XXXVII PhD Course in

*Applied Biology and Experimental Medicine*

DEPARTMENT OF CHEMICAL, BIOLOGICAL,

PHARMACEUTICAL AND ENVIRONMENTAL SCIENCES

University of Messina

---

# *Antitumor effect of SOS-1/KRAS inhibitor BAY-293 against head and neck carcinoma*


PhD thesis of:

Dr.ssa Deborah Mannino

BIOS-11/A

Supervisor:

Prof.ssa Michela Campolo



Coordinator:

Chiar.ma Prof.ssa Emanuela Esposito


---


Anno Accademico 2021/2024

# ABSTRACT

Head and neck cancer (HNC) is a heterogeneous disease that affects multiple anatomical sites and histological subtypes. Among these tumors, head and neck thyroid cancer is one of the endocrine-derived HNC. The most aggressive and lethal type of thyroid cancer (TC) is anaplastic thyroid carcinoma (ATC). Another aggressive type of HNC is oral squamous cell carcinoma (OSCC) which originates in the squamous cells lining the mucosa of the mouth. Although ATC and OSCC are two totally different types of tumors in terms of origin, prognosis, and treatment, a known oncogene common in the pathogenesis of both tumors is the Kirsten Rat Sarcoma Viral Oncogene Homolog (KRAS) oncogene. Recent studies have indicated that increased expression levels of mutated KRAS genes may play a key role in the development and progression of ATC and OSCC. KRAS is one of the well-known proto-oncogenes that belongs to a group of small guanosine triphosphate (GTP)-binding proteins known as the RAS superfamily or RAS-like GTPases. Overexpression of KRAS can be caused by a mutation of the KRAS gene or by hyperactivation of growth factor receptor tyrosine kinases. Despite its recognized importance in cancer malignancy, KRAS is considered non-druggable and has been never studied in the field of HNC. Recently, it has been shown that an interesting approach to target K-RAS and its interaction with GTP cargo could be through the Son of Sevenless 1 (SOS1) protein, a key regulator of KRAS function. In this context, a new synthetic molecule, BAY-293, has recently been developed, able to selectively inhibits the KRAS–SOS1 interaction. Based on these findings, the aim of this thesis was to evaluate for the first time the antitumor effect of BAY-293 in the field of ATC and subsequently in the field of OSCC. The study of ATC was performed using an *in vitro* and *in vivo* model, investigating the main signaling pathways related to KRAS. The *in vitro* model was performed using different TC cell lines to study the effect of BAY-293 on the modulation of Mitogen-activated protein kinase (MAPK) pathways , apoptosis and cell migration. To

confirm the *in vitro* mechanism and better mimic the complex tumor microenvironment, an *in vivo* orthotopic model of ATC was used. This involved in situ inoculation of ATC cells into the thyroid of mice, followed by treatment with BAY-293. Histological analysis and Masson's trichrome staining of mouse thyroids were performed to evaluate the effects of BAY-293 on tumor growth and progression, and Western blot analysis was used to examine markers related to KRAS/MAPK and apoptosis pathway. The results of the ATC study indicate that BAY-293, both *in vitro* and *in vivo*, effectively blocked the KRAS/MAPK/ERK pathway and β-catenin that act as essential downstream effectors for cell migration and increased the apoptotic process by slowing the progression of ATC. The study of BAY-293 in the field of OSCC was performed using an *in vitro* model. In the *in vitro* model of OSCC, BAY-293 significantly reduced the cell viability of CAL-27 cells by modulating the activation of NF-κB/IκBα pathway and the release of inflammatory mediators. In addition, BAY-293 reduced the expression of eNOS and TGFβ, two important markers of angiogenesis, and significantly increased the apoptosis pathway in OSCC cells. Overall, these results demonstrated that KRAS/SOS1 inhibition could be a promising therapeutic target for the treatment of ATC and OSCC and highlighted BAY-293 as a novel molecule that requires further research to fully evaluate its efficacy in these types of tumors.

## *INTRODUCTION*

Head and neck cancers (HNC) include tumors that arise in the oral cavity, pharynx, larynx, paranasal sinuses, nasal cavity, and salivary glands [1]. This group of tumors also includes malignant tumors of neural, mesenchymal, and other cellular origin, such as malignant tumors of the salivary glands and thyroid. Among these tumors, head and neck thyroid cancer is one of the HNC of endocrine origin. Thyroid cancer (TC) accounts for 95% of all endocrine tumors, and its incidence continues to increase worldwide. The most aggressive and lethal type of TC is anaplastic thyroid carcinoma (ATC) [2] . ATC usually develops in elderly patients, presenting rapidly growing and infiltrative neck mass [3]. The prognosis of ATC is severe with a median survival period of less than 6 months and mortality rate of more than 90% [4]. Nuclear pleomorphism, tumor necrosis, increased mitosis, and infiltrative growth are key features for a conclusive diagnosis of ATC, and immunohistochemistry Ki67 is useful to confirm ATC and other high-risk thyroid carcinomas [5]. Therapeutic approaches for ATC are very limited. ATC often results in poor surgical resectability and radioactive iodine treatment is ineffective [6]. TC guidelines therefore recommend the use of target therapy [7]. Hence, the therapy depends on the result of the molecular test and the mutations involved. Other recommended regimens include treatment with chemotherapy, which are generally not very effective for advanced anaplastic disease, but in some cases may contribute to disease response or maintenance of stable disease [8]. Another type of aggressive HNC is oral squamous cell carcinoma (OSCC). OSCC originates in the squamous cells that line the mucosa of the mouth and can affect different areas of the oral cavity, including the tongue, gums, hard palate, floor of the mouth, and cheeks. Even for this type of tumor, the survival rate of affected patients remains very low due to its high aggressiveness and ability to metastasize. Although ATC and OSCC are two totally different

types of tumors in terms of origin, prognosis, treatment, risk factors, and epidemiology, they share some common characteristics such as aggressive neoplasms. Moreover, a known oncogene common in the pathogenesis of both ATC and OSCC is the rat sarcoma virus (RAS) oncogene. Activating mutations in RAS genes have been found in both these tumors and recent *in vitro* and *in vivo* studies have suggested that increased expression of mutated RAS genes may play a crucial role in the development and progression of ATC and OSCC [9-12]. RAS is a family of guanosine triphosphate (GTP) -binding proteins, upstream of v-RAF murine sarcoma viral oncogene homolog B1 (BRAF), that acts through Mitogen-activated protein kinase (MAPK) signaling pathways. HRAS, KRAS, and NRAS encode four different but related proteins (H-Ras, N-Ras, K-Ras4A, and K-Ras4B) that are cardinal in the control of cell growth, differentiation, and survival [13]. In particular, the KRAS protein transduces extracellular signals through cell surface receptors from the inactive state (bound to Guanosine-diphosphate, GDP) to the active state (bound to Guanosine-5'-triphosphate, GTP). KRAS protein activation orchestrates intracellular signaling cascades that regulate tumor cell survival and proliferation [14]. Aberrant activation of KRAS occurs in approximately 1 in 7 of all human tumors, making it the most frequently mutated oncogene [15]. This aberration can be caused by deregulated upstream signaling, loss of GTPase-activating protein function, or oncogenic mutations that result in increased GTP-bound KRAS and persistent downstream signaling [16]. But in addition to the KRAS mutation, other variables could also play a role in the hyper-activation of this protein. These include overexpression of RAS scaffold proteins and hyperactivation of growth factor receptor tyrosine kinases, which can result in persistent KRAS activation [17]. Therefore, significant efforts and progress have recently been made in the development of novel therapies that target functionally important receptor tyrosine kinase (RTK)/KRAS effector pathways, such as the MAPK or Phosphoinositide 3-kinase (PI3K) pathways. However, in most cases, the development of acquired resistance is inevitable and the toxicity of combination therapies may become prohibitive to tolerate [18]. This requires the development of new strategies to overcome these clinical dilemmas. An attractive

approach to target KRAS and its interaction with GTP cargo could be through the Son of Sevenless 1 (SOS1) protein [19]. SOS1, also known as guanine nucleotide exchange factor (GEF), increases GTP turnover and regulates the fraction of KRAS in the active state and cell proliferation. Furthermore, SOS1 can not only promote the production of active GTP-bound K-RAS at the catalytic site, but also enhance its GEF function allosterically. Therefore, given its direct protein-protein interaction with KRAS, targeting SOS1 may have advantages over other indirect approaches for suppressing KRAS signaling. In addition, targeting the SOS1-KRAS interaction, due to the functional compensation of its paralog SOS2 and the lack of requirement in normal versus tumor cells, might also be less toxic [20]. Several small molecule inhibitors, such as BAY-293, have been developed to abolish Guanosine-5'-triphosphate (GTP) recharging and to impair the interaction between SOS1 and KRAS, resulting in antiproliferative activity [21]. The compound BAY-293 is a novel synthetic molecule that selectively inhibits the KRAS–SOS1 interaction and it has demonstrated a relatively broad spectrum of antitumor activity in a large panel of tumor cell lines [22-24]. This molecule is attractive for its KRAS inhibition independently of the type of KRAS mutations [22]. However, its antitumor effect in the field of HNC has never been investigated before. Based on this evidence, the purpose of this investigation was to study the efficacy of the KRAS inhibitor BAY-293 for the treatment of ATC and OSCC. Our study focused primarily on TC, and we then extended the analysis to OSCC. This approach allowed us to explore not only the specificities of each tumor type, but also to highlight the connections and similarities they have in common within this oncological category.

# 1. *CARCINOMAS OF THE HEAD AND NECK*

HNC are a heterogeneous group of malignant neoplastic entities, comprising malignant neoplasms that originate below the level of the skull base and above the thoracic inlet. It includes subsites such as the oral cavity, oropharynx, nasal cavity, nasopharynx, hypopharynx, and larynx, typically affecting the squamous epithelial cells (~90%) lining the mucosal surfaces of the upper aerodigestive tract [25]. In addition, this group of tumors also includes malignant neoplasms of neural, mesenchymal, and other cellular origin, such as malignant neoplasms of the salivary glands and thyroid glands [26]. HNC is the seventh most common cancer globally, with over 660,000 new cases and 325,000 deaths annually [27]. However, due to differences in presenting symptoms, treatment regimens, and prognosis in each anatomical subsite, HNCs are considered separate entities. Among these TC is an HNC that belongs to endocrine tumors and accounts for approximately 95% of them [28]. Excluding skin and TC, over 90% of head and neck cancers are squamous cell (epidermoid) carcinomas, while most of the remainder are adenocarcinomas, sarcomas, and lymphomas. Among squamous cell carcinomas, the most frequent and of greatest scientific interest is oral squamous cell carcinoma (OSCC).

## *1.1 THYROID CARCINOMAS*

### 1.1.1 Anatomy and function of the thyroid gland

The thyroid is a gland located in the anterior region of the neck, in front and lateral to the larynx and trachea. It is located at the height of the fifth cervical vertebra, just above the base of the neck. The thyroid consists of two lateral lobes, joined by a median isthmus. The two lobes have a conical shape and extend from the mid-height of the thyroid cartilage to the fifth tracheal ring. They have a length of approximately 3 cm and a thickness that varies from 0.5 cm at the apex to

2 cm at the base. The isthmus joins the two lobes near their base, at the height of the first two tracheal rings. From the upper edge of the isthmus a glandular extension of variable length can branch upwards, which is called the pyramidal lobe. It represents a testimony of the path taken by the gland during its embryonic development [29]. The overall size of the thyroid varies greatly depending on age and gender. The thyroid is located on the ventral surface of the larynx and the first two tracheal rings, partially covered by the sternocleido-mastoid, sternothyroid and omohyoid muscles, and by the middle cervical fascia. Posterior to the gland, in close continuity, the parathyroid glands are located. The gland is located inside a fibrous sheath (thyroid sheath), through which it is in contact with surrounding organs. Connective branches depart from behind the thyroid sheath and secure the organ to the larynx (suspension ligament), to the laryngeal cartilage and to the first tracheal rings (internal lateral ligaments), and to the sheath that surrounds the vascular-nervous bundle of the neck (external lateral ligaments). Posteriorly, the left lobe is also in contact with the pharyngo-esophageal tube, where the inferior laryngeal nerve runs. The gland is covered from the inside to the outside by its own connective sheath, by the dangerous thyroid space (a network of arteries and veins of the organ) and by the peri-thyroid sheath. The thyroid is supplied by the right and left superior thyroid arteries, branches of the external common carotids, and by the right and left inferior thyroid arteries, branches of the thyrocervical trunk of the subclavian artery. The division branches of the inferior thyroid artery are in close contact with the inferior laryngeal (or recurrent) nerve, branch of the vagus nerve. The waste veins from the intra-thyroid circulation form a plexus in the thyroid dangerous space, from which the thyroid veins originate upper right and left (tributaries of the ipsilateral internal jugular vein) and lower right and left (tributaries of the ipsilateral brachio-cephalic vein). The lymphatic vessels are tributaries of the internal jugular chain (upward) and of the para-tracheal and pre-tracheal lymph nodes (downward). The thyroid receives nerves from the cervical sympathetic nerve and the two laryngeal nerves of the vagus nerve. The thyroid gland is divided into lobules, formed by slender

shoots that branch out from the connective capsule. The vessels and nerves reach the individual functional units with the connective branches (Figure 1) [30].

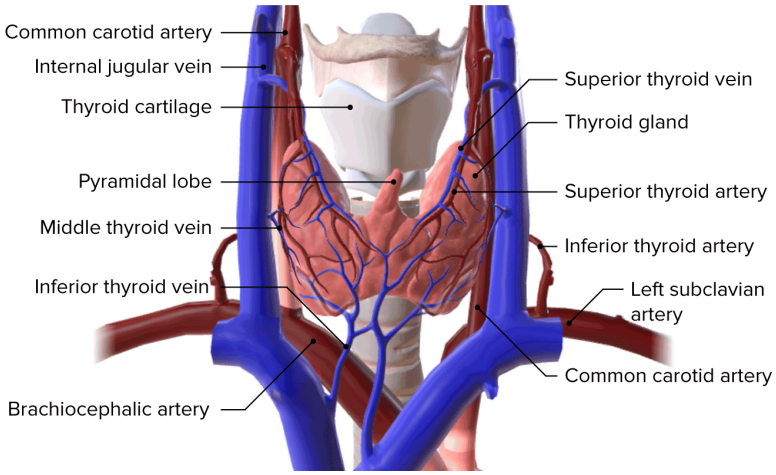


**Figure 1.** Anatomy of the thyroid gland [31].

From a structural point of view, the thyroid is composed of a series of small spherical vesicles, called thyroid follicles. These circular cavities represent the functional units of the thyroid. Thyroid follicles are hollow spherical vesicular units whose wall is formed by a single layer of epithelial cells, the thyrocytes, which delimit the follicular lumen containing the thyroid colloid inside, amorphous glycoprotein substance, where thyroglobulin (Tg), is stored glycoprotein characterized by the presence of tyrosine residues which they can be iodized after iodide oxidation and condensed to form the thyroid hormones T3 and T4 [32]. Thyroglobulin is an iodinated glycoprotein secreted and poured into the follicular lumen via secretory vesicles. Thyrocytes are cells with clear polarity: the basal pole lies on the basement membrane, while the apical pole delimits the follicular lumen in irregular manner due to the presence of numerous microvilli. The stimulation of the secretion of thyroid hormones induces variations in the shape and activity of the thyrocytes: from the flattened shape typical of the quiescent cell, a columnar appearance is assumed and pseudopodic extrusions emerge from the apical membrane which

incorporate the colloid allowing reabsorption via pinocytosis. Adjacent to the follicular cells, there are rare parafollicular cells or C cells that secrete calcitonin (Figure 2) [33].


**Figure 2.** Histology of follicular epithelium [34].

Thyrocytes synthesize thyroxine and triiodothyronine under the control of thyrotropin (TSH) and based on the availability of iodine, the main constituent of thyroid hormones. TSH is produced by the pituitary gland in response to hypothalamic thyrotropin-releasing hormone (TRH) stimulation and is regulated through the negative feedback of circulating thyroid hormones. TSH, a 25 kDa glycoprotein, is made up of an α subunit shared with other glycoprotein hormones (hCG, LH and FSH) and a β subunit, which confers biological specificity. The TSH receptor, expressed on the basal plasma membrane of the thyrocyte, belongs to the superfamily of G protein-coupled membrane receptors and consists of seven hydrophobic transmembrane domains, an extracellular hormone-binding domain, and a cytosolic carboxy-terminal domain. The interaction of TSH with its receptor, which occurs through a cAMP-dependent mechanism, stimulates the uptake of iodide, hormonesynthesis and the secretion of thyroid hormones by modulating the expression of the genes for the NIS (Na/I cotransporter), Tg and thyroperoxidase

(TPO) [35]. Furthermore, TSH stimulates the proliferation and differentiation of thyrocytes. The thyroid hormone T3 is the main mediator of the determined effects by thyroid hormones, as most of the T4 hormone is transformed into T3 through a desiodation process by of the desiodase enzyme. The physiological actions of the T3 hormone are mediated by its interaction with specific nuclear receptors called thyroid hormone receptors (THRs). The action of thyroid hormones occurs in target tissues through genomic and non-genomic mechanisms. The genomic actions are mediated by the binding of the hormone to the specific thyroid nuclear receptor THR which allows their translocation into the nucleus where they regulate the transcription of certain genes by binding to specific sites on the DNA. The genomic effect mainly translates into a regulation of proliferation and cellular differentiation. Based on the effects of the ligand on transcription, responsive elements can be classified as positive (pTRE) or negative (nTRE). The binding of the hormone to the receptor when it binds pTREs leads to the dissociation of the corepressor and the recruitment of coactivators and therefore to activation of gene expression [36]. However, when there is a link with nTREs, the THRs activates gene expression in its absence of the ligand and binding of the hormone leads to repression of transcription. The actions of thyroid hormone that do not depend on binding to the THR are defined as non-genomic. These effects are caused by interaction with proteins that are not directly involved in the regulation of gene expression. Moreover, these effects are characterized for the rapidity of onset (seconds or minutes), for the fact of not require new protein synthesis, and for the use of signaling pathways that originate in the cell membrane and which generally involve the activation of protein kinases. The result is normally an increase in the activity of some proteins important for cellular metabolism, such as some ion transporters (especially the sodium-potassium pump). In particular, they regulate adult metabolic activity by having thermogenetic action and effects on the cardiovascular system, regulating glucose metabolism and protein synthesis and intervening in lipolysis and lipogenesis [37].

### 1.1.2 Definition of TC

Thyroid carcinoma (TC) represents approximately 95% of all endocrine cancers and 2.5% of all malignancies, making it the most common neoplasm of the endocrine system. There is a lot of variation in the cellular, molecular, genetic, and clinical features of TCs. This significant phenotypic heterogeneity typically arises from the combination of genetic and non-genetic factors and may have consequences for comprehending the mechanisms behind treatment resistance and formulating successful tactics. Current developments in multiscale tumor profiling have enhanced knowledge of the tumor landscape and may enable the discovery of novel molecular targets and biomarkers for prognosis and treatment [38].

### 1.1.3 Epidemiology

The incidence of thyroid cancer worldwide continues to increase. In 2020, approximately 586,000 cases of thyroid cancer were reported worldwide, making thyroid cancer the tenth most common cancer [39]. The female incidence was estimated at 449,000 compared to the male incidence of 137,000, making thyroid cancer three times more common among women. However, mortality rates remain low, but differ by gender. The mortality among males was 15,900 compared to 27,700 deaths in females. In another way, the cumulative risk for females is estimated at 0.05 compared to that for males at 0.04, making male mortality from thyroid cancer disproportionate to the incidence [39]. The incidence of the disease does not have a uniform impact on all areas of the world and varies according to socioeconomic development. Indeed, the level of increase can vary depending on the geographic location and the prevalence of imaging modality use. Countries with a high sociodemographic index are home to a third of thyroid cancer patients [40]. In fact, the World Health Organization (WHO) revealed that the Western Pacific region had the highest rates of thyroid cancer diagnoses in 2020 with 279,035, making it the 9th

most common cancer in that area [41]. In terms of the percentage of the population, the Western Pacific region represented 25.4% of the global population in 2018 but was responsible for 47.6% of thyroid cancer cases and 31.9% of deaths attributed to the disease in 2020. The African region had the highest percentage of cases causing mortality (number of deaths due to thyroid cancer divided by the prevalence of thyroid cancer cases multiplied by 100) at 11.25%. This was followed by the Southeast Asia region at 7.01% with single-digit percentages for the remaining regions (5.87%, 2.13%, 1.51%, and 1.49% for the Eastern Mediterranean region, Europe region, Americas region, and Western Pacific region, respectively) [41]. Furthermore, it has been suggested that geographic areas worldwide with previously high mortality rates secondary to thyroid cancer include regions with iodine deficiency, associated with benign thyroid disease, which is a known risk factor for the development of thyroid cancer, such as iodine-deficiency goiter. Overall, the estimated number of incident cases of thyroid cancer from 2020 to 2040 is projected to increase by 29.9%. and thyroid cancer mortality is estimated to increase by 67% for both sexes [42].

### 1.1.4 Risk factors

Thyroid carcinogenesis can be caused by a variety of risk factors, both intrinsic and extrinsic. Several studies have discovered a relationship between environmental pollutants and thyroid cancer incidence rates. These factors have been shown to contribute to the development of thyroid cancer, so further investigation is needed to discover how they function and influence thyroid pathology. Identifying the pathophysiology associated with these environmental risk factors may allow for more rapid development of risk reduction plans, exposure remedies, and medical treatments to prevent and perhaps even reverse the course of the disease. Age, biological sex and family and hereditary conditions are examples of innate, non-modifiable factors [43]. Genetic susceptibility and mutations play an essential role in predisposition to thyroid cancer.

Otherwise, extrinsic factors include ionizing radiation, pesticides, persistent organic pollutants (POPs), endocrine disrupting chemicals (ECDs), bisphenol A (BPA), phthalates, heavy metals and polychlorinated biphenyls (PCBs). Furthermore, another environmental factor related to the risk of thyroid cancer incidence is dietary iodine intake (deficiency or sufficiency of nutritional iodine) [44]. Low and high iodine intake can alter TSH and induce the development of carcinogenic substances. Some scientific investigations have shown that iodine deficiency, rather than an excessive intake, has more of a promoting effect than a direct carcinogen [45,46]. This results in an increase in TSH, which stimulates thyroid epidermal growth factor (EFG), and a reduction in transforming growth factor 1 (TGF1), which simultaneously promotes angiogenesis and tumor growth. The presence of follicular and anaplastic carcinomas in the population from iodine-deficient regions has been demonstrated in numerous studies confirming this observation [47,48]. Preexisting benign thyroid disease is one of the constitutional etiologic factors associated with the development of computed tomography (CT). Goiter, benign nodular or multinodular thyroid disease, and autoimmune disorders, such as Graves' disease and Hashimoto's disease, may increase the risk of developing TC, according to a series of case-control and prospective studies [49]. Furthermore, females and males have been observed to differ markedly in the presence of TC after puberty and during the reproductive period [50]. Thus, scientific research suggests that the development of TC may be linked to estrogenic effects [51,52]. Obesity is another risk factor identified by numerous case-control studies. The exact pathophysiological mechanism is not yet fully understood, but the increase in TSH associated with this condition could cause an altered interaction with insulin-like growth factor 1, activating the MAPK and PI3K pathways. This could contribute to the pathogenesis of TCs [53]. Furthermore, the clinically relevant risk of thyroid cancer trends positively with age; however, the risk of malignancy of such nodules paradoxically decreases with age [54]. The increase in cancer incidence observed in the 1990s has come to an end, except for thyroid cancer in young adults. Furthermore, many environmental factors have not yet been sufficiently studied to adequately infer the impact of environmental

pollutants on the human endocrine system, making prevention strategies for this pathology more challenging [55]. Notably, increasing awareness of environmental risk factors related to thyroid cancer is considered an essential tool for cancer prevention through risk prevention/management.

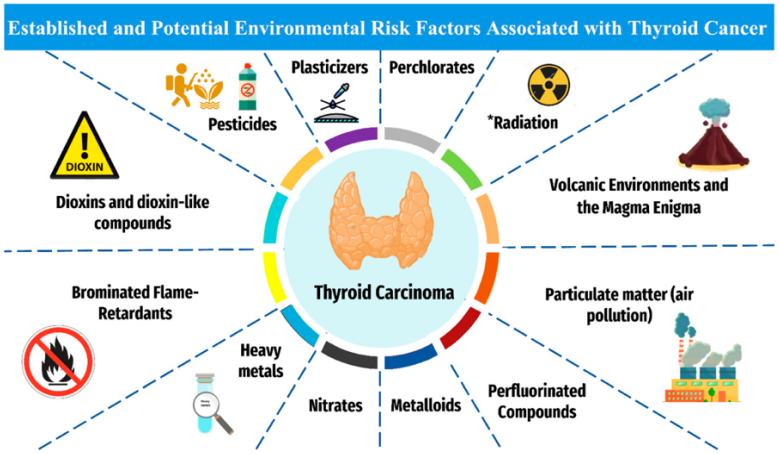


**Figure 3.** The established and plausible environmental risk factors for thyroid cancer [56].

### 1.1.5 Molecular pathogenesis of thyroid cancer

Understanding the etiopathogenesis of thyroid cancer, i.e., the factors that contribute to its onset and development, is essential to improve prevention, diagnosis, and treatment strategies. This etiopathogenesis is influenced by a combination of genetic, environmental, and hormonal factors. Genetic factors play a crucial role in the pathogenesis of thyroid cancer, significantly contributing to the onset and progression of the disease. Among the various subtypes of thyroid cancer, several genetic mutations and chromosomal rearrangements have been identified as key factors. In this context, recent molecular biology has revealed a variety of genetic alterations related to thyroid cancer oncogenesis. Mutations in the rearranged during transfection (RET) gene (12 % of cases), RAS mutations (15 %) and BRAF mutations (60 % of cases) are among the most important mutations [57]. These alterations lead to an altered function of various pathways signal, among which the most important are the MAPK/extracellular signal-regulated kinase (ERK) pathway and the PI3K- Protein kinase B (Akt) pathway. MAPKs are serine/threonine kinases that transmit

extracellular stimuli and regulate cell proliferation, differentiation, motility and survival; alterations of this pathway have been linked to the tumorigenic process in various organs, including thyroid [58]. PI3K-Akt is another signaling pathway that has various functions: it regulates accumulation glucose, survival, migration and cell proliferation.

In addition to the activation of specific signaling pathways, the tumorigenic process that characterizes thyroid cancer involves other mechanisms such as the evasion of immune surveillance. Tumor cells can develop mechanisms to evade immune surveillance, such as the expression of immunosuppressive molecules and reduction of antigen presentation [59]. Therefore, immune evasion allows tumor cells to avoid elimination by the immune system and proliferate uncontrollably. Furthermore, tumor growth requires an adequate supply of nutrients and oxygen, provided by angiogenesis, the process of formation of new blood vessels. Thyroid tumors can produce pro-angiogenic factors, such as vascular endothelial growth factor (VEGF), to stimulate the formation of blood vessels. Angiogenesis is essential for tumor growth and metastasis, as it provides access to the circulatory system [60].

### 1.1.6 Classification

In March 2022, the World Health Organization (WHO) released the fifth edition of its Classification of Endocrine and Neuroendocrine Tumors [61] (Figure 4). This edition includes a hierarchical taxonomic classification of tumor types, assigned based on biological behavior, pathological or molecular characteristics, and the cell of origin. Type, subtype, family, and category are the four primary taxonomic ranks. Follicle epithelial cells are the primary source of thyroid cancers; C cells that secrete calcitonin are responsible for a tiny percentage of cases. Benign tumors, low-risk malignancies, and malignant malignancies are the three categories into which follicular cell-derived malignancies fall. Based on both molecular pathogenesis and classical histopathology, the classification of thyroid tumors has changed over time [62].

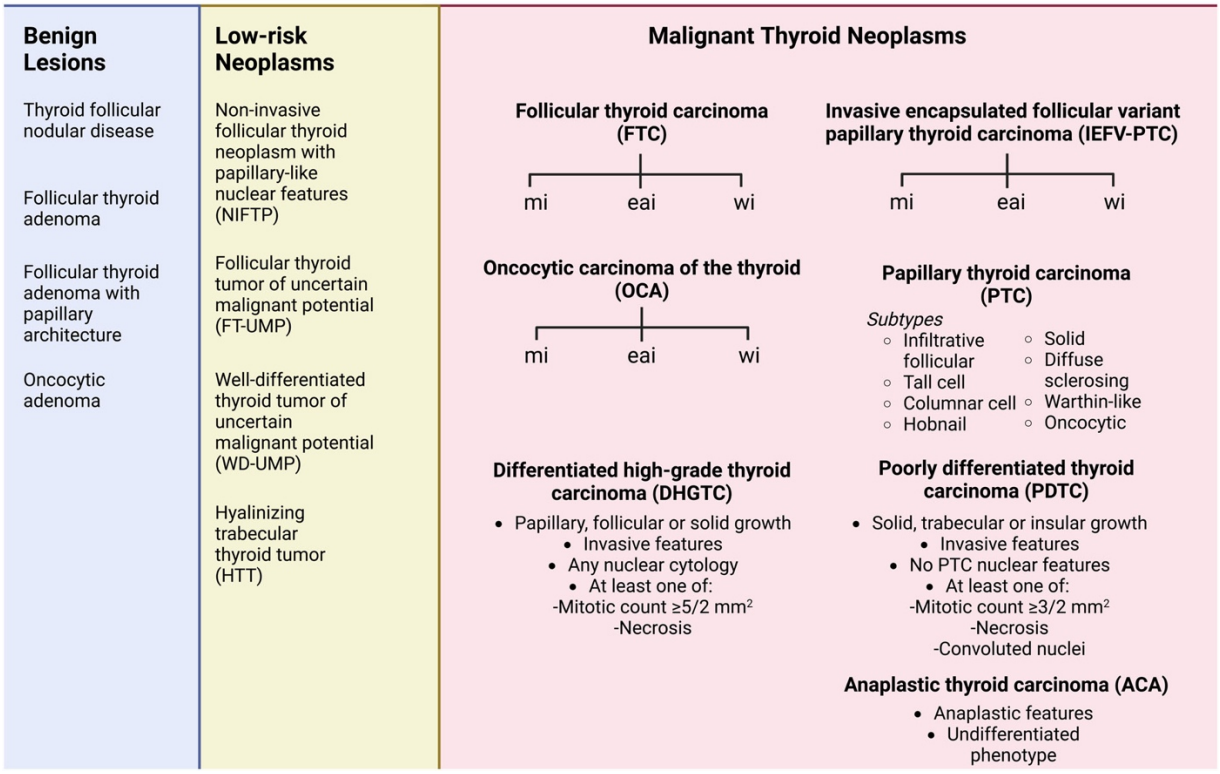


**Figure 4**. The 2022 WHO classification of thyroid tumors [61].

TC are classified into:

- **Benign follicular cell-derived thyroid tumors**

Benign follicular cell-derived thyroid tumors are noncancerous growths that arise from the follicular cells of the thyroid gland. These tumors often present as a painless, slow-growing thyroid nodule. They are usually discovered incidentally during routine examinations or imaging studies. However, benign follicular thyroid tumors generally have an excellent prognosis, with no risk of metastasis or invasion. Benign follicular cell-derived thyroid tumors are the most common type of benign thyroid tumor, usually well-demarcated and noninvasive. This type of tumor is often encapsulated and has intra-follicular centripetal papillary growth [63]. These tumors are often associated with autonomic hyperfunction and may therefore appear as warm or

tepid nodules on radionuclide thyroid scans [64]. Molecular analyses have shown that these tumors are driven by TSHR, guanine nucleotide-binding protein, alpha stimulating (GNAS), or enhancer of zeste 1 polycomb repressive complex 2 subunit (EZH1) mutations and alterations that activate the protein kinase A (PKA) pathway [65,66]. These tumors can also occur in the context of McCune-Albright complex and Carney syndromes; both are PKA pathway-related conditions driven by guanine nucleotide-binding protein alpha stimulating activity polypeptide (GNAS) and protein kinase A regulatory subunit 1 Alpha (PRKAR1A) mutations, respectively [67]. Furthermore, nonfunctional follicular adenomas with papillary architecture can harbor double-stranded RNA-specific endoribonuclease (DICER1) mutations, and a subset of these has been reported in association with DICER1 syndrome [68,69]. Therefore, the association between thyroid function and related tumor syndromes makes the distinction between these tumors clinically significant [69,70].

- **Low-risk follicular cell-derived thyroid neoplasms**

Low-risk thyroid neoplasms derived from follicular cells are a category of thyroid tumors that, although they have neoplastic features, have a less aggressive clinical behavior than more advanced malignant neoplasms. These tumors behave neutrally, as their behavior is neither benign nor malignant, but intermediate between these two forms. They have the potential to metastasize, but the chances are low. These tumors arise from follicular cells of the thyroid and include three types of low-risk neoplasms, such as noninvasive follicular neoplasm with papillary nucleus (NIFTP), tumors of uncertain malignant potential (UMP) and hyalinizing trabecular tumor (HTT) [71]. NIFTP has recently been recognized as a new diagnostic entity. In the past, these tumors were often classified as variants of papillary thyroid carcinoma but have been reclassified because of their favorable clinical behavior. These tumors are characterized by growth in a follicular pattern with nuclei that show features like those of papillary carcinoma,

but without invasion of the capsule or blood vessels. In fact, because it is considered a very low-risk neoplasm, NIFTP does not pose a risk of metastasis or recurrence if completely excised [72]. UMPs are rare lesions in which histologic confirmation of capsular and vascular invasion is erroneous. Because an invasive focus alone would disqualify these diagnoses, these tumor entities require thorough microscopic evaluation of the entire capsule/tumor interface [73]. Tumors in this category are encapsulated, have a follicular pattern, and have architectural and cytologic criteria that do not meet all the criteria for malignancy. In UMP, angioinvasion and capsular infiltration are present, which were not seen in NIFTP [74]. HTT are follicular cell-derived thyroid neoplasms with nuclear atypia, trabecular growth, extracellular hyaline matrix [75]. Intertrabecular hyaline material is produced by an active basement membrane protein. Due to overlapping features with papillary and medullary thyroid carcinomas, the diagnosis of this tumor is always challenging. Apart from HTT, these neoplasms are mostly RAS-driven, and detection of any non-RAS-like molecular signature (e.g., BRAF p.V600E) or high-risk molecular alterations (e.g., TERT promoter mutations) requires reassessment of pathological features to exclude overt malignancy [61].

- **Follicular thyroid carcinoma and follicular variant of papillary thyroid carcinoma**

Because of their distinct nuclear morphologies, follicular variant of papillary thyroid carcinoma (FVPTC) and follicular thyroid carcinoma (FTC) were nearly identical. Compared with FTC, FVPTC has a worse prognosis and more lymph node metastases. An oncocytic cell population that exceeds 75% is defined as FTC oncocytic carcinoma. The degree of invasion determines the prognosis for both types of tumors. Accordingly, there are differences in prognosis for tumors that are extensively invasive, angioinvasive, or mildly invasive [76]. Many FVPTCs have varying levels of disease-free survival after 40 months, resulting in 45% for highly invasive FTC and 97% and 81% for minimally and extremely invasive FTC, respectively [77,78]. The receptor

tyrosine kinase (RTK), PI3K/Akt and MAPK pathways are prevalent in FTC, suggesting the role of these signalling pathways mediated by growth factors and oncogenes like RAS in these tumours [79]. The presence of RAS mutation may suggest their role in early steps of thyroid carcinogenesis. In this context, Miller et al. used *in vivo* models to demonstrate that oncogenic transformation into invasive and metastatic cancers required simultaneous activation of KRAS and P13K signaling [80]. Follicular cancers that harbor RAS mutations may be at a risk of dedifferentiating into anaplastic thyroid cancers [81,82]. In fact, mutations of RAS gene are associated with poor histological features and poor patient survival [83].

FVPTCs are now divided into infiltrative and encapsulated subtypes. Infiltrative FVPTCs are BRAF-driven tumors with florid nuclear atypia and invasion of the surrounding thyroid parenchyma and lymphatics. Encapsulated FVPTCs are RAS-driven lesions with an invasive pattern like FTCs (capsular and/or propensity for vascular rather than lymphatic invasion) [61]. Concerning therapy, regardless of whether it is FTC or FVPTC, total thyroidectomy with neoadjuvant therapy is the treatment of choice for both tumors [84].

- **Papillary thyroid carcinoma**

Papillary thyroid carcinoma (PTC) is the most common type of thyroid cancer, accounting for approximately 80-85% of cases. It is generally considered a slow-growing tumor with an excellent prognosis, especially when diagnosed early. However, there are several variants and characteristics that can influence the management and prognosis of the tumor [85]. Histological subtyping of PTC has been the focus of the fifth edition of the WHO classification. Oncogenic BRAF mutations have been shown to be present in 50–60% of all PTCs and are specifically overrepresented in columnar cell and hobnail subtypes with the highest risk of lymph node metastasis, loco-regional recurrence, distant metastasis, and poor outcomes [5]. Therefore, even sub centimeter PTCs should be histologically subtyped, as small subsets of these lesions have

been observed to have an aggressive clinical course like their large counterparts. Several histological subtypes are listed to date in addition to classical PTC. The most common are infiltrative follicular, tall cell, columnar cell, hobnail, solid, diffuse sclerosing variant. The WHO classified these subtypes in 2022 based on their histological definitions and molecular profiles. The new classification requires the exclusion of PTCs with high-grade features (tumor necrosis and mitosis) from a new diagnostic category, as for other forms of differentiated thyroid carcinoma [5].

- **Poorly differentiated thyroid carcinoma and differentiated high-grade thyroid carcinoma**

Poorly differentiated thyroid carcinoma (PDTC) and differentiated high-grade thyroid carcinoma (DHGTC) are more aggressive forms of thyroid cancer than differentiated carcinomas such as PTC and FTC. PDTC is considered an intermediate form between well-differentiated thyroid carcinomas (such as PTC and FTC) and anaplastic thyroid carcinomas (ATC), which are highly aggressive [86]. It is characterized by solid, insular, or trabecular growth, and displays histological features that distinguish it from well-differentiated carcinomas, such as a high nuclear/cytoplasmic ratio, the presence of necrosis, and high mitotic activity [87]. PDTC retains some features of differentiated carcinomas but loses the ability to organize cells into typical follicular or papillary structures. This makes it more aggressive, with worse biological behavior. The criteria for the diagnosis of PDTC include a solid, trabecular, or insular growth pattern, the absence of typical nuclear features of papillary carcinoma, and the presence of at least one of the following criteria: convoluted nuclei, tumor necrosis, and mitotic activity [5,64,88]. In some cases, PDTC cells show small nuclei with clumped dark chromatin with a resinous appearance, reminiscent of the nuclei of PTC. A distinctive feature of PDTC is necrosis with the presence of necrotic tumor cells and nuclear dust [87].

DHGTC is an emerging category that includes papillary or follicular thyroid carcinomas that exhibit high-grade histologic features, such as increased mitotic activity, focal necrosis, and extensive vascular invasion. Although derived from well-differentiated carcinomas, these tumors exhibit more aggressive behavior and a poorer response to radioiodine therapy. Some variants of PTC, such as the tall cell variant and the columnar cell variant, may be considered DHGTC due to their more aggressive clinical behavior [89]. DHGTC shows a papillary development pattern that is comparable to well-differentiated tumors. Nuclear features typical of papillary thyroid carcinoma may be present throughout the tumor, although some regions of the tumor may show pleomorphism and nuclear expansion [90]. Distinctive histologic features that support the diagnosis include necrosis and excessive mitotic activity. Moreover, along with invasion beyond the thyroid, blood vessels, nerves, and lymphatic involvement are frequently detected [91]. Both PDTC and DHGTC exhibit positive immunohistochemical staining for thyroid transcription factor 1 (TTF1), PAX8, cytokeratins (often CK-7), and thyroglobulin (TG). In addition, the Ki67 proliferation index is high, usually between 10% and 30% [92]. According to molecular biology, PDTC and DHGTC have BRAF $^{V600E}$ or RAS mutation. In fact, most DHGT are BRAF $^{V600E}$ driven because they mainly have a papillary carcinoma-like cytoarchitecture [90]. This explains why DHGTC have a higher tendency to develop cervical lymph node metastases. In addition, PDTC and DHGTC also have severe secondary mutations, usually in the telomerase reverse transcriptase (TERT) promoter but occasionally in phosphatidylinositol-4,5-bisphosphate 3-kinase catalytic subunit alpha (PIK3CA) and tumor protein p53 (TP53 or p53) [93].

- **Anaplastic thyroid carcinoma**

ATC represents a rare, undifferentiated form of thyroid cancer, accounting for less than 0.2% to 1%–2% of cases [94]. Nonetheless, it is regarded as one of the deadliest neoplasms, with a significant reduction in quality of life and a median survival of only 4 to 6 months [95]. Patients

with incurable or metastatic disease have had only patchy results from multimodal therapy involving chemotherapy and external beam radiation, with less than 20% of patients surviving for a full year [96]. The existence of neck tumors that are growing quickly frequently results in serious and sometimes fatal consequences. These tumors can invade several different structures, including lung, the major blood vessels, which can result in symptoms of intermittent cerebral ischemia or superior vena cava syndrome, the esophagus causing dysphagia, the trachea leading to airway obstruction and asphyxia. Moreover, ATC can invade laryngeal nerve causing paralysis, and the neural plexuses causing persistent pain [97]. The most prevalent molecular alterations were discovered in the TERT promoter (75%), TP 53 (63%), BRAF (45%), RAS (22%), PIK3CA (18%), eukaryotic translation initiation factor 1A X-linked (EIF1AX) (14%), and Phosphatase and tensin homolog (PTEN) (14%), in a recent series of 126 samples of ATC analyzed by Next Generation Sequencing (NGS). The first two are more common in ATC than the others, and they can be seen in either DTC or PDTC [98,99]. Moreover, histone methyltransferases (KMT2A, KMT2C, KMT2D, and SETD2) and the chromatin remodeling SWI/SNF complex (ARID1A, SMARCB1, PBRM1, etc.) have been found to be altered in 24% and 36% of ATC samples, respectively [100]. In addition, ATC tumors are characterized by an important infiltration of Tumor-Associated Macrophages (TAMs) which can represent 40 to 70% of the total tumor mass and could play some role as an immunosuppressive tumor stroma, in treatment resistance and in the poor prognosis of the disease. TAMs may have an immunosuppressive effect on the tumor stroma, contribute to treatment resistance, and worsen the prognosis of the disease [101]. In ATC, three histological types can be seen in any ratio or combination: sarcomatoid, giant cell, and epithelial. Immunohistochemistry Ki67 is helpful in confirming ATC and other high-risk thyroid carcinomas. Nuclear pleomorphism, tumor necrosis, increased mitosis, and infiltrative growth are important characteristics for a definitive diagnosis of ATC [102].

- **Medullary thyroid carcinoma**

Medullary thyroid carcinoma (MTC) is an uncommon neuroendocrine tumor arising from the thyroid parafollicular C cells. In 75% of cases, MTC is sporadic, and in 25% of cases, it is familial. Somatic mutations in the RET gene or, less frequently, the RAS genes are the most common cause of the sporadic form. A recent worldwide investigation has proposed a two-tiered classification system for medullary thyroid cancer. Stronger correlations have been found between high-grade pathologic features like tumor necrosis and an increased mitotic count or Ki67 proliferation index and poorer patient outcomes [103-106]. Using this method, MTCs are classified as high-grade tumors if at least one of the subsequent characteristics is present: tumor necrosis, a Ki67 proliferation index of at least 5%, and/or a mitotic count of at least five per 2 $mm^2$. The fifth edition of the WHO classification of thyroid neoplasms highlights this grading system as an independent predictor of worse outcome, independent of TNM stage, RET mutational status, and several other clinical parameters, to help identify patients at higher risk of recurrence and unfavorable outcome [105].

### 1.1.7 Diagnosis

The diagnostic workup for thyroid carcinomas involves both preoperative and postoperative pathologic and molecular evaluations. Guidelines for the diagnosis of these carcinomas recommend thyroid ultrasound in conjunction with cervical lymph node examination in patients with suspected thyroid nodules. The clinical goal of thyroid ultrasound is to identify nodules at high risk for cancer. The presence of features such as microcalcifications, irregular margins, and marked hypoechogenicity indicates an increased risk of malignancy. Existing guidelines classify thyroid nodules into risk categories based on these suspicious features and provide recommendations for biopsy. In the Thyroid Imaging Reporting and Data System (TI-RADS)

developed by the American College of Radiology (ACR), nodules were reclassified and scored based on echogenic foci, irregular margins, taller than wide shape, and the presence of calcifications and microcalcifications [107]. The risk category of the nodules was assessed according to these characteristics. The nodules were classified as benign (TR1, 0 points), very low suspicion (TR2, 2 points), low suspicion (TR3, 3 points), intermediate suspicion (TR4, 4-6 points), and high suspicion (TR5, ≥7 points). According to the guidelines, fine needle aspiration biopsy (FNAB) is recommended for nodules of 1 cm and larger with high or moderate suspicion, for nodules of 1.5 cm and larger with low suspicion, and for nodules of 2 cm and larger with very low suspicion [108]. Cytological results are classified into diagnostic categories associated with different risks of malignancy. Most malignant thyroid tumors can be identified cytologically, with some notable exceptions such as FTC and NIFTP, which are usually classified as indeterminate in various thyroid cytology reporting systems. Cytological diagnosis of PDTC is also difficult unless there is evidence of increased mitotic activity and/or necrosis [109,110]. Diagnosis with FNAB may be aided by evaluation of malignancy markers (including proteins commonly overexpressed in tumors, such as human bone marrow endothelial cell marker-1(HBME1) or galectin-3 and molecular profiling to detect specific alterations associated with malignancy (e.g., BRAF, RAS, TERT, TP53, RET mutations, and other novel genetic alterations) [111]. Resected thyroid carcinomas are classified histologically according to the World Health Organization (WHO) criteria updated in 2022.

### 1.1.8 Treatments strategy: conventional treatments and targeted therapy

There are several treatment options available to manage TCs, including surgery, which is the mainstay of treatment for most patients, except for ATC. Surgery may consist of a lobectomy, in which one lobe of the thyroid is removed, or a thyroidectomy, in which all or part of the thyroid gland is removed. If the entire gland is removed, the operation is called a "total thyroidectomy,"

while if most of the gland is removed, it is called a "subtotal thyroidectomy." After thyroidectomy, the patient's body will no longer be able to produce thyroid hormone, which is essential for regulating metabolism, so levothyroxine is needed. Moreover, treatment after thyroidectomy may include radioactive iodine therapy (RAI or I-131) [112]. It is a radioactive isotope of iodine, in which radioactive iodine is absorbed by thyroid cells throughout the body. RAI is also often used as a primary treatment for DTC after thyroidectomy. It is given to the patient in liquid or tablet form and concentrates in the thyroid cells [111]. The resulting radiation kills the malignant thyroid cells without harming the rest of the body [113]. However, the issue of the development of secondary primary malignancies following RAI continues to be debated [114]. The rate of RAI-related malignancy may vary depending on the study design and detection method. Some studies suggest a correlation between the dose of RAI and the risk of secondary primary malignancies, including leukemia [115-117]. Another treatment modality for thyroid cancer is external beam radiation therapy (EBM), which uses high-energy radiation (or particles) to destroy cancer cells or stop their growth [118]. This type of radiation therapy is usually not indicated for patients with DTC, who respond well to radioiodine treatment. However, EBM is commonly used as part of the treatment for patients with MTC and ATC and aims to mitigate symptoms and improve the quality of life for the patient.

Approximately 15% of patients with DTC progress to PDTC or ATC due to insensitivity to RAI. Therefore, several targeted drugs have emerged as promising new therapeutic options. Targeted therapy is an innovative approach in the treatment of thyroid cancer, especially in cases where the disease does not respond to conventional treatments such as surgery or radioactive iodine therapy. This therapeutic modality focuses on specific molecules and signaling pathways that are crucial for the growth and survival of tumor cells. Targeted drugs inhibit tumor cell growth through the RET/RAS/RAF/MEK/ERK and PI3K/AKT/mTOR signaling pathways to treat advanced TCs. Among these, the most studied are tyrosine kinase inhibitors (TKIs). These drugs can bind one or more tyrosine kinase receptors (TKRs), inhibiting their tyrosine kinase activity

[119]. Tyrosine kinases (TKs) are enzymes responsible for controlling mitogenic signals by phosphorylating/dephosphorylating many intracellular proteins involved in the MAPK signal transduction cascade. Therefore, the enhanced catalytic activity that is responsible for uncontrolled cell growth is the molecular rationale for the use of TKIs in the treatment of thyroid cancer. Over the past decade, several targeted drugs have been approved by the Food and Drug Administration (FDA) in the United States for the treatment of advanced thyroid cancer, including multi-targeted kinase inhibitors for radioiodine-refractory differentiated thyroid cancer (RR-DTC): lenvatinib and sorafenib, multi-targeted kinase inhibitors for MTC: vandetanib and cabozantinib, selective kinase inhibitors for MTC: selpercatinib and pralsetinib, and BRAF and MEK inhibitors for ATC: dabrafenib and trametinib. Although kinase inhibitors play an antitumor role by inhibiting aberrant hyperactivated MAPK signaling or PI3K signaling, tumor cells can reactivate these signaling pathways through some molecular mechanisms such as epigenetic alterations, driver gene mutations, and gene amplifications and thus develop drug resistance [120]. Furthermore, considering that PI3K/AKT/mTOR pathway is another important pathway in the development of thyroid tumors, other drugs have been explored. The most studied group of drugs related to this pathway in TC is that of mammalian target of rapamycin (mTOR) inhibitors. Recently, due to the limited efficacy of these compounds in the treatment of solid tumors, new drugs, like BEZ235 have been developed to act on both PI3K and mTOR [121]. The possible synergistic effects of gene amplifications, copy number increases, PIK3CA alterations and BRAF mutations suggest that a more effective outcome could be achieved by simultaneously targeting the PI3K/AKT and MAPK pathways. Another pathway highly involved in the pathogenesis and progression of thyroid cancer is angiogenesis [122]. Angiogenesis, the formation of new blood vessels, facilitates tumor growth and the spread of cancer cells to other parts of the body. It is promoted by VEGF, which is overexpressed in response to intratumoral hypoxia via hyperactivation of HIF1α [123,124]. A major target of HIF1α is the MET oncogene, which is upregulated in many thyroid tumors and promotes angiogenesis, as well as cell motility,

invasion, and metastasis [125]. Many TKIs target the VEGF receptor (VEGFR) with varying affinities, but only one of them (e.g., cabozantinib) also blocks HIF1α signaling. Another promising drug targeting angiogenesis is combretastatin A-4 phosphate (CA4P), a microtubule-depolymerizing agent [126]. This drug is closely related to colchicine, the well-known tubulin-binding agent discovered in the 1930s for its negative effect on tumor vascularization. This vessel-targeting agent, also known as fosbretabulin, impairs the function of tumor blood vessels, reduces blood flow to the tumor, and causes ischemic tumor necrosis. CA4P works through two mechanisms. First, it binds to tubulin dimers, interferes with microtubule polymerization, and causes mitotic arrest and apoptosis in endothelial cells. Second, it prevents endothelial cell migration and hinders the formation of new capillaries.

In addition to TKIs, the development of immunotherapies and immune checkpoint inhibitors, such as anti-cytotoxic T-lymphocyte-associated protein 4 (CTLA-4) and anti-programmed death 1 (PD-1) molecules, are being investigated in clinical trials for the treatment of advanced thyroid cancer [127,128]. Overexpression of PD-1 ligand 1 (PD-L1) has been documented in DTC. PD-L1 expression by tumor cells has also been linked to a higher risk of recurrence in PTC [129]. Therefore, targeting these components of the immune system may also prove useful in the treatment of TC. In a clinical study, pembrolizumab (PD-1 inhibitor) showed high tolerability in patients diagnosed with PTC or FTC who had progressed on standard therapy. Clinical trials are ongoing on different combinations with immunotherapy drugs such as the evaluation of encorafenib (BRAF inhibitor) and binimetinib (MEK inhibitor) with or without nivolumab (anti-PD-1 antibody) in patients with BRAF V600-positive metastases and RAIR-DTC [130]. To date, favorable results encourage the use of MAPK inhibitors in combination with immunotherapy. Despite innovative therapies, tumors can develop resistance to targeted drugs. In fact, over time, tumor cells further mutate and activate alternative signaling pathways, making treatment less effective. However, while further experiments and clinical trials are needed to further

demonstrate efficacy, adverse effects, and resistance issues, the targeted agent represents a promising approach for the treatment of ATC.

## 1.2 ORAL SQUAMOUS CELL CARCINOMA

### 1.2.1 Definition of OSCC

Oral Squamous Cell Carcinoma (OSCC) is the most common type of oral cancer. It arises from the squamous cells that line the mouth, lips, and throat. OSCC can affect various parts of the oral cavity, including the tongue, floor of the mouth, cheeks, gums, and palate. OSCC is the 16th most common cancer in the world with an annual prevalence of >377,000 cases, 70 % of which are men [131]. Middle-aged to elderly men are the most susceptible to OSCC, which affects more men than women [132]. The greatest incidence of OSCC is found on the posterior lateral border of the tongue, where an estimated 50% of cases occur [133]. Therefore, oral tongue tends to be the most common oral cavity subsite in OSCC patients. The deformity and functional impairments caused by OSCC, such as difficulty swallowing, speaking, and taste, significantly lower patients' quality of life.

Through lymphatic outflow, OSCC primarily invades the ipsilateral lymph nodes of the neck, though it can also invade the contralateral or bilateral lymph nodes. Metastases of OSCC usually occur in the liver, bones, and lungs [134]. Metastasis, recurrence, and resistance to treatment, are the main cause of treatment failure in OSCC patients. The variable composition of this tumor, which is made up of various cancer cell lineages, is mostly responsible for this phenomenon. Therefore, it is crucial that early disease detection be the primary focus of the fight against OSCC. Moreover, as most patients develop the disease because of risk factors, effective preventive measures are essential to the worldwide battle against OSCC.

### 1.2.2 Risk factors

The main risk factors include tobacco use (smoking and smokeless tobacco) and excessive alcohol consumption. Although risk factors act alone, they appear to work together. 75 % of oral cancer cases are linked to tobacco smoking. Tobacco smoking increases the risk of developing oral cancer six times compared to non-smokers. Alcohol drinkers are also six times more likely to develop oral cancer than non-drinkers. Users have a fifteen-fold increased risk of oral cancer compared to non-users if they consume tobacco and alcohol together [135]. In addition to tobacco and alcohol, it is important to consider other risk factors for OSCC, such as betel quid chewing, popular in Indian and Taiwanese populations, and the use of areca nut, narcotics, and cannabis [132,136]. Moreover, it was demonstrated that human papillomavirus (HPV), nutritional insufficiency, immune deficiency and hereditary conditions could lead to the development of oral potentially malignant disorders increasing the risk of developing OSCC. HPV has been linked to the development of OSCC by causing precancerous squamous intraepithelial neoplasia, which has the potential to turn malignant [137]. Oral cancer risk is also associated with inadequate nutrition, especially in the areas of plant-based foods and vitamin D [138]. Apart from people with normal physiological function, those with rare hereditary diseases like dyskeratosis congenital (DC) and Fanconi anemia (FA) and suppressed immune systems are more prone to OSCC. Persistent exposure to these risk factors results in genetic alterations, epigenetic modifications, and a dysregulated tumor microenvironment, all of which contribute to the occurrence and transformation of oral potentially malignant disorders to OSCC [139].

### 1.2.3 Molecular pathogenesis of OSCC

The molecular pathogenesis of OSCC is a complex process involving multiple genetic and molecular alterations. These changes contribute to the transformation of normal epithelial cells into malignant cells, characterized by uncontrolled growth, invasiveness, and the ability to metastasize. OSCC results from a combination of an individual's genetic predisposition and

exposure to environmental carcinogens. Individual genes and larger parts of genetic material, such as chromosomes, can be damaged by continued exposure to carcinogens [140]. Genetic damage can result in mutations or amplification of oncogenes, which promote cell survival and proliferation. General DNA hypomethylation, hyper- or hypomethylation of some genes such as cyclin D, and chromatin alterations are examples of mutations [141]. The main oncogenes are growth factor receptors, transcription factors, intracellular signal transducers, apoptosis inhibitory factors and cell cycle regulators. Upregulated oncogenic signaling pathways that promote OSCC progression include the EGFR pathway, PI3K/AKT/mTOR pathway, JAK/STAT pathway, MET pathway, and Wnt/β-catenin pathway [142]. Recently, it has been shown that among the oncogenes that transduce intracellular signal, there are RAS genes. In fact, the RAS-RAF-MEK-ERK1/2 signal represents an important pathogenic factor of OSCC. RAS activation in turn induces the phosphorylation of transcription factors that cause OSCC, such as cellular Myc (c-Myc), Erythroblast Transformation Specific 1 (ETS-1), Activator Protein 1 (AP-1) and nuclear factor of kappa light polypeptide gene enhancer in B-cells inhibitor, alpha (NF-κB). Among them, NF-κB plays a key role in the tumor microenvironment as it regulates the release of inflammatory mediators and increases the production of reactive oxygen species (ROS) and reactive nitrogen species (RNS) highly involved in the pathogenesis of OSCC [143]. Indeed, the interplay between cancer cells and their surrounding stroma, including inflammatory cells, immune cells, fibroblasts, and extracellular matrix components, significantly influences tumor growth and the response to treatment [132]. Research also underscores the importance of tumor-infiltrating immune cells in OSCC's prognosis. In an immunohistochemistry study on specimens of OSCC, Caruntu et al. reported that the density, distribution, and characteristics of the immune cells within the tumor microenvironment significantly affected patient outcomes [144]. The increased infiltration of CD8-positive lymphocytes and CD56-positive cells was independently correlated with the improved survival of patients treated for OSCC. These findings need to be further investigated, because the characteristics of the tumor microenvironment could influence

the efficacy of immunotherapy and could set the base for the optimized profiling of patients. However, different signaling pathways and tumor microenvironment may interact with each other and further contribute to OSCC progression.

### 1.2.4 Prognosis and therapeutic approaches

Prognosis is the prediction of the potential cause, duration, and outcome of the disease based on general knowledge of the pathogenesis and the presence of risk factors. The prognosis for early OSCC is generally accepted, especially for those that are well-differentiated and have not metastasized [145]. Unfortunately, most OSCCs are diagnosed when the disease is in an advanced stage. However, the prognosis for OSCC varies based on perineural invasion, staging, presence of angiogenesis and the expression of specific biomarkers [146]. In particular, the presence of marked angiogenesis has been linked to an increased likelihood of nodal metastases and may indicate that additional intensified treatment is required after surgery. Furthermore, angiogenesis in OSCC is associated with the parameters of lymph node size (T) and involvement (N), a reliable indicator of tumor recurrence. Other prognostic biomarkers of OSCC include Ras-GTPase-activating protein SH3-domain-binding protein 1 (G3BP1), B7-H6, and the sequence similarity family 3 member C (FAM3C). Patients with overexpressed G3BP1 mRNA have a lower overall survival rate. In OSCC, G3BP1, a protein belonging to the B7 family of molecules, which are involved in the regulation of immune responses, has a direct relationship with Ki67 and an inverse relationship with Cleaved-caspase 3 [147]. OSCC tissues express high levels of the B7-H6 protein compared to normal oral mucosa. This protein is related to differentiation, in fact OSCC patients with lower B7-H6 expression may have a better prognosis. In addition, FAM3C is an additional essential prognostic indicator for epithelial-mesenchymal transition (EMT) in OSCC. EMT is a process during which epithelial cells lose their apico-basolateral characteristics and acquire mesenchymal properties, including increased mobility and invasiveness. Indeed, in OSCC patients with high FAM3C expression are more likely to have a poor prognosis [148].

Regarding therapeutic interventions for OSCC, treatments include surgery followed, if necessary, by postoperative radiation therapy or chemotherapy. In most cases, surgery is the first-line treatment for oral cancers. Inadequate removal of tumor cells increases the likelihood of local and regional recurrence, thus decreasing long-term survival rates. The goal of surgical resection is to remove sufficient tumor tissue. In advanced cases, postoperative radiation therapy, chemoradiation, oncogene-targeted therapy, and immunotherapy may be administered [149]. Because irradiated tissue cannot be surgically removed, radiation therapy is usually administered postoperatively. Regeneration is less effective when the tissue is fibrous. The size of the primary tumor, positive surgical margins, and the presence of perineural, lymphatic, and vascular invasion determine whether radiation therapy should be given to the primary site. Treatment of the neck to prevent the possibility of metastasis and recurrence, especially in lymph nodes with extracapsular dissemination, is also common [150]. Recently, chemotherapy is becoming an adjunctive treatment for locally advanced OSCC. Although chemotherapy is not considered a curative treatment for oral cancers, it can be given before surgery or in conjunction with radiation before or after surgery. Additionally, immunotherapy is an alternative treatment that has shown promise in the management of OSCC. Anti-PD-1/PD-L1 agents have promoted an immune response against tumors by blocking immune checkpoint suppression signals [151]. In particular, multi-cytokine biological preparations derived from homologous cells are being studied and have demonstrated efficacy against tumor inflammatory cytokines [152]. However, despite progress, the development of new therapeutic approaches for the treatment of OSCC remains a key goal of oncology research.

## *2. KRAS ONCOGENE AND HUMAN HEAD AND NECK CANCER*

### 2.1 Ras family

The RAS family of monomeric GTPase proteins is a gene family often mutated in tumors. It is present in all eukaryotes and carries out numerous crucial physiological functions such as proliferation, differentiation and cell death [153]. It was initially identified in the 1960s by Harvey and Kirsten as a retroviral oncogene when sarcomas were induced in rodents from a murine leukemogenic virus preparation; hence it's named- Kirsten rat sarcoma 2 viral oncogene homolog [154] (Figure 5).

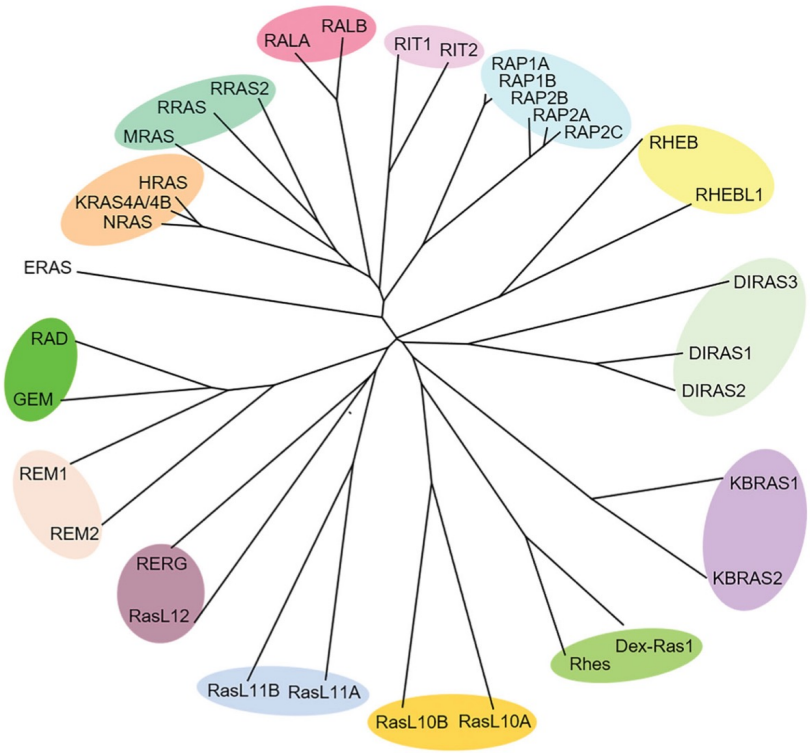


**Figure 5.** Members of the RAS family [154].

In mammals, this family includes three major protooncogenes: Harvey (H)-ras, Kirsten (K)-ras, and Neuroblastoma (N)-ras, identified over a quarter of a century ago due to their frequent oncogenic activation in human tumors. They are the founding members of the largest superfamily

of monomeric small G proteins, which includes over 150 small GTPases divided into at least five subfamilies (RAS, RHO/RAC, RAB, ARF and RAN) based on primary sequence [155]. The KRAS gene produces, through alternative splicing of exon 4, two proteins: KRAS4A and KRAS4B. The mRNA level for the 4B isoform is higher than that for the 4A isoform, so KRAS4B is often simply called KRAS. The three human RAS genes share a common structure: a first noncoding exon and four coding exons. Introns vary in size and sequence but have conserved splice sites. The HRAS, NRAS and KRAS proteins weigh 21 kDa and contain 189 amino acids, except the KRAS4A isoform which has 188 [156]. The protein products show almost 100% homology in the first 165 N-terminal amino acids, where the catalytic site and the effector interaction domain are located, but differ in the 25 C-terminal residues, which represent the hypervariable region (HVR). The HVR region ends with a CAAX motif (C= cysteine, A= aliphatic amino acid). For the KRAS4B isoform, the polybasic domain of six lysines (175-180) in the HVR region is involved in trafficking control and membrane anchoring via electrostatic interactions with anionic phospholipids of the inner membrane [157]. The three RAS isoforms localize to specific membrane microdomains based on the type of lipid anchor. This differential localization has important consequences on the activation of downstream signaling pathways and could explain the different biological effects of RAS on proliferation, survival, cell differentiation and cytoskeletal modifications. The palmitoyl groups of HRAS and NRAS mediate a strong association with lipid rafts, membrane regions rich in sphingolipids, glycolipids and cholesterol. Furthermore, it seems that HRAS is in a dynamic equilibrium between lipid rafts and non-raft microdomains and that binding to GTP. This change in localization appears necessary for the activation of downstream effectors. NRAS, however, appears to move in the opposite direction compared to HRAS when activated [158]. KRAS is normally localized outside the lipid rafts and the absence of hydrophobic acyl groups facilitates its movement from the intracellular organelles to the plasma membrane, via a Golgi-independent mechanism (still not well understood), contrary to what happens for H-RAS and N-RAS [159]. The release of K-RAS

from the plasma membrane is driven by phosphorylation at amino acid residues in the polybasic region. Phosphorylation at serine 181, mediated by the protein kinase C (PKC), promotes the localization of the protein in the outer membrane of the mitochondria, triggering apoptosis. These posttranslational modifications influence the interaction of different RAS isoforms with downstream effectors, determining the specific function of each isoform [160]. All RAS proteins can bind and hydrolyze GTP. The membrane-associated protein RAS is inactive when binding GDP, while it is active when binding GTP. The exchange occurs thanks to the SOS-1 protein, which stimulates the dissociation of GDP. The RAS protein has a weak intrinsic GTPase activity that allows it to hydrolyze GTP into GDP; this activity is significantly accelerated by the GAP protein (GTPase activating protein) [161]. An activation and deactivation cycle are thus formed.

## 2.2 KRAS structure and function

KRAS is a 21 kDa monomeric GTPase on the membrane. It has a conserved domain, known as the G domain (residues 1–165), and a less conserved domain on the C tail, known as the hypervariable domain (residues 166–188) [162]. KRAS consists of five helices (2-1) and six sheets. The GTPase has two switches: switch I (residues 30–38) and switch II (residues 60–76). These switches undergo significant conformational changes when the guanine nucleotide changes from GTP to GDP or vice versa [163]. During its GDP-bound (inactive) and GTP-bound (active) states, the phosphate-binding ring (P-ring, residues 10–17) of KRAS participates in the induction of conformational change. The γ-phosphate of GTP interacts with tyrosine (Tyr) 32 and threonine (Thr) 35 residues of the switch region I. Furthermore, the conserved Gly 60 in the switch region II interacts with the γ-phosphate. The C-terminal Cys-A-A-X motif, where A is isoleucine, leucine, or valine and X is methionine or serine, is in the KRAS HVR region. The C-terminal Cys-A-A-X motif of KRAS undergoes several post-translational modifications (PTMs) that facilitate its trafficking to the inner surface of the plasma membrane [161] (Figure 6).

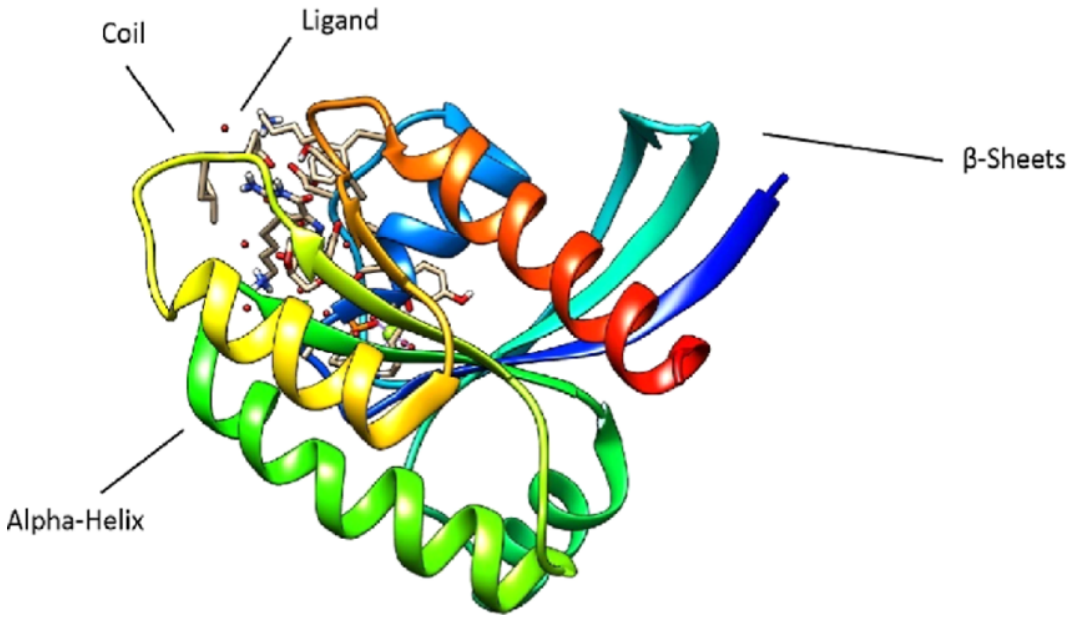


**Figure 6.** Crystal structure of KRAS [164].

Like all RAS proteins, KRAS is synthesized as a biologically inactive cytosolic propeptide (Pro-RAS). The first modification of this propeptide is catalyzed by Farnesyltransferase (Ftase) and involves the covalent addition of the 15-carbon Farnesyl group (C-15) from Farnesyl Diphosphate (FDP) onto the cysteine residue of the CAAX sequence [165]. Subsequently, the -AAX sequence is cleaved by a CAAX protease which converts CAAX endopeptidase 1 also known as RAS converting enzyme 1 (RCE1). This is followed by methylation of the carboxy-prenylated cysteine residue via isoprenylcysteine carboxyl methyltransferase (ICMT). Finally, palmitoyl transferase (Ptase) catalyzes the addition of palmitic acid (a 16-carbon fatty acid) to upstream cysteine residues. These modifications to KRAS enhance the proteins' hydrophobicity and anchoring to the plasma membrane, and membrane-anchored K-RAS proteins cycle between the active GTP-bound form and the inactive GDP-bound form [166]. The associated conformational changes of KRAS serve as master moderators of many signaling pathways involved in various cellular processes. K-RAS is involved in the regulation of cell differentiation through the MAPK kinase cascade and in cell survival through the PI3K

pathway, which, once activated, activates the AKT signaling pathway, which promotes cell survival by preventing apoptosis (programmed cell death). Furthermore, KRAS plays other physiological roles such as cellular response to various external stimuli, including growth factors and stress signals. In fact, by interacting with tyrosine kinase receptors such as epidermal growth factor receptor (EGFR) and platelet-derived growth factor receptor (PDGFR), it activates pathways that modulate the cell's response to environmental stimuli. Furthermore, K-RAS affects cytoplasmic organization and cytoskeletal dynamics, playing a role in cell morphology and motility. These processes are essential for cell movement and interaction with the surrounding environment. However, when mutated, K-RAS can become an oncogene and contributes to the formation and progression of numerous types of cancer [167].

## 2.3 Oncogenic K-RAS signaling pathways

Oncogenic mutations in KRAS primarily occur at residues G12, G13, and Q61. Due to these mutations, KRAS is unable to hydrolyze GTP to GDP, which keeps it perpetually "ON" and triggers downstream signaling that leads to cellular transformation. KRAS-associated signaling pathways persistently activated in many tumors participate in cell growth and proliferation, differentiation, protein synthesis, glucose metabolism, cell survival, and inflammation. KRAS is activated by GEF proteins such as: SOS1 and SOS2 (two sons of Sevenless 1 and 2), GRB2 (growth factor receptor-related protein 2), RASGRF2 (guanine nucleotide releasing factor specific for the Ras protein 2) or Ras-GRP (Ras guanine nucleotide releasing protein). In turn the GEF proteins are activated upstream by transmembrane receptors G protein-coupled receptors (GPCRs) and receptor tyrosine kinases (RTKs) such as EGFR or PDGFR [168]. Indeed, when a signaling molecule binds to a receptor tyrosine kinase it dimerizes and activates its kinase activity. Phosphorylated RTK are recognized by the Src homology 2 (SH2) domain of an adapter protein GRB2 which, in turn, recruits GEF protein via an SH3 domain [169].

Finally, GEF, by interacting with RAS and stimulating GDP/GTP exchange, modifies its conformation, making it capable of interacting with its effectors and activating numerous downstream pathways. KRAS-dependent human oncogenesis is characterized by some effector pathways such as the Raf-MEPK -ERK pathway, PI3K-Akt-mTOR pathway and Ral selective guanine nucleotide exchange factors (Ral-GEF) pathway (Figure 7).

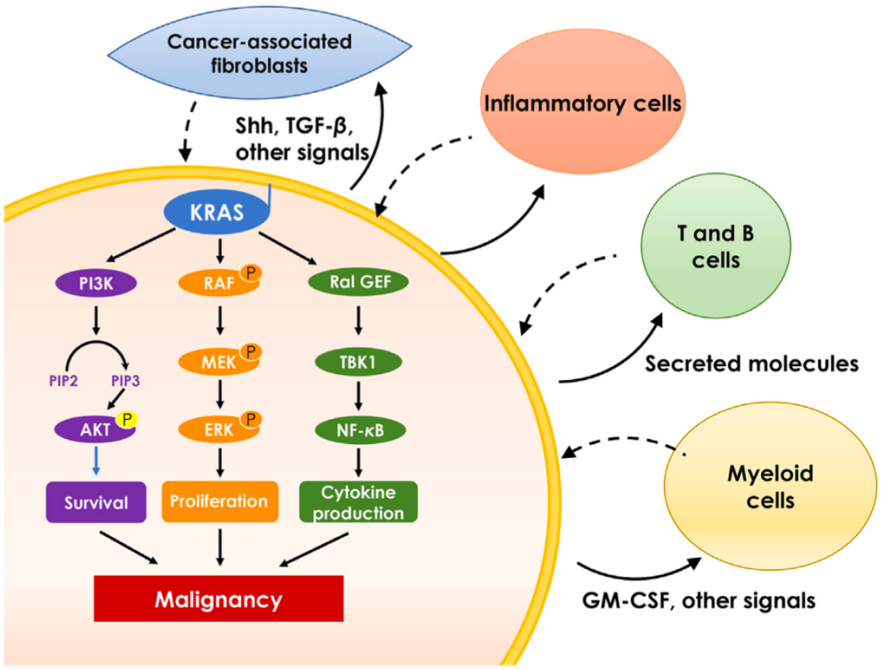


**Figure 7.** The principal effector pathways of KRAS. Intracellular PI3K, MAPK, or RAL-GEF pathways are triggered by oncogenic KRAS in order to enhance cell viability, proliferation, and cytokine release. In turn, these stroma cells encourage the malignancy of cancer [170]

### 2.3.1 Raf-MEPK-ERK Pathway

The Raf/mitogen-activated protein kinase (MEK or MAPK)/ERK pathway is a well-characterized KRAS-associated pathway that leads to cell growth, suppression of cell death, cell cycle progression, invasiveness, and induction of angiogenesis. This pathway is activated by stimulation of membrane RTKs. Specific receptors respond to ligands such as growth

factors, such as fibroblast growth factor (FGF) or EGF [171]. After binding of the ligand to the receptor, the receptor dimerizes and autophosphorylates, which leads to signal transduction in the cell. Its intracellular signaling begins with the recruitment of GRB2 to the phosphorylated site of the receptor and subsequent binding of SOS to GRB2. SOS, which is a GTP exchange factor, allows the activation of K-Ras-GDP to K-Ras-GTP. SOS is divided into SOS1 and SOS2. Although the structures of the two are highly homologous, current research demonstrates that the function of SOS1 is stronger than that of SOS2 in controlling cell proliferation and migration [172]. Following KRAS/SOS1 interaction, activation and dimerization of RAF, a member of a family of serine/threonine (Ser/Thr) kinases, occurs. Subsequently, RAF stimulates mitogen-activated protein kinases 1 and 2 (MEK1 and MEK2), which in turn activate downstream extracellular signal-regulated kinases 1 and 2 (ERK1 and ERK2). MEK1 and MEK2 belong to the dual-specificity kinase (DSK) family, which phosphorylate Tyr and Ser/Thr residues within the activation loop of their substrate MAP kinases, and these phosphorylation depend on the phosphorylation of serine 218 and 222 in their segments of activation by the RAF [173]. Activated MEKs directly interact with ERK which then translocates to the nucleus, where it phosphorylates and activates various transcriptional factors, including the ternary complex factor (TCF) Elk-1 and the serum response factor accessory proteins Sap-1a, Ets1, c- Myc and Tal. These activations upregulate immediate-early c-Fos protein expression, allowing cell cycle progression through G0/G1 mitogenic signals.

### 2.3.2 PI3K-Akt-mTOR Pathway

PI3-K, which is activated by a variety of pathways, is the second most well-characterized Ras effector [174]. PI3K is important for the detection of tumors with mutant profiles guided by the KRAS because it regulates cell growth, entry into the cell cycle, cell survival, cytoskeleton, reorganization, and metabolism. The PI3K isoforms are classified into three classes based on

their structural and biochemical characteristics. The Class I PI3K are heterodimers that contain one of four catalytic subunits (p110) (p110α (PI3CA), p110β (PIK3CB), p110γ (PIK3CG), and p110δ (PIK3CD)) and one regulatory subunit (p85α, p85β, p55γ, p101 e p84). There are three isoforms of the class II PI3K: PI3K-C2α (PIK3C2A), PI3K-C2β (PIK3C2B), and PI3K-C2γ (PIK3C2G). The class III PI3K contains two subunits: a regulatory subunit (Vps15) and a catalytic subunit (Vps34). Members of the PI3K family are activated by RTKs or GPCRs at the plasma membrane. The binding of extracellular growth factor to its receptor tyrosine kinase, which causes the receptor monomer to dimerize and then autophosphorylate [175]. Subsequently, the catalytic site of the phosphorylated dimer is bound by Insulin Receptor Substrate-1 (IRS-1). After attaching itself to the dimer, IRS-1 acts as PI3-K's binding and activation site. Direct binding of PI3-K with GTP-bound Ras is a completely distinct mechanism of PI3-K activation. Phospholipidinositol bisphosphate (PIP2) is phosphorylated to phosphatidylinositol (3,4,5) trisphosphate (PIP3) by the activated PI3-K, which then migrates to the inner aspect of the cell membrane and activates a protein kinase AKT [174]. Once activated, AKT mediates cell growth and survival by phosphorylation of mTOR (mammalian serine/threonine kinase target of rapamycin), which acts in two functionally distinct complexes, namely the RAPTOR-associated mTOR complex 1 (mTORC1) and the mTOR complex associated with RICTOR 2 (mTORC2). Recently, it was reported that mTORC2 and Akt constitute a positive feedback loop through phosphorylation of the mTORC2 subunit SIN1 (stress-activated protein kinase interacting protein 1), and phosphorylation of this subunit leads to phosphorylation of Akt serine (Ser) 473 [176].

### 2.3.3 The RalGEF-Ral Pathway

The Ral- GEF pathway is the third best characterized effector of KRAS-dependent human oncogenesis. Like RAS, Ral proteins (RalA and RalB) are small GTPases that cycle between

an inactive, GDP-bound state and an active, GTP-bound state. However, the GTPase Ral depends on RALG-EF and GTPase activating proteins (RALGAP) to catalyze GDP–GTP exchange due to its weak intrinsic GTPase activity. Mutated KRAS activates RalGEFs, leading to the formation of the GTP-bound active state of Ral GTPases. Activated Ral GTPases stimulate a broad spectrum of downstream effectors and regulate their activations. RAL signaling activates the transcriptional activity of nuclear factor-κB (NfκB) via TANK-binding kinase 1 (TBK1) [177]. Indeed, active TBK1 phosphorylates and promotes the nuclear localization and activation of NfκB that plays important roles in proliferation, survival, metastasis, reorganization of the actin cytoskeleton, regulation of transcription and intracellular membrane trafficking [178].

## 2.4 Role of K-RAS signaling in ATC

Activated KRAS family oncogenes have been identified in a wide range of solid tumors and malignancies, especially lung and colon carcinomas. However, a very high frequency of KRAS oncogene activation has recently been highlighted also in TCs, particularly in ATC. Indeed, a key role for abnormalities in RAS/Raf-MAPK signaling in ATC tumorigenesis has been established. Downstream of KRAS there are multiple signal transduction pathways responsible for executing RAS-mediated cellular effects. The most widely validated ones that contribute to ATC tumorigenesis include Raf-MAPK [179]. Indeed, constitutive activation of the K-RAS/MAPK signaling pathway is frequently observed in various histological subtypes of ATC.The mutation causes the KRAS protein to remain permanently active, promoting uncontrolled cell growth and contributing to the formation of tumors. The most representative proteins of this pathway and also the most important players are RAF, MEK and ERK. They are involved in various cellular programs such as differentiation, proliferation and apoptosis [180].. Recent genomic studies of thyroid tumors have identified mutually exclusive activating

mutations in proteins of this pathway. Genome analyses using next-generation sequencing have found that activating KRAS mutations and $BRAF^{V600E}$ mutation are the most common driver mutations in ATC. In fact, mutations of the RAS gene family (NRAS, HRAS and KRAS) represent the majority (about 70%) of all mutated cases, especially in indeterminate cytology, and can be observed in histologically benign and malignant thyroid nodules [181]. Actually, the malignancy risk associated with KRAS mutations has been reported to range from 23 to 76% [182,183]. However, besides KRAS mutation, other factors may contribute to its hyper-activation in thyroid tumors. These include hyperactivation of growth factor receptor tyrosine kinases and over-expression of RAS scaffold proteins that may lead to chronic KRAS activation. Among these most common aberrations in thyroid tumors are EGFR mutations, which cause constitutive activation of the receptor that acts upstream of KRAS [17]. Furthermore, it has been previously shown that galectin-3 (Gal-3) acts as a selective intracellular scaffold of KRAS. Gal-3 is an extracellular marker that acts as a β-galactoside binding protein [184], while intracellularly it acts as a scaffold of the KRAS protein. Gal-3 acts as a driving force for K-Ras nanoclustering and increases its signaling [185]. Ran Levy et al. demonstrated that overexpression of Gal-3 in tumor cells increases KRAS signal output. An important finding was that relatively high levels of Gal-3 expression can be detected in TCs, whereas relatively low levels of Gal-3 are detected in benign tumors or normal glands [186,187]. Therefore, the increase in KRAS is not only mediated by gene mutations but also by other mechanisms. However, KRAS hyperactivation in TCs leads to a significant alteration of the RAS-Raf-MAPK-ERK pathway. In particular, the p38-MAPK pathway activated by KRAS can usually have a dual role in cancer as it can promote or inhibit tumor development depending on the cellular context [58]. However, in the context of aggressive tumors such as ATC, p38-MAPK promotes survival, invasion and metastasis [188,189]. Furthermore, once activated p38-MAPK promotes the activation of p-ERK which leads to the transcription of genes involved in cell division. In fact, when aberrantly activated, p-ERK promotes cell differentiation and survival,

contributing to the oncogenic phenotype [190]. Based on these evidence, K-Ras inhibitors could be considered as a potential targeted therapy for highly malignant thyroid carcinomas.

## 2.5 Role of KRAS signaling in OSCC

In the context of OSCC, the KRAS is one of genetically altered oncogene. The first study of activation of the RAS genes in OSCC has been reported in oral cancer cell lines by Tsuchida and his group in 1989 [191]. To date, more than 40 independent studies on genetic alterations of RAS oncogenes in OSCC have been reported [192]. Indeed, RAS is the most frequently mutated gene in OSCC with 20% of cases [192]. The etiology of OSCC is explained by hyperactive mitogenic signaling caused by amplification of the wild-type KRAS gene in HNC, which in turn causes increased tumor proliferation and survival [193]. Activated KRAS facilitates several signaling cascades, including activation of RAL signaling that activates the NfκB pathway (Figure 8). NF-κB is a nuclear transcription factor that is present in cells and participates in functions such as proliferation, survival, and apoptosis. Activated following activation of the KRAS pathway, NfκB is closely related to inflammation and immunoregulation of OSCC. Some downstream effectors of NF-κB include chemokines and cytokines that contribute to tumor growth by stimulating inflammatory cell infiltration into the tumor microenvironment and angiogenesis markers [194]. In addition, NF-κB has been found to suppress the apoptotic potential of chemotherapeutic and radiotherapy agents, linking it to chemoresistance. NF-κB is also responsible for the increased expression of matrix metalloproteinase (MMP)-degrading enzymes in many tumors. This may be related to the ability of tumors to metastasize through the breakdown of supporting structures. Thus, the KRAS gene regulates cell proliferation, mutation, and apoptosis. The KRAS pathway can regulate the downstream silk/threonine protein Akt by regulating the p110 subunit of PI3K. Activation of this pathway promotes protein synthesis and vascular endothelial growth factor secretion and inhibits cell apoptosis,

contributing to the progression of OSCC [195]. Therefore, based on these evidences, KRAS protein could be a potential target to achieve an effective molecular therapy for OSCC.

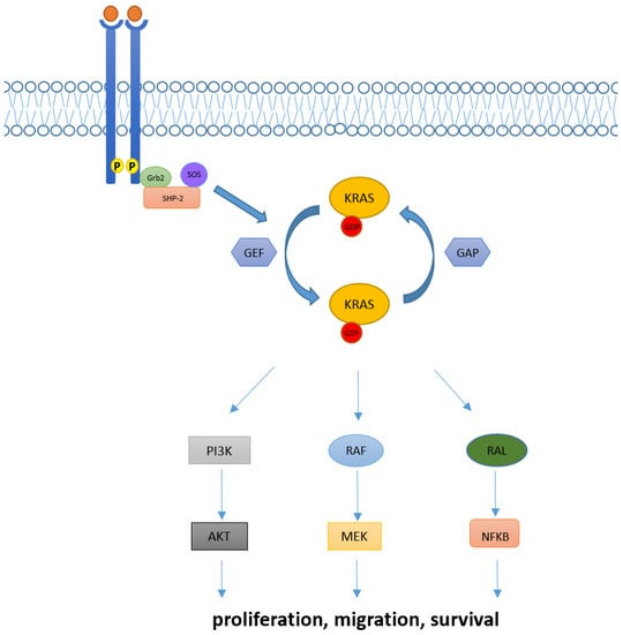


**Figure 8. KRAS signaling pathway.** The RAS GTPase protein is involved in transmitting cell proliferation and survival signals from cell surface growth factor receptors. Activated KRAS triggers several signaling pathways including PI3K, RAF and RAL that are implied in the regulation of cellular proliferation, migration, and death [196].

# 3. SOS1–KRAS INTERACTION INHIBITOR BAY-293

Based on the comprehensive understanding of the molecular pathways involved in KRAS activity, various attempts have been made in the past decades to block the oncogenic activity of KRAS. However, direct inhibition of KRAS has been a significant challenge due to the picomolar affinity of KRAS protein for guanine nucleotides, the abundance of GDP and GTP in the micromolar range, and the absence of favorable binding sites for small molecules on the surface of K-RAS protein [197]. Consequently, several strategies have been developed to target the downstream signaling pathways of KRAS associated with its tumor-inducing effect. In recent years, a breakthrough has been made in the development of molecules that may offer a promising alternative as they allow inhibition for any KRAS variant [198]. In this regard, an interesting approach to target KRAS and its interaction with GTP loading is through the SOS1 protein. SOS1 can not only promote the production of active GTP-bound K-RAS at the catalytic site but also enhance its GEF function allosterically. Indeed, inhibition of the direct interaction of SOS-1 with K-RAS could have several advantages over other indirect approaches to suppress KRAS signaling [199,200]. In this context, a small molecule inhibitor known as BAY-293 has been recently developed. This compound is a novel synthetic molecule that selectively inhibits KRAS-SOS1 interaction and is highly attractive for its pan-RAS inhibition regardless of the type of KRAS mutations [201].

## 3.1 Chemical and Physical Properties

BAY-293 is a 6,7-dimethoxy-2-methyl-N-[(1R)-1-[4-[2-(methylaminomethyl)phenyl]thiophen-2-yl]ethyl]quinazoline-4-amine with a molecular weight of 448.6 g/mol (Figure 9). It is a selective and potent inhibitor of KRAS–SOS1 interaction with an IC50 of 21 nM. To elucidate the mechanism of action, a series of biophysical assays such as isothermal titration calorimetry

(ITC) and native mass spectrometry (native MS) were performed. These analyses showed that the Kd (dissociation constant describing the affinity between two molecules) of BAY-293 had values of 18 nM which were consistent with the IC50 data obtained from the KRAS–SOS1 interaction assay [200,201]

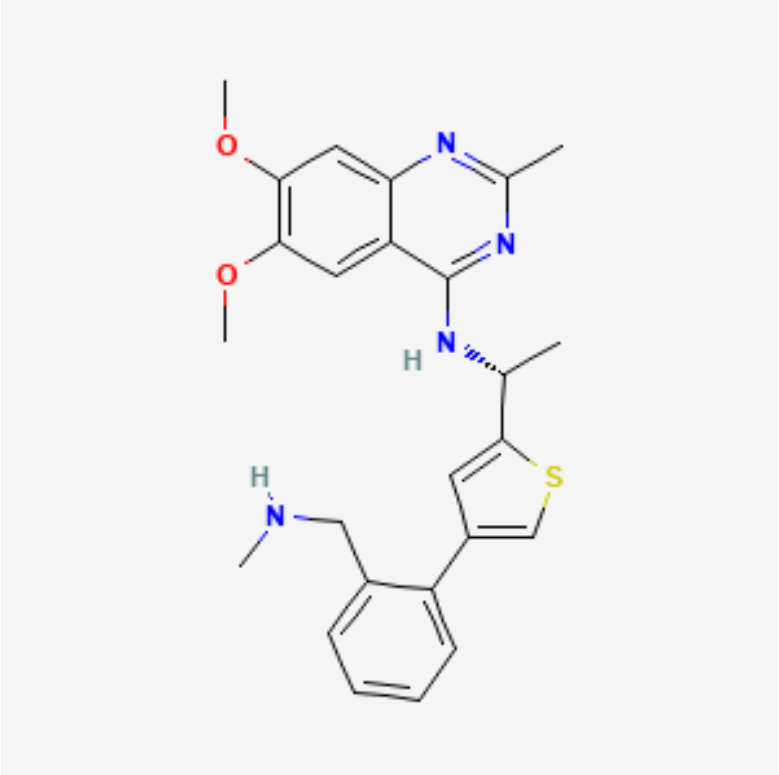


**Figure 9.** BAY-293 chemical structure.

### 3.2 Interactions and Pathways

BAY-293 was shown to inhibit K-RAS activation in HeLa cells, with IC50 values in the submicromolar range, and showed efficient antiproliferative activity against wild-type K-RAS cell lines (K-562, MOLM-13) and KRASG12C mutant cell lines (NCI-H358, Calu-1) [200]. In addition, this compound effectively inhibited p-ERK levels in K-562 cells, without having any effect on total ERK protein levels, thus reducing cell proliferation. What is quite interesting is that SOS1 inhibition shows a synergistic antiproliferative potential when combined with covalent direct inhibitors of KRASG12C (e.g., combined with ARS-853 in a KRASG12C mutant cancer

cell line) [202]. Furthermore, an *in vitro* study on pancreatic cancer cells demonstrated that BAY-293 effectively inhibited cell proliferation by blocking KRAS activation and reducing the phosphorylation of downstream effectors such as MAPKs [24]. The same study demonstrated that BAY-293 induced apoptosis in some pancreatic cancer cell lines, by increasing cleaved poly (ADP-ribose) polymerase (PARP) (a marker of cell apoptosis), thus suggesting another possible antitumor mechanism of this molecule. Roman C. Hillig et al. further demonstrated that in Hela tumor cells with wild-type K-RAS, BAY-293 completely inhibited the RAS-RAF-MEK-ERK pathway [201]. Despite the studies conducted, there are few in-depth studies of BAY-293 in the scientific literature to date, which limits our complete understanding of its mode of action. BAY-293 is a compound that has shown potential as a kinase inhibitor, but it is important to recognize that the cellular signaling pathways it affects may be numerous and complex. For this reason, further research is needed that analyzes in detail the different signaling pathways that BAY-293 may affect. Additionally, a deeper understanding of the mechanisms of action of BAY-293 could help identify potential side effects or interactions with other metabolic pathways, thus allowing for the targeted use of this compound in the treatment of cancer.

## *4. AIM OF THE THESIS*

Over the past decades, numerous scientific evidence has demonstrated a significant tumorigenic role of KRAS in HNC. Among these tumors, those with the highest incidence rate and greatest malignancy are ATC, an HNC belonging to endocrine tumors, and OSCC. To date the KRAS pathway is blocked only by inhibitors of upstream or downstream marker proteins; however, due to tumor cells mutation and activation of alternative signaling pathways, these inhibitors have proven ineffective. ATC is a complex, multigenic KRAS mutational tumor with evident tumor heterogeneity. Therefore, targeting KRAS could has great advantages. However, because of the numerous mutations in KRAS gene, it is difficult to develop specific compounds that act on each allele of the specific mutation. Similarly, recent *in vitro* and *in vivo* studies have demonstrated increased levels of expression of KRAS genes that play an important role in the development and progression of OSCC. However, selective inhibition of KRAS protein has never been investigated in OSCC. Recently, a new potential pharmacological approach has been discovered to inhibit KRAS protein by blocking its interaction with its primary regulator, SOS-1. In this context, a new small molecule known as BAY-293 has been developed, able to selectively inhibit KRAS-SOS-1 interaction and has demonstrated an antiproliferative effect in some tumor cell lines. The main innovation of BAY-293 lies in its targeting, as it is able to target all KRAS mutation variants, thus overcoming the problem of selectivity towards a single mutation. Therefore, based on this scientific evidence, the aim of this project was to investigate, for the first time, the effect of BAY-293 in the context of ATC. This evaluation was conducted through both *in vitro* and *in vivo* ATC models and aimed to specifically investigate the KRAS/SOS1/MAPK signaling pathway, apoptosis, and cell proliferation and corroborate the efficacy of this inhibitor. In addition, to better understand the mechanism of BAY-293, it was examined in an *in vitro* model of OSCC, with particular attention to the analysis of the NF-κB pathway, tumor inflammation, as well as the study of the apoptotic pathway and angiogenesis markers. Given the limited treatment options and drug resistance challenges in ATC and OSCC, there is a growing interest in finding new possible drug

targets to suppress or reverse the early stages of carcinogenesis. Therefore, this research, exploring KRAS-SOS1 inhibition, using BAY-293, as a novel pharmacological approach, could represent a significant advance in the therapy of aggressive tumors such as ATC and OSCC.

# *5. MATERIALS AND METHODS*

## 5.1 Materials

BAY-293 was provided by Sigma-Aldrich Company (Milan, Italy; cat. SML2703). Every chemical used was of the best commercial grade possible. Nonpyrogenic saline (0.9% NaCl; Baxter Healthcare Ltd., Thetford, Norfolk, UK) was used to make all stock solutions.

## 5.2 *In vitro* TC studies

### 5.2.1 Cell cultures

Human FTC cell line, FTC-133, human PTC cell line, K1 and human ATC cell line, 8305C were acquired from ATCC (American Type Culture Collection, Rockville, MD, USA). The culture media used for the TC cells was RPMI-1640 (Sigma-Aldrich, St. Louis, MO, USA cat. R8758), which was enhanced with 10% fetal bovine serum (FBS, Life Technologies, Gibco®; Carlsbad, CA, USA), 100 U/ml of penicillin, and 100 µg/ml of streptomycin (Sigma-Aldrich® Catalog No. P4333; St. Louis, MO, USA). Every cell line was maintained in incubators at a temperature of 37 °C and 5% $CO_2$.

### 5.2.2 Cell viability (MTT Assay)

Tetrazolium dye (MTT) (M5655; Sigma-Aldrich), a mitochondria-dependent dye for living cells, was used to assess the cell viability of FTC-133, K1, 8305C cells and CAL-27 cells. Cells were plated at a density of $4 \times 10^4$ cells/well on 96-well plates. Following a 24-hour period, BAY-293 was applied to cells at progressively higher doses of 1 µM, 10 µM, 25 µM and 50 µM, dissolved in dimethyl sulfoxide (DMSO) for a whole day. Following a 24-hour incubation period at 37°C with MTT (0.2 mg/mL) for one hour. Cells were lysed using 100 µl of DMSO and the optical density at 540 nm (OD540) was measured to determine the degree of reduction of MTT to formazan [203].

### 5.2.3 Experimental groups:

1. Control group (CTR): TC cell lines, FTC-133, K1 and 8305C;
2. BAY-293 1 μM group: FTC-133, K1 and 8305C cells were treated with BAY-293 1 μM for 24 hrs;
3. BAY-293 10 μM group: FTC-133, K1 and 8305C cells were treated with BAY-293 10 μM for 24 hrs;
4. BAY-293 25 μM group: FTC-133, K1 and 8305C cells were treated with BAY-293 25 μM for 24 hrs;

We limited our research to BAY-293 concentrations of 1 μM, 10 μM, and 25 μM, as these were found to be the lowest concentrations with the greatest cytotoxic effect according to the MTT experiment. Furthermore, as BAY-293 had comparable effects on cell survival across all three cell lines, we opted to focus our analysis solely on the 8305C cell line, which is one of the most widely utilized cell lines in the ATC area and the most commonly used cell line in experimental mice models of orthotopic thyroid carcinoma [204,205].

### 5.2.4 Western Blot Analysis

The methodology for the Western blot analysis was as previously reported [206]. To prepare cell lysates, 8305C cells were twice washed in ice-cold phosphate buffered saline (PBS), collected, and then resuspended in lysis buffer that contained a protease cocktail of inhibitors (Catalog No. 11836153001; Roche, Switzerland), 150 μl of NaCl, 10 mM NaF, and 20 mM Tris-HCl pH 7.5. Cell lysates were centrifuged at 12,000 rpm for 15 minutes at 4 °C after 40 minutes. Using bovine serum albumin as a standard, the Bio-Rad protein assay (Bio-Rad Laboratories, Hercules, CA, USA) was used to quantify the protein concentration. Following a 5-minute heating period to 95 °C, the samples were separated into equal volumes of proteins using 10%–15% sodium dodecyl sulfate–polyacrylamide gel electrophoresis (SDS-PAGE) and then transferred to a

polyvinylidene difluoride (PVDF) membrane (Immobilon-P, catalog # 88018; ThermoFisher Scientific). Anti-PTEN (1:500; sc-7974; Santa Cruz Biotechnology) and anti-SOS1 (1:500; sc-17793; Santa Cruz Biotechnology), anti-p-p38 MAPK (1: 500; Santa Cruz Biotechnology, Dallas, TX, USA; sc- 166182), p38 MAPK (1: 500; Santa Cruz Biotechnology, Dallas, TX, USA; sc-7972), anti-pERK(1: 500; Santa Cruz Biotechnology, Dallas, TX, USA; sc-7383), ERK (1: 500; Santa Cruz Biotechnology, Dallas, TX, USA; sc-514302), β-Catenin (1: 500; Santa Cruz Biotechnology, Dallas, TX, USA; sc-7963), anti-BID (1:500; sc-11423; Santa Cruz Biotechnology), anti-BAX (1:500; sc-20067; Santa Cruz Biotechnology) and anti-p53 (1:500; sc-126; Santa Cruz Biotechnology ) were the primary antibodies utilized. Dilutions of the antibodies were prepared in PBS, 5% w/v milk powder, and 0.1% Tween-20 (PMT), the membranes were incubated at 4° C for a whole night. After that, the membranes were treated for one hour at room temperature with a secondary antibody (1: 2000; Jackson ImmunoResearch, West Grove, PA, USA). Additionally, we used β-actin antibody (cytosolic fraction 1: 500; sc-47778; Santa Cruz Biotechnology) to guarantee that equivalent amounts of protein lysate have been loaded. Enhanced chemiluminescence (ECL) detection system mixture (Thermo Fisher, Waltham, MA, USA) was used to detect the signals.

### 5.2.5 Wound healing assay (Scratch test)

The impact of BAY-293 on the migration of 8305C cells was assessed using the previously published Wound Healing Assay (Scratch test) [207]. To obtain a confluent monolayer, $2 \times 10^6$ 8305C cells were plated on 60 mm plates (Corning Cell Culture, Tewksuby, MA, USA). A straight line was created by scratching the cell monolayer 24 hours later with a P200 pipette tip. Following, cells were washed in Phosphate Buffered Saline (PBS) to remove debris from each plate and were subjected to 24 hours of treatment with BAY-293 at increasing doses (1 μM, 10 μM, and 25 μM). In contrast, standard culture media was employed in the control group. In order to document the extent of the wound and, consequently, the cell migration capacity, phase contrast

microscopy images of every plate were taken at 0 and 24 hour. *I*mage *J* software was used to calculate the cell migration rate.

### 5.2.6 Colony formation assay

To perform the colony formation assay, 1,000 8305C cells were cultivated on six-well plates and exposed to of BAY-293 treatment at the concentrations of 1 μM, 10 μM, and 25 μM, or solvent alone as a control. Following a 24-hour treatment period, RPMI-1640 media supplemented with 10% FBS was added to the wells. After an incubation period of 10 days, the cells underwent two PBS washes before being stained with 0.1% (w/v) crystal violet. Using a bright-field microscope, the stained cells were photographed (Zeiss) [208].

### 5.2.7 DNA fragmentation assay

Induction of apoptosis was analyzed by detection of DNA fragmentation performed by agarose gel electrophoresis, using the 8305C cells. Briefly 1.5 x $10^6$ cells were plated and treated with BAY-293 for 24 hours. Then the DNA was extracted using (REDExtract-N-Amp Tissue PCR Kit, XNAT-100RXN) according to the manufacturer's instructions. After, electrophoresis was performed for 30 min at 100 V through 2% agarose gel. The gels were photographed under ultraviolet light [209].

## 5.3 *In vivo* TC studies

### 5.3.1 Animals

For in vivo studies BALB/c nude male mice (25-30 g; 6-8 weeks of age) were used and purchased from Envigo (Milan, Italy). Mice were safely placed in a controlled environment and were fed with a standard diet and water ad libitum under pathogen-free conditions with a 12 h light/12 h

dark. Animal study was approved by the University of Messina in accordance with Italian regulations on the use of animals (D.M.116192) and Council Regulation regulations (EEC) (O.J. of E.C. L 358/1 12/18/1986).

### 5.3.2 Orthotopic model of ATC

For the in vivo study an orthotopic mouse model of ATC with 8305C cells was performed. 3% isoflurane was used to anesthetize the BALB/c- nude mice before the injection. In the orthotopic model of ATC, 5 x$10^5$ 8305C cells, resuspended in 50 µl of PBS, are injected into the right lobe of the thyroid using an insulin syringe with a 28G 1/2 needle. Following the operation, the animals were observed every day, and their overall health was evaluated by periodic weighing. After receiving the injection, 13 days later, the mice were treated intraperitoneally with BAY-293 for 2 weeks, at two doses (10 and 50 mg/kg). The solubility of BAY-293 in 10% DMSO was used to prepare the final solutions administered. This final DMSO concentration of 10% (v/v) is a concentration commonly used in preclinical studies, which does not cause toxicity in animals [210]. The animals were sacrificed at the conclusion of the experiment, and the thyroids were removed, weighed, and examined [211].

The mice were randomly divided into four experimental groups, as described below:

1. SHAM group (n=8): intraperitoneal administration of saline solution containing 10% of DMSO;
2. ATC group (n=8): mice that received tumor cell inoculation intraperitoneal administrated with saline for two weeks starting at day 13 after tumor cells inoculation.
3. ATC + BAY-293 10 mg/kg group (n=8): mice that received tumor cells inoculation, intraperitoneal administrated with BAY-293 at the dose of 10 mg/kg once daily for two weeks starting at day 13 after tumor cells inoculation.

4. ATC + BAY-293 50 mg/kg (n=8): mice that received tumor cells inoculation, intraperitoneal administrated with BAY-293 at the dose of 50 mg/kg once daily for two weeks starting at day 13 after tumor cells inoculation.

### 5.3.3 Histological evaluation

Hematoxylin and Eosin staining for the histological evaluation was performed [206]. Samples of thyroid tissue were promptly extracted using 10% buffered formalin. Following dehydration in xylene and graded ethanol, the samples were embedded in paraffin and sectioned at a thickness of 7 μm. Sections were examined under a Nikon Eclipse Ci-L optical microscope following hematoxylin and eosin staining. The histology findings are displayed with a 20x (50 μm bar scale) and 40× (20 μm bar scale) magnifications. Every histological analysis was carried out in a blinded way.

### 5.3.4 Masson's Trichrome staining

Using the Masson's trichrome kit (Bio-Optica cat: 04-010802), morphological examination of the tumors was carried out on 5 μm sections following the manufacturer's instructions. Using a Nikon Eclipse Ci-L microscope, the images were obtained at a magnification of 20x (50 μm bar scale) [212].

### 5.3.5 Immunohistochemistry assay

The expression of the tumor proliferation marker Ki67, was evaluated by immunohistochemical analysis [213]. The thyroid sections of 7 μm were were incubated overnight (O/N) with the anti-Ki-67 (1:100; sc-8426 Santa Cruz Biotechnology, Dallas, TX), primary antibodies. Then, the

sections were washed with PBS and incubated with secondary antibody for 1 h. The reaction was revealed by a chromogenic substrate (brown DAB), and counterstaining with nuclear fast red. All stained sections were observed and analyzed in a blinded manner with a Nikon Eclipse Ci-L microscope. Immunohistochemistry results were showed at 20x magnification (50 μm scale bar) and 40x magnification (20 μm scale bar).

### 5.3.6 Western Blot Analysis

Thyroid sample protein levels were measured according to earlier instructions [207]. Cytosolic proteins were processed and sorted using electrophoresis and transferred to nitrocellulose membranes. After blocking the membranes with 5% (w/v) dried nonfat milk in buffered saline (PM) for 45 minutes at room temperature, the membranes were probed using the following specific antibodies: anti-PTEN (1:500; sc-7974; Santa Cruz Biotechnology) and anti-SOS1 (1:500; sc-17793; Santa Cruz Biotechnology), anti-p-p38 MAPK (1: 500; Santa Cruz Biotechnology, Dallas, TX, USA; sc- 166182), anti-pERK (1: 500; Santa Cruz Biotechnology, Dallas, TX, USA; sc-7383), ERK (1: 500; Santa Cruz Biotechnology, Dallas, TX, USA; sc-514302), β-Catenin (1: 500; Santa Cruz Biotechnology, Dallas, TX, USA; sc-7963), and anti-Caspase 3 (1: 500; Santa Cruz Biotechnology, Dallas, TX, USA; sc-70498) in 1× PBS, 5% w/v dried nonfat milk, and 0.1% Tween-20 (PMT) at 4 °C overnight. After goat anti-mouse IgG secondary antibody (1:2000, Jackson ImmunoResearch, West Grove, PA, USA) or goat anti-rabbit IgG secondary antibody (1:5000, Jackson ImmunoResearch, West Grove, PA, USA) conjugated with peroxidase were incubated on membranes for 1 hour at room temperature. As directed by the manufacturer (Thermo, Waltham, MO, USA, cat# 457), signals were detected using an enhanced chemiluminescence (ECL) detection system reagent. Protein band relative expression was measured using densitometry

and the Bio-Rad ChemiDoc XRS+ software. The results were normalized to the levels of β-actin (sc-8432, 1:500; Santa Cruz Biotechnology, Dallas, TX, USA), which served as an internal control.

## 5.4 *In vitro* OSCC studies

### 5.4.1 Cell cultures

Human oral tongue squamous carcinoma cell line CAL-27 was used in this study and was purchased from ATCC (American Type Culture Collection, Rockville, MD, USA) CAL-27 cells were cultured in 75 cm2 flask with respectively Dulbecco's Modified Eagle Medium (DMEM—Sigma-Aldrich® Catalog No. D5030; St. Louis, MO, USA) supplemented with 10% fetal bovine serum (FBS, Sigma-Aldrich® Catalog No. 12103C St. Louis, MO, USA) and antibiotics (penicillin 1000 units—streptomycin 0.1 mg/L, Sigma-Aldrich® Catalog No. P4333; St. Louis, MO, USA), in incubators under 5% $CO_2$ at 37°C.

### 5.4.2 Cells treatments

CAL-27 cells were plated on 96-well plates at a density of 4 × 104 cells/well to a final volume of 150 µl. After 24 hours, CAL27 cells were treated with BAY-293 (MedChemExpress USA, Cas No.: 2244904-70-7) for 24 hours at increasing concentrations 1 µM, 10 µM, 25 µM and 50 µM dissolved in dimethyl sulfoxide (DMSO).

### 5.4.3 Cell viability assay (MTT assay)

Cell viability of CAL27 was performed using 3-(4,5-dimethylthiazol-2-yl)-2,5-diphenyltetrazolium bromide assay (MTT assay). Cal-27 cells were plated on 96-well plates (Corning Cell Culture, Corning, NY, USA) at a density of 4 × 104 cells/well to a final volume of 150 µL and after 24 hours cells were treated with increasing concentrations of BAY-293 (1 µM, 10 µM, 25 µM and 50 µM). After 24 hours, cells were incubated at 37 ◦C with MTT (0.2 mg/mL)

for 1 h. Then, medium was removed, and cells were lysed with DMSO (100 µL). The amount of reduction of MTT to formazan was quantified by measurement of optical density (OD) at 550 nm with a microplate reader.

### 5.4.4 Western blot analysis

Western blot analysis was performed on Cal-27 cells lysates. 1 × 106 Cal-27 cells were plated in 6-well plates (Corning Cell Culture, Tewksuby, MA, USA) and after 24 hours cells were treated with BAY-293 at the concentrations of 10 µM and 25 µM for 24 hours. Subsequently, Cal-27 cells were washed twice with ice-cold phosphate-buffered saline (PBS), collected, and resuspended in 20 mM Tris-HCl pH 7.5, 10 mM NaF, 150 µL NaCl, 1% Nonidet P-40 and protease inhibitor cocktail (Roche, Basel, Switzerland). Then cell lysates were centrifuged at 16,000 × g for 15 minutes at 4 ° C and protein concentration was estimated by the Bio-Rad protein assay using bovine serum albumin as standard. The samples were then heated to 95 ◦C for 5 minutes and equal amounts of proteins were separated on a 12% SDS-PAGE gel and transferred to a Polyvinylidene fluoride (PVDF) membrane. The membranes were then incubated overnight at 4 ° C with the following primary antibodies: NF-κB (1: 500; Santa Cruz Biotechnology, Dallas, TX, USA; sc-372), IκBα (1: 500; Santa Cruz Biotechnology, Dallas, TX, USA; sc-1643), iNOS (1: 500; Santa Cruz Biotechnology, Dallas, TX, USA; sc-7271), COX-2 (1: 500; Santa Cruz Biotechnology, Dallas, TX, USA; sc-376861), IL-6 (1: 500; Santa Cruz Biotechnology, Dallas, TX, USA; sc-28343), TNF- α (1: 500; Santa Cruz Biotechnology, Dallas, TX, USA; sc-4564), anti-Caspase 3 (1: 500; Santa Cruz Biotechnology, Dallas, TX, USA; sc-56046), anti-BID (1: 500; Santa Cruz Biotechnology, Dallas, TX, USA; sc-11423), BAX (1: 500; Santa Cruz Biotechnology, Dallas, TX, USA; sc-20067), Bcl2 (1: 500; Santa Cruz Biotechnology, Dallas, TX, USA; sc-7382). Primary antibodies against β-actin or Lamin A/C were used as an endogenous control for protein expression of blots. A secondary antibody was added to the membrane (1:2000, Jackson ImmunoResearch, Jackson Laboratories, Bar Harbor, ME, USA) for 1 h at room temperature. Antibodies were diluted

in PBS, 5% w/v nonfat dried milk and 0.1% Tween-20 (PMT). The signals were detected with the Advanced Chemiluminescence Detection System (ECL) reagent according to the manufacturer's instructions (Thermo Fisher, Waltham, MA, USA). The relative expression of the protein bands was quantified by densitometry with the BIORAD ChemiDocTMXRS + ImageLab software [206].

### 5.4.5 Measurement of Nitric oxide (NO) levels

The effect of BAY-293 on NO production by Cal-27 cells was investigated by colorimetric Griess reaction. After treatment with different concentration of BAY-293 (10 μM and 25 μM) for 24h, cell culture supernatant from each group was collected from plates and the NO released into the media was measured. 100 μL of supernatant was transferred to microplate wells and 100 μL Griess reagent (1% sulfanilamide and 0.1% N-naphthylethyl-ethylenediamine dihydrochloride in 5% phosphoric acid were mixed at a ratio of 1:1) was added, respectively. The mixture was incubated for 10 min at room temperature. The absorbance was measured by a microplate reader at 540nm, and NO concentration was determined using a curve calibrated on sodium nitrite standards.

### 5.4.6 Enzyme-linked immunosorbent assay

The concentration of TNF-α in cell culture supernatant was measured using enzyme-linked immunosorbent assay (ELISA) (Rapidbio, Transhold, China), according to the manufacturer's protocol. Briefly, the samples (50 μL) were added in anti-dog TNF-α biotin-coated well plates and incubated at 37 °C for 60 min; plates were washed five times with washing buffer 1X. Then 100 μL of the horseradish peroxidase (HRP) was added to each well and incubated for 30 min at room temperature and plates were washed five times with washing buffer 1X. TMB (3,3′5,5′ tetramethyl-benzidine) substrate solution (100 μL) was added and incubated for 15 min at room temperature, then 100 μL of stop solution was added and incubated for another 30 min at room

temperature. The TNF-α concentration was determined spectrophotometrically at an absorbance of 450 nm and interpolated with a standard curve.

### 5.5 Statistical Analysis

The mean ± standard deviation (SD) of N observations is used to express all values. Three replicate samples were used for each analysis, which was carried out three times overall. One-way analysis of variance (ANOVA) was used to evaluate the data, and for multiple comparisons, a Bonferroni post hoc test was performed. A p-value $< 0.05$ was deemed significant.

# 6. RESULTS

## 6.1 *In vitro* results for TC study

### 6.1.1 The effect of BAY-293 on reducing TC cell viability

The MTT assay was performed to evaluate the viability of FTC-133, 8305C, and K1 cells after a 24-hour treatment with BAY-293. Our findings demonstrated that BAY-293 treatments were able to reduce cell viability in a concentration-dependent way (Figure 10 panel A-C). Based on these results we chose to do additional investigation focusing just on BAY-293 at concentrations of 0,4 g/L, 4,4 g/L and 11,2 g/L, as these were found to be the lowest concentration with the greatest cytotoxic effect. Furthermore, since BAY-293 demonstrated superior effects on 8305C cell viability, we have chosen to focus our investigation only on the anaplastic carcinoma cell line, which is the most aggressive form of thyroid carcinoma with a poor prognosis and few therapeutic options.

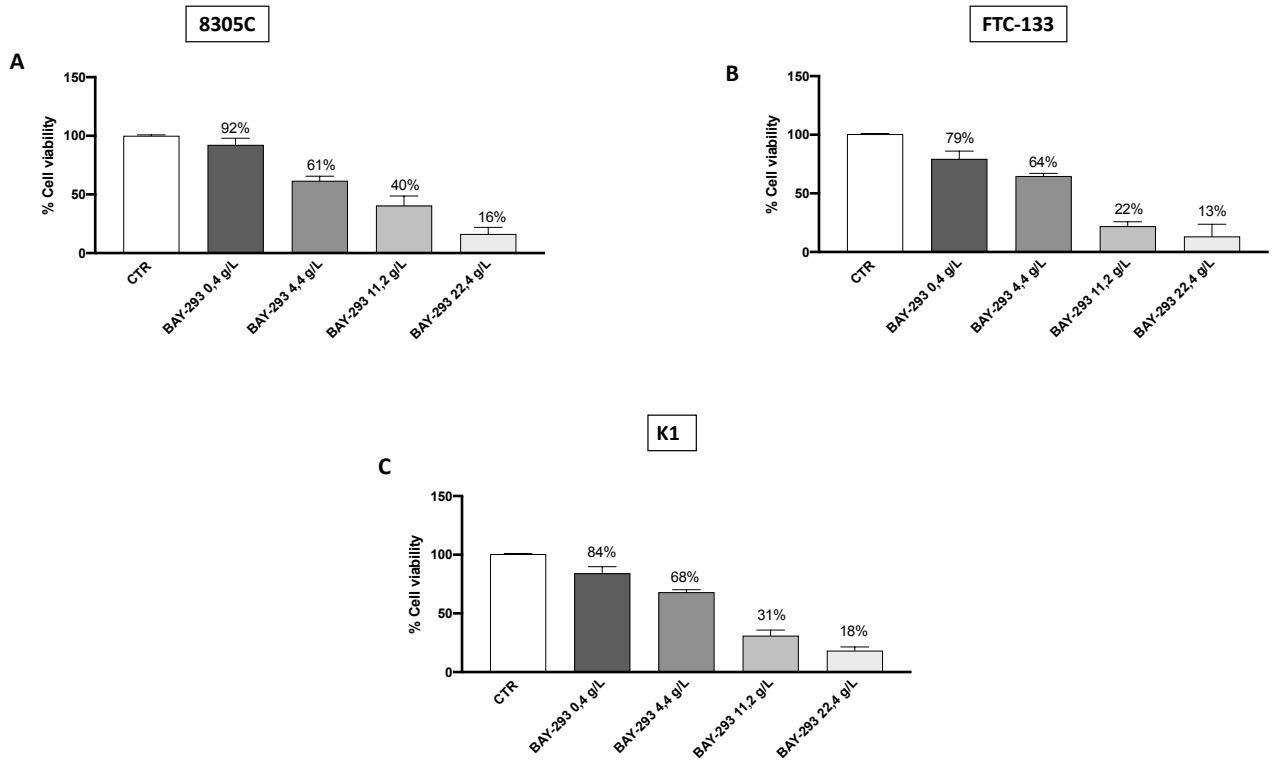


**Figure 10. Effect of BAY-293 on cell viability.** BAY-293 treatment was able to significantly reduce cell viability in a concentration dependent manner on 8305C cells (A), FTC-133 cells (B) and K1 cells (C). Data are representative of at least three independent experiments.

### 6.1.2 ATC cell migration and proliferation were reduced by BAY-293 treatment

By preventing the transition from inactive GDP to active GTP, BAY-293 alters the interaction between SOS1 and KRAS, resulting in antiproliferative activity [214]. Therefore, we assessed the ability of 8305C cells to form colonies after the treatment with BAY-293 at the concentrations of 0,4 g/L, 4,4 g/L and 11,2 g/L. According to the 0.1% (w/v) crystal violet staining results, BAY-293 considerably reduced colonies development of 8305C cells at all the concentrations (Figure 11 A, see colony formation rate panel A1). In addition, BAY-293's impact on 8305C cell migration was assessed through an *in vitro* wound healing assay. Confluent cells were scratched at time zero (T=0) and then subjected to BAY-29 treatment for 24 hours (T=24) (figure 11 B). Calculation of the percentage of migrating cells in the scratched area showed that CTR cells

migrated and filled the free zone. Conversely, treatment with BAY-293 for 24 hours at concentrations of 0,4 g/L, 4,4 g/L and 11,2 g/L significantly reduced the number of 8305c cells migrating into the scratched area compared to control cells (CTR) as showed in Figure 11 B, see % of wound closure panel B1.

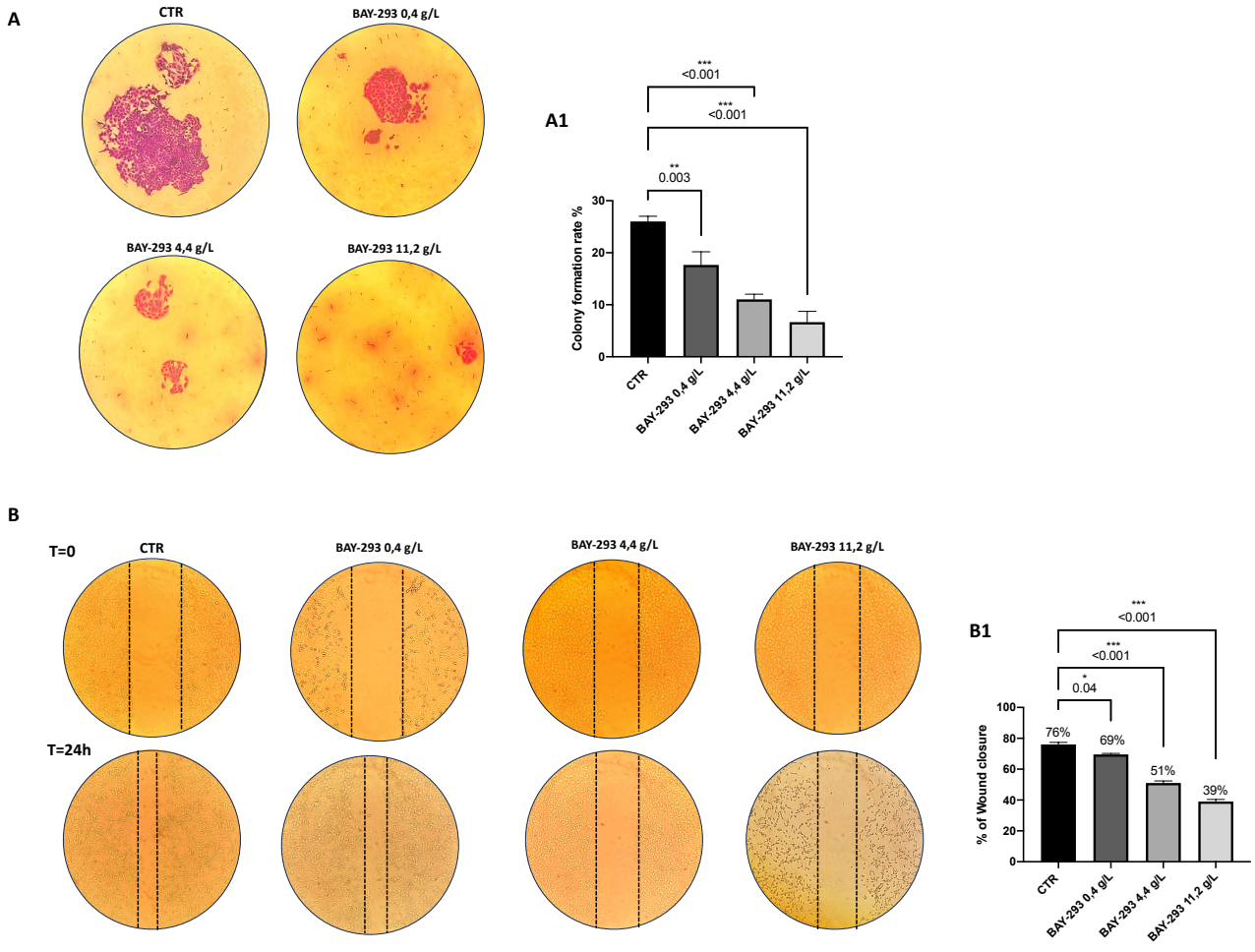


**Figure 11. Effect of BAY-293 on colony formation and migration.** The colony formation assay of 8305C cells treated with BAY-293 for 24h, at the concentration of 0,4 g/L, 4,4 g/L and 11,2 g/L, showed a significant reduction of colonies formation compared to untreated 8305C cells (CTR) (A). ** $p < 0.01$ vs. CTR; ***$p < 0.001$ vs. CTR. The Wound healing assay (Scratch test) revealed a significant reduction in the number of cells migrating to the scratched area, and thus a reduced percentage of wound closure, following 24 hours of BAY-293 treatment at the concentrations of 0,4 g/L, 4,4 g/L and 11,2 g/L (D). *$p < 0.05$ vs. CTR; ** $p < 0.01$ vs. CTR;

***p < 0.001 vs. CTR. Data are representative of at least three independent experiments. Values are means ± SEM. We used one-way ANOVA test followed by Bonferroni post hoc test for multiple comparisons.

### 6.1.3 The impact of BAY-293 on the modulation of K-RAS/SOS-1 pathway

BAY-293 has been extensively demonstrated to influence multiple molecular mechanisms, such as MAPK signaling pathway and apoptosis, providing further insight into its antitumor activity [215]. To confirm the action on the target, we used western blot analysis to evaluate the expression of KRAS/SOS-1 pathway related proteins (SOS-1, PTEN, p-p38 MAPK, p-ERK, β-Catenin). Figure 3 displays the considerable reduction in SOS-1 after BAY-293 treatment compared to untreated cells, confirming the inhibition of the target (Figure 12 A, panel A1). SOS1 inhibition results in a blockade of the Ras/MAP kinase pathway and in a high reduction in p-ERK activity [216]. Furthermore, it has recently been demonstrated that hyperactivation of the K-RAS/SOS1 signal, via a positive feedback loop through the MAPK-ERK pathway, leads to the accumulation of β-catenin. In ATC cells, β-catenin can translocate from the cytoplasm to the nucleus and trigger the expression of target genes involved in migration on tumor cells contributing to tumorigenesis and malignant transformation [217,218]. Our results showed a significant downregulation of p-p38 MAPK following treatment with BAY-293 at the concentration of 4,4 g/L, and 11,2 g/L (Figure 12 D, panel D1) and reduced levels of p-ERK1 following treatment with BAY-293 at the concentration of 11,2 g/L (Figure 12 E, panel E1). Moreover, we observed a significant reduction of β-Catenin levels in 8305C cells treated with BAY-293 at the concentrations of 0,4 g/L, 4,4 g/L and 11,2 g/L (Figure 12 B, panel B1) suggesting a role in the inhibition of KRAS/MAPK pathway. Simultaneously, our data showed that BAY-293 treatment results in an upregulation of tumor suppressor protein PTEN, particularly at the higher concentrations of 4,4 g/L and 11,2 g/L (Figure 12 C, panel C1). PTEN contributes to KRAS

signaling by negatively modulating the PI3K-Akt pathway. PTEN, through its phosphatase action capable of converting PIP3 to PIP2, inactivates the signaling pathway, reducing tumor growth. Therefore, these data provide the idea that BAY-293 could reduce the MAPK/ERK pathway in 8305c cells. Moreover, although the PI3K-Akt pathway was not directly assessed, a possible modulation of this pathway by BAY-293 could be hypothesized, considering the significant reduction of the main upstream protein, SOS-1, and the concomitant increase in PTEN levels, which is closely related to this pathway [219].

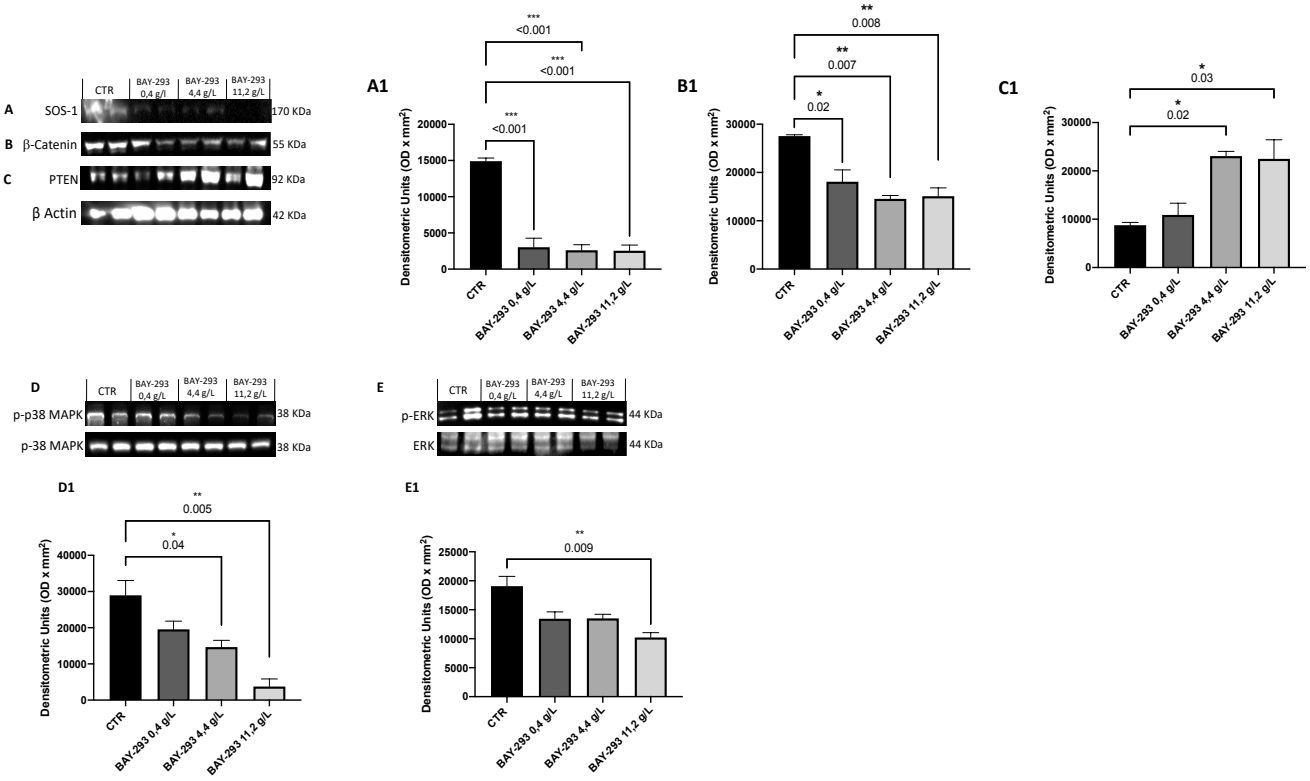


**Figure 12. Effect of BAY-293 on K-RAS/SOS-1 pathway in 8305C cells.** The blots revealed a significant modulation of K-RAS/SOS-1 markers expression following BAY-293 treatment. BAY-293 at the concentrations of 0,4 g/L, 4,4 g/L and 11,2 g/L was able to significantly reduce the expression of SOS-1 (A, see densitometric analysis panel A1), β-Catenin (B, see densitometric analysis panel B1) compared to untreated 8305C cells. At the concentration of

4,4 g/L and 11,2 g/L BAY-293 significantly reduced p-38 MAPK (D, see densitometric analysis panel D1) levels compared ti untreated cells, while only the highest concentrations of 11,2 g/L was able to significantly reduce p-ERK levels (E, see densitometric analysis panel E1). Treatment with BAY-293 (4,4 g/L and 11,2 g/L) was also able to increase the expression of tumor suppressor protein PTEN (C, see densitometric analysis panel C1). *** $p < 0.001$ vs CTR; ** $p < 0.01$ vs CTR; * $p < 0,05$. Our data are the result of three experimental replicates. Data are representative of at least three independent experiments. Values are means ± SEM. We used one-way ANOVA test followed by Bonferroni post hoc test for multiple comparisons.

### 6.1.4 BAY-293 activated apoptotic process on ATC cells

SOS1 promotes cell survival through the activation of the RAS-MAPK and PI3K-AKT pathways, enhancing the expression of anti-apoptotic proteins and inhibiting pro-apoptotic factors [220]. Treatment with BAY-293 revealed that the SOS1 inhibition can lead to reduce cell proliferation by promoting apoptosis in ATC cells. The effect of BAY-293 treatment on the expression of apoptotic markers such BAX, p53, and BCL-2 was assessed by Western blot analysis. According to our findings, BAY-293 was able to significantly increase the levels of pro-apoptotic proteins BAX and p53 and to decrease the expression of the anti-apoptotic BCL-2 protein compared to the control cells (Figure 13 A-C, panel A1-C1). The induction of the apoptotic process was confirmed by the DNA fragmentation assay. Following agarose gel electrophoresis of 8305C cells treated with BAY-293 a typical ladder pattern of internucleosomal fragmentation was observed in cells after 4,4 g/L treatment for 24 h (Figure 13 D).

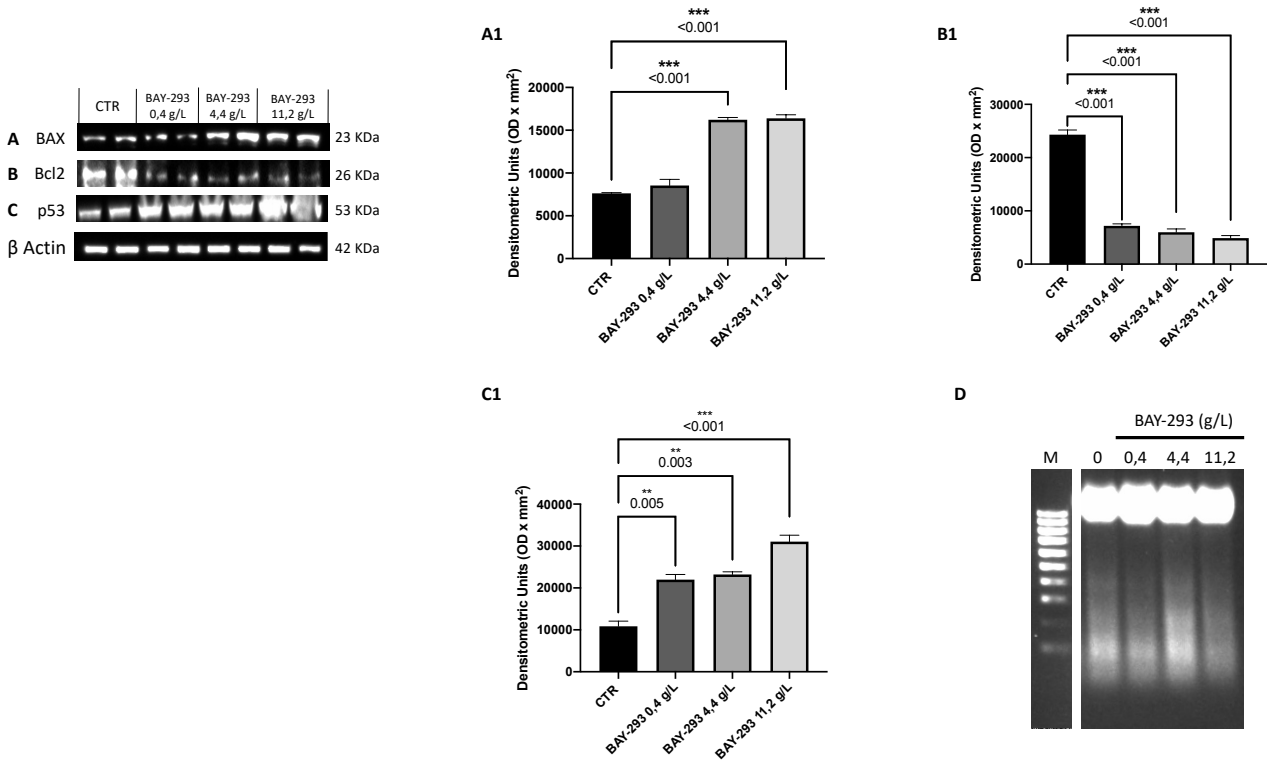


**Figure 13. Effect of BAY-293 on apoptosis markers expression in 8305C cells.** Western blots analysis revealed a significant modulation of apoptosis markers expression following BAY-293 treatment. BAY-293 was able to significantly increase the levels of pro-apoptotic marker BAX (A, see densitometric analysis panel A1) and p53 (C, see densitometric analysis panel C1) and significantly reduced the expression of anti-apoptotic protein Bcl-2 (C, see densitometric analysis panel C1). Analysis of genomic DNA fragmentation in 8305c cells after treatment with BAY-293 at the concentration of 0,4 g/L, 4,4 g/L and 11,2 g/L for 24 hours (D). *** $p < 0.001$ vs CTR; ** $p < 0.01$ vs CTR; * $p < 0.05$ vs CTR. Data are representative of at least three independent experiments. Values are means ± SEM. We used one-way ANOVA test followed by Bonferroni post hoc test for multiple comparisons.

## 6.2 *In vivo* results for TC study

### 6.2.1 BAY-293 improved histopathological features on ATC orthotopic model

The histological evaluation of the ATC group (Figure 14 B, B1 score panel E) revealed characteristics of a high-grade malignant tumor, including necrosis, significant cellular pleomorphism, high-grade nuclear atypia and extensive neutrophilic inflammation compared to sham group (Figure 14 A, A1 score panel E) [205]. As showed in Figure 14, our findings revealed that BAY-293 treatment at doses of 10 and 50 mg/kg was able to improve these pathological characteristics (Figure 14 C-D, C1-D1, score panel E). In addition, malignant tumor cells can induce the formation of a supporting stroma, consisting of collagen types I and III fibers, which in most solid tumors evolves into fibrosis [221]. Masson's trichrome-stained histological sections were performed to assess the extent of fibrosis in 8305C orthotopic tumors. Comparing the ATC group (Figure 14 G) with the sham group (Figure 14 F), it is evident that the ATC group shows greater infiltration of collagen fibers around the tumors. According to our data, these fibrotic characteristics could be reduced by BAY-293 treatments at doses of 10 and 50 mg/kg, as shown in the Figure 14 panel H and I. Moreover, our results demonstrated that no significant changes in body weight were reported in all mice during the experiment (from day 0 to day 13) (figure 14 panel J).

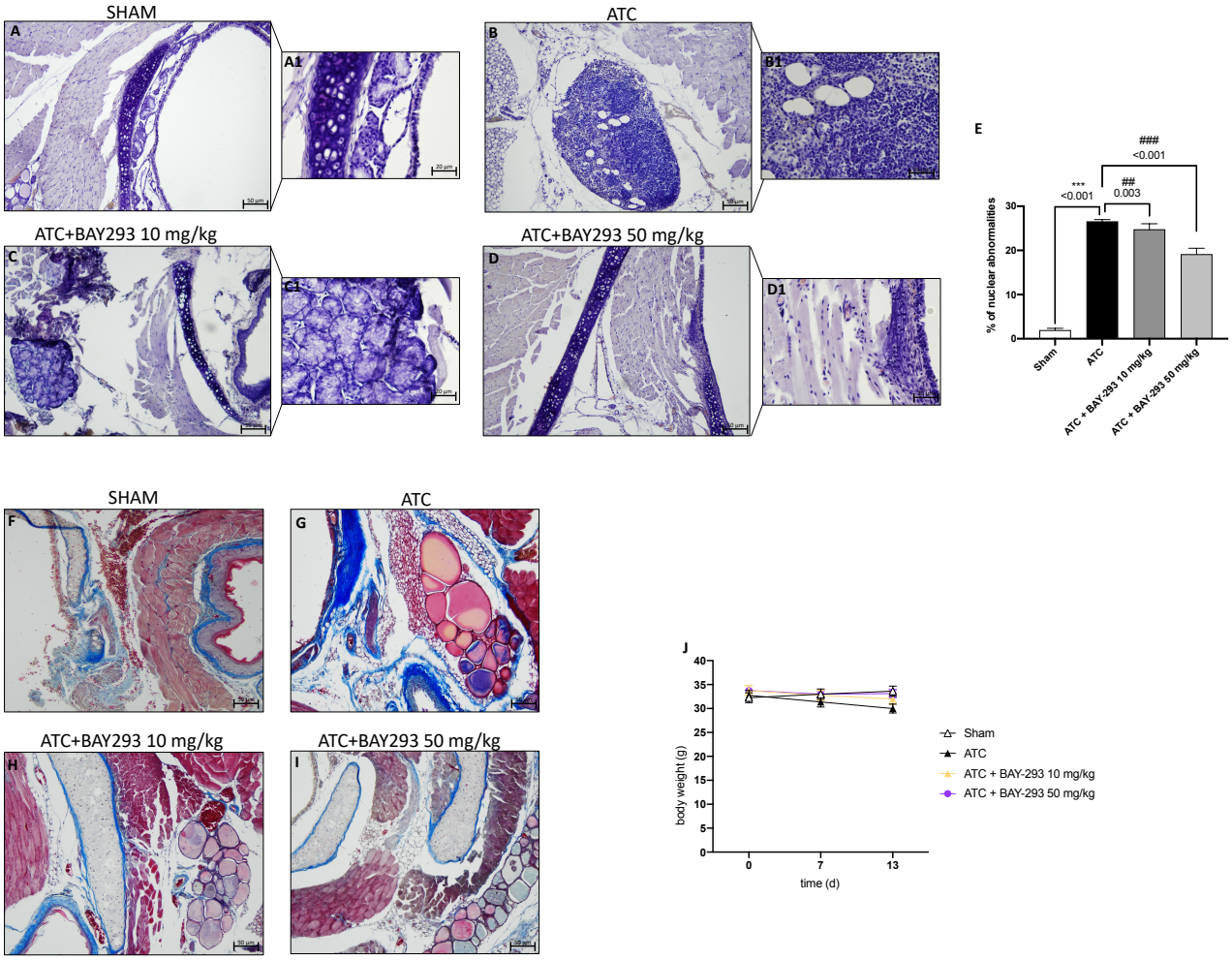


**Figure 14. Effect of BAY-293 on tumor growth in an orthotopic model of ATC.** Hematoxylin and eosin staining revealed that BAY-293 treatment at the dose of 10 mg/kg (C) and 50 mg/kf (D) was able to reduce features of a high-grade malignant neoplasm such as high-grade nuclear atypia, marked cellular pleomorphism, necrosis, and neutrophil infiltration compared to the ATC mice (B, see score panel D). Masson's trichrome staining of ATC tumors, the collagen is stained in blue cytoplasm is stained in red (F-I). No important change in the animals' body weight was showed during the experiments (J). Values are means ± SD. Distribution of values come from individual animals. One-way ANOVA test followed by Bonferroni post hoc test for multiple comparisons. ***$p < 0.001$ vs Sham; ###$p < 0.001$ vs ATC.

### 6.2.2 BAY-293 reduced Ki67 expression and increased apoptosis process in the orthotopic model

Among the histopathological features beyond to necrosis, extensive neutrophilic inflammation and the presence of fibrous tissue, ATC is characterized by a high Ki-67 proliferation index or a percentage of positive tumor nuclei (>30%) [222]. Ki-67 overexpression correlates with adverse outcomes in undifferentiated thyroid cancer [223]. According to our findings, the ATC group (Figure 15 B, B1, see score E) showed a significant overexpression of Ki-67 positive nuclei compared to the sham group (Figure 15 A, A1, see score E). Figure 15 illustrates how BAY-293 treatments at doses of 10 and 50 mg/kg significantly reduced the expression Ki-67 in orthotopic tumors, thereby contributing to the reduction of tumoral proliferation and invasion (Figure 15 panel C, C1 and D, D1, see score panel E). Moreover, Western blot results conducted on thyroid samples collected in the orthotopic model confirmed that BAY-293 was able to induce activation of programmed cell death. Treatment with BAY-293 led to a downregulation of the antiapoptotic marker BCL-2 (Figure 15 F, F1) and to an increase in the expression levels of the pro-apoptotic proteins BAX (Figure 15 G, G1) and Caspase 3 (Figure 15 H, H1), confirming the results obtained *in vitro*.

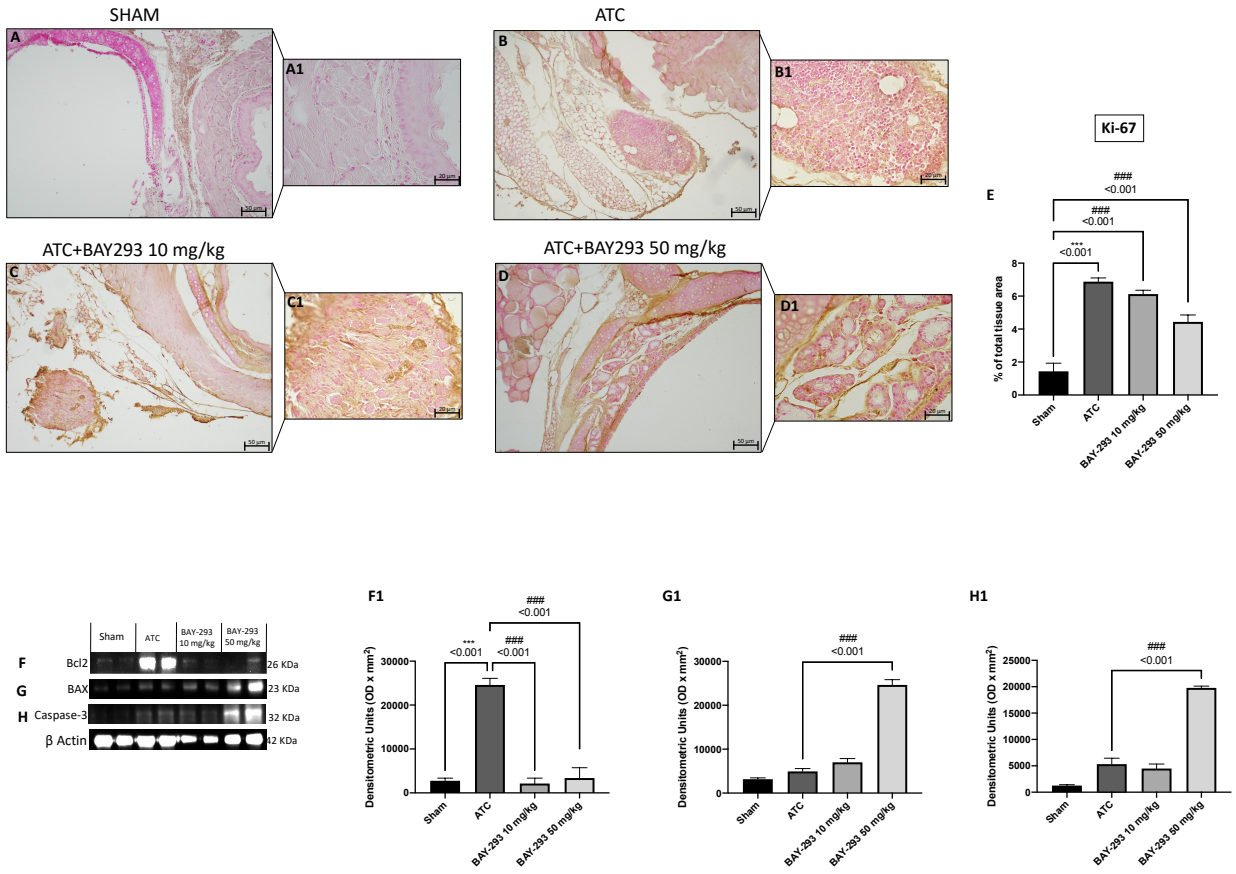


**Figure 15. Effects of BAY-293 on the cell proliferation marker Ki-67 and apoptosis pathway.** Immunohistochemical analysis of Ki-67 demonstrated that ATC tissues (B, see score panel E) showed a high number of ki-67-positive cells compared to tissues from the Sham group (A, see score panel E). BAY-293 treatment at the dose of 10 mg/kg (C, see score panel E) and 50 mg/kg (D, see score panel E) significantly reduced the number of Ki-67 positive cells compared to the ATC group. Western blot analysis conducted on thyroid tissues lysates for evaluation of Bcl-2 (F, score F1), BAX (G, score G1), Caspase-3 (H, score H1). Values are means ± SD. Distribution of values come from individual animals. One-way ANOVA test followed by Bonferroni post hoc test for multiple comparisons. ***$p < 0.001$ vs Sham; ## $p < 0.01$ vs ATC ; ###$p < 0.001$ vs ATC.

### 6.2.3 BAY-293 confirms the inhibition of K-RAS/SOS1 pathway in the orthotopic ATC model

To confirm the action on the target and the consequent modulation of the downstream factors of the KRAS/SOS1 pathway, we also performed molecular biology analyses on the thyroid samples collected in the orthotopic model. Our results showed elevated levels of SOS1 in the ATC group compared to the Sham group (Figure 16 A, see densitometric analysis panel A1). However, treatment with BAY-293 at both doses of 10 mg/kg and 50 mg/kg was able to significantly downregulate SOS1 levels (Figure 16 A, see densitometric analysis panel A1 and D, see densitometric analysis panel D1). In addition, we observed that BAY-293 at the highest dose of 50 mg/kg significantly reduced p-38 MAPK levels compared to the ATC group (Figure 16 C, see densitometric analysis panel C1), while both doses were able to reduce p-ERK levels compared to the ATC group (Figure 16 D, see densitometric analysis panel D1). Furthermore, the expressions of β-catenin were significantly elevated in the ATC group compared to the sham group (Figure 16 B, see densitometric analysis panel B1). Otherwise, β-catenin levels were significantly reduced following treatment with BAY-293 at doses of 10 and 50 mg/kg compared to the ATC group.

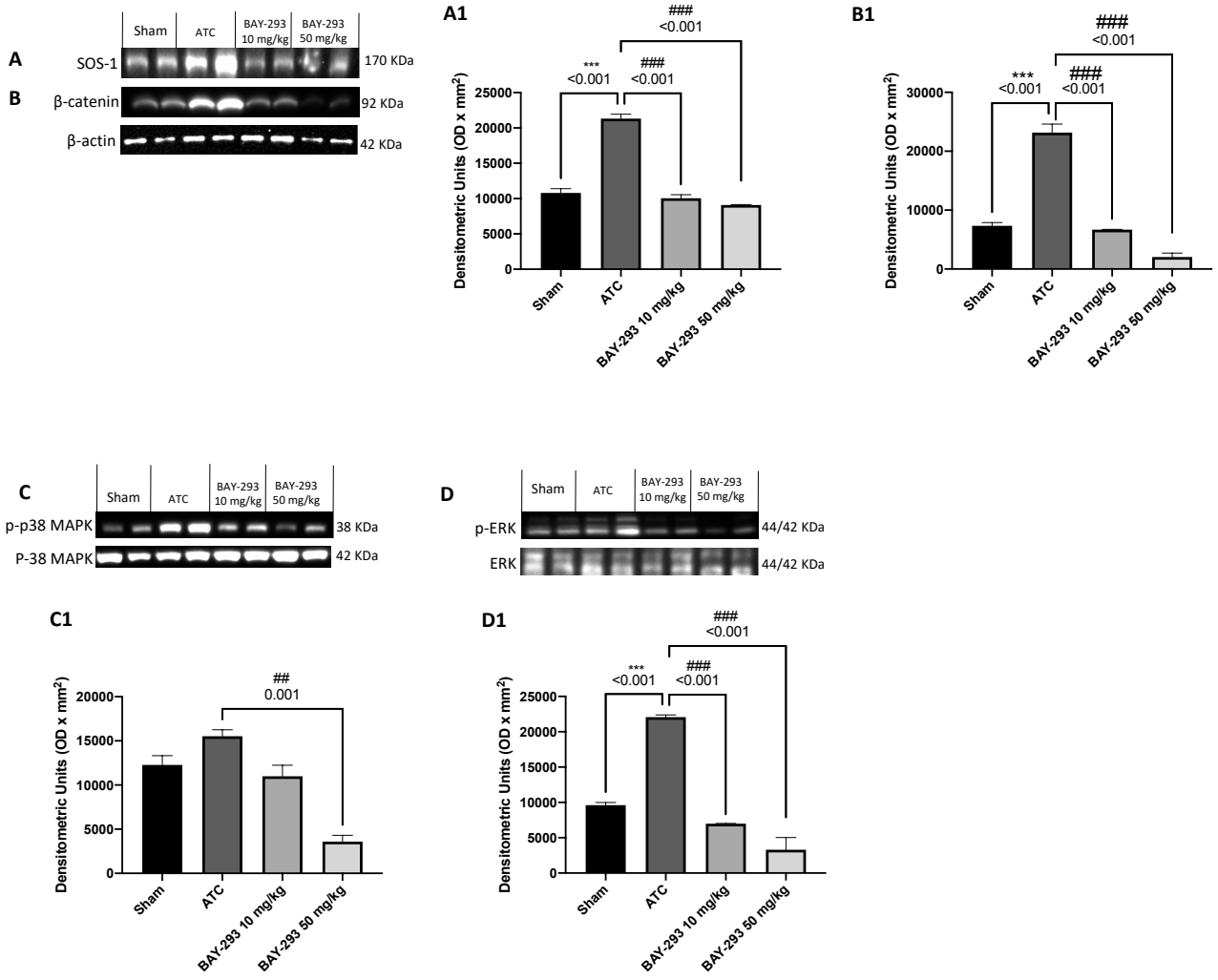


**Figure 16. Effect of BAY-293 on KRAS/SOS-1 pathway in an orthotopic model of ATC.** The blots revealed a significant reduction of SOS-1 (A, densitometric analysis panel A1), β-catenin (A, densitometric analysis panel A1), and p-ERK (D, densitometric analysis panel D1) following treatment with BAY-293 at the doses of 10 mg/kg and 50 mg/kg. Only the highest dose of 50 mg/kg of BAY-293 was able to significantly reduce the expression of p-38 MAPK (C, densitometric analysis panel C1) compared to ATC group. Values are means ± SD. Distribution of values come from individual animals. One-way ANOVA test followed by Bonferroni post hoc test for multiple comparisons. ***$p < 0.001$ vs Sham; ## $p < 0.01$ vs ATC ; ###$p < 0.001$ vs ATC.

## 6.2 *In vitro* results for OSCC study

### 6.3.1 BAY-293 reduced CAL-27 cell viability

CAL27 represents one of the most frequently used cell line in the field of OSCC and validated from neck and head tumor sites [224-226]. CAL-27 cell viability was assessed following 24 hours of treatment with BAY-293 at different concentrations. The treatment with BAY-293 at the concentrations of 10 μM and 25 μM was able to reduce viability of CAL-27 cell line (CTR) as shown in Figure 17. Since the concentration of 25 μM and 50 μM of BAY-293 showed similar effects on cell viability, we decided to continue to analyze the effect of BAY-293 only at the concentration of 10 μM e 25 μM which are the lowest concentration with the greatest cytotoxic effect on CAL27 cell line.

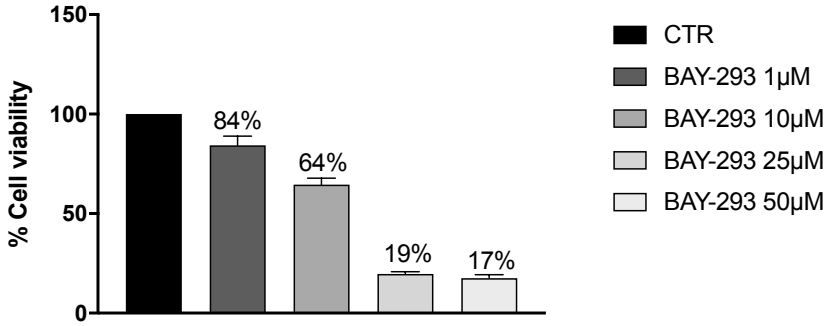


**Figure 17. Effect of BAY-292 on CAL-27 cell viability.** BAY-293 treatment at concentrations of 10 μM and 25 μM reduced cell viability compared to untreated cells (CTR). Data are representative of at least three independent experiments. Data are representative of at least three independent experiments.

### 6.3.2 BAY-293 modulated OSCC inflammation through NF-κB pathway

KRAS and its downstream interactors are described to affect the tumor microenvironment through the induction of NF-kB signaling, which in turn promotes the transcription of several cytokines and chemokines, including interleukin, IL-6, and tumor necrosis factor α (TNF-α), and pro-inflammatory enzymes such as iNOS and COX-2. In turn, activation of these pro-inflammatory mediators may contribute to the accumulation of immunosuppressive cells that promote immune escape and tumor growth [227]. Our results demonstrated that selective inhibition of the SOS-1/KRAS interaction after BAY-293 treatment significantly increased IKB-α levels at both concentrations compared to untreated cells (CTR) (Figure 18 A, see densitometric analysis panel A1). IκBα binds to NF-κB dimers in the cytoplasm, preventing their translocation into the nucleus. After activation, IκBα is phosphorylated by the IκB kinase (IKK) complex, leading to its ubiquitination and subsequent degradation, which releases NF-κB, allowing it to translocate into the nucleus and activate gene transcription. In OSCC, dysregulation of IκBα/NF-κB signaling due to KRAS hyperactivation may play a significant role in tumor development. In agreement, the obtained data demonstrated that the selective inhibitor BAY-293 significantly reduced the transcription factor NF-κB at concentrations of 10 μM and 25 μM compared to CTR cells (Figure 18 B, see densitometric analysis panel B1). Furthermore, BAY-293 at the highest concentration of 25 μM significantly reduced the levels of the pro-inflammatory enzyme iNOS (Figure 18 C, see densitometric analysis panel C1) and at both concentrations reduced the levels of the pro-inflammatory enzyme COX-2 compared to CTR cells (Figure 18 D, see densitometric analysis panel D1). KRAS appear to promote increased levels of IL-6 and TNF-α via NF-kB. Our data demonstrated that selective inhibition of the KRAS/SOS-1 interaction following BAY-293 treatment significantly reduced the levels of IL-6 (Figure 18 E, see densitometric analysis panel E1) and TNF-α (Figure 18 F) at both concentrations. It is well known that an increasing number of cytokines and other signaling enzymes such as iNOS in the tumor microenvironment

are responsible for the production of nitrite and nitrate. Therefore, the conditions existing in the tumor microenvironment are conductive to the generation of high concentrations of nitrosative stress and may be an important mediator of inflammation-associated carcinogenesis [228]. The results obtained by the Griess assay demonstrated that BAY-293 treatment was able to significantly reduce the concentrations of nitrate (Figure 18 G) and nitrite (Figure 18 H) in the cell supernatant compared to untreated CTR cells.

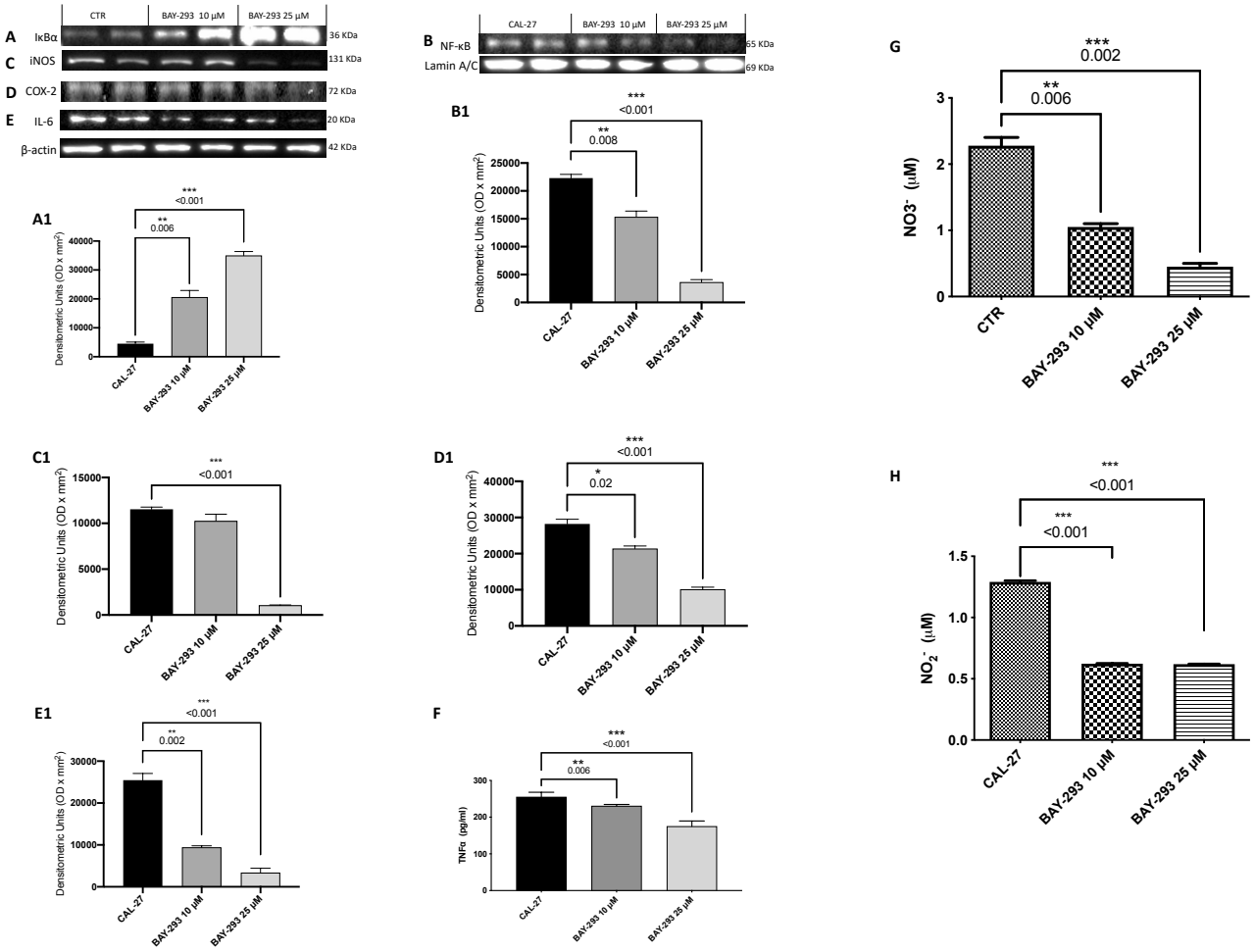


**Figure 18. Effect of BAY-293 on inflammation – associated cancer.** BAY-293 treatments at the concentrations of 10 μM and 25 μM was able to significantly increase the expression of IKB-α (A, densitometric analysis A1) and reduce the expression of pro-inflammatory marker NF-κB (B, densitometric analysis B1), iNOS (C, densitometric analysis C1), COX-2 (D, densitometric analysis D1) and IL-6 (E, densitometric analysis E1) compared to untreated CAL-27 cells. The

ELISA assay revealed a significant decrease of TNF-α, following BAY-293 treatments at all the concentrations (F). BAY-293 treatment at both concentrations significantly reduced nitrosative stress as observed by Griess assay for nitrate (G) and nitrite (H). *** $p < 0.001$ vs CTR; ** $p < 0.01$ vs CTR; * $p < 0,05$. Our data are the result of three experimental replicates. Data are representative of at least three independent experiments. Values are means ± SEM. We used one-way ANOVA test followed by Bonferroni post hoc test for multiple comparisons.

### 6.3.3 BAY-293 reduced tumor angiogenesis marker in OSCC cells

Considering the critical role that SOS-1/KRAS interaction plays in tumor angiogenesis [229,230], we examined the effect of BAY-293 on eNOS and TGFβ expression by Western Blot analysis. Our data demonstrated that following BAY-293 treatment at the concentration of 25 μM, TGFβ expression was significantly reduced compared to untreated cells (CTR) (Figure 19 A, see densitometric analysis panel A1). Furthermore, both concentrations of BAY-293 significantly reduced eNOS expression compared to CTR cells (Figure 19 B, see densitometric analysis panel B1). Therefore, targeting SOS1/KRAS interaction in OSCC can potentially mitigate abnormal cell proliferation through eNOS and TGFβ modulation.

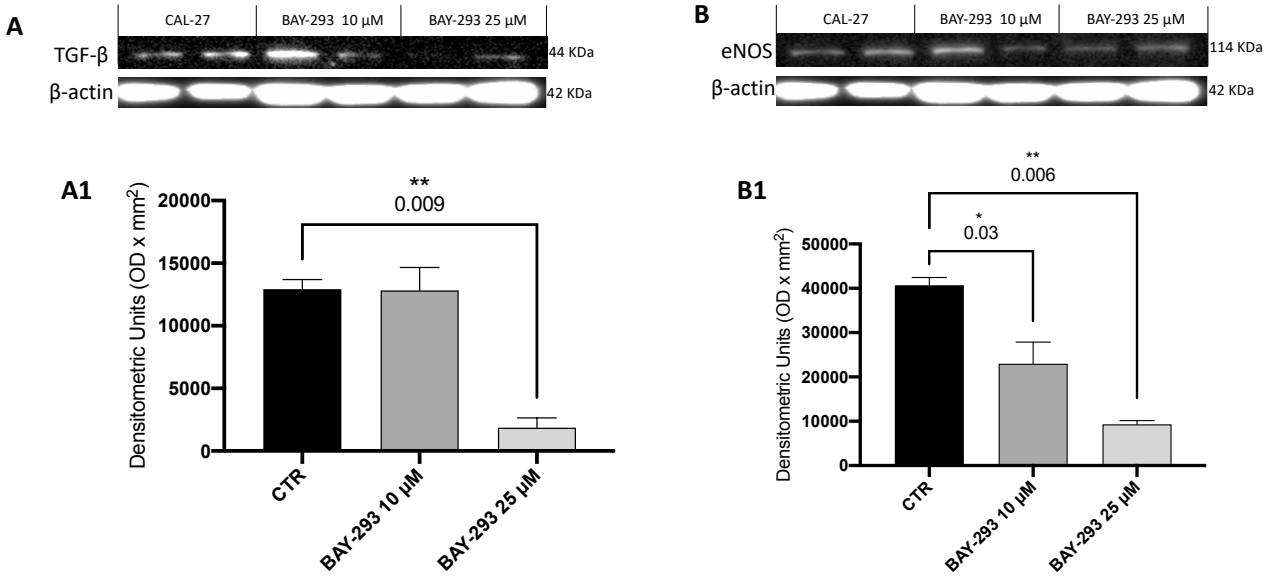

**Figure 19. BAY-293′s impact on TGFβ and eNOS levels in CAL27 cells.** BAY-293 treatment at the concentration of 25 μM reduced TGFβ levels compared to CTR cells (A, see densitometric analysis panel A1). Moreover, BAY-293 at both concentration, reduced eNOS levels compared to CTR cells (B, see densitometric analysis panel B1. ** $p < 0.01$ vs CTR; * $p < 0,05$. Our data are the result of three experimental replicates. Data are representative of at least three independent experiments. Values are means ± SEM. We used one-way ANOVA test followed by Bonferroni post hoc test for multiple comparisons.

### 6.3.4 Inhibition of SOS-1/KRAS interaction increased apoptosis pathway in OSCC cells

Western blot analysis was performed to evaluate the effect of BAY-293 on the expression of apoptotic markers such as Caspase-3, BID, BAX and Bcl-2. Our results showed that BAY-293, only at the concentration of 10 μM, significantly enhanced the levels of the pro-apoptotic proteins Caspase-3 and BID (Figure 20 A-B, see densitometric analysis A1-B1 ). Instead, both concentrations significantly increased the levels of the pro-apoptotic protein BAX and reduced the expression of the anti-apoptotic protein BCL-2 compared to untreated CTR cells (Figure 20 B-C, see densitometric analysis B1-C1).

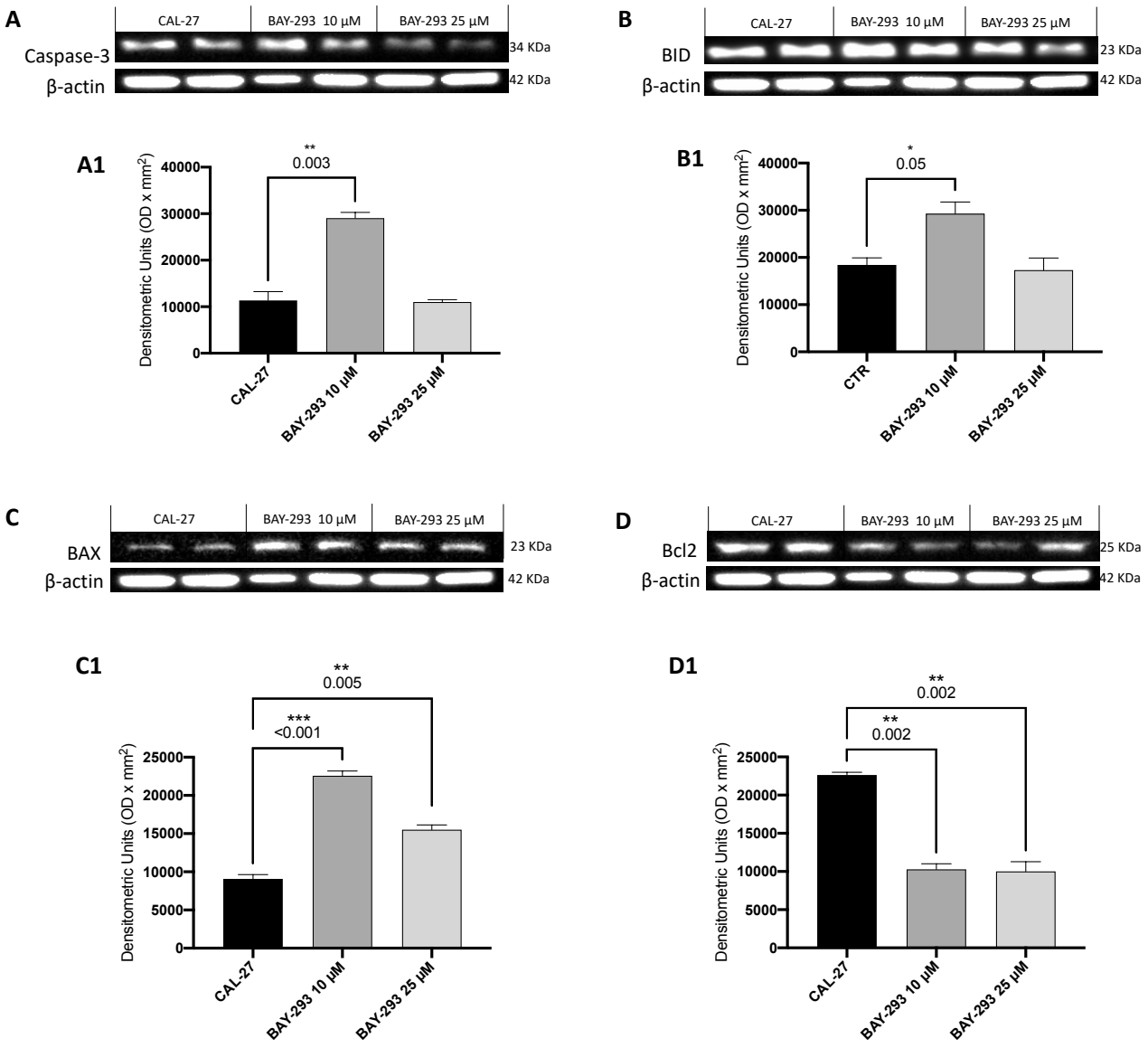


**Figure 20. Effect of BAY-293 on apoptosis markers expression in CAL-27 cells.** The blots revealed a significant modulation of apoptosis markers Caspase-3 and BID following BAY-293 treatment at the concentration of 10 µM (A-B, densitometric analysis A1, B1). BAY-293 at the concentration of 10 µM and 25 µM was able to significantly increase the expression of BAX (C, densitometric analysis C1) and to reduce the expression of BCL-2 (D, densitometric analysis D1) markers compared to untreated CAL-27 cells; *** $p < 0.001$ vs CTR; ** $p < 0.01$ vs CTR; * $p < 0.05$ vs CTR. Data are representative of at least three independent experiments. Values are means ± SEM. We used one-way ANOVA test followed by Bonferroni post hoc test for multiple comparisons.

## *7. DSCUSSION*

Several studies on HNC have identified KRAS mutation as an important prognostic factor [231,232]. In HNC, several mechanisms can activate KRAS, such as RTK activation, changes in upstream signaling molecules such as growth factor receptors or GEFs, and epigenetic alterations. These factors trigger downstream signaling events that ultimately lead to KRAS activation, which plays a significant role in MAPK, (PI3K)/AKT or RAL pathway activation [231,232]. In this study, we used a potent blocker of the interaction between KRAS and its primary regulator SOS1, called BAY-293, to investigate, for the first time, whether KRAS inhibition could influence the proliferation and migration of endocrine HNC, ATC, and OSCC. Considering that both ATC and OSCC fall into the broader category of head and neck cancers, the study focused primarily on ATC and subsequently the analysis was extended to the study of OSCC. This approach allowed us to explore the role of KRAS and its key downstream signals in both tumors. Regarding ATC, it is a rare and aggressive cancer that in most cases is diagnosed late and characterized by a poor prognosis, leading in 90% of cases to death within one year of diagnosis [233]. The management of ATC involves a multimodal therapeutic approach that combines surgical resection and chemoradiotherapy [234]. However, the efficacy of the current therapeutic approach is limited. KRAS mutations are among the main drivers in poorly differentiated carcinomas and occurring in 29% of ATCs [235]. In this aggressive form of thyroid cancer, mutations in KRAS can lead to constitutive activation of the RAS/MAPK pathway [236]. BAY-293, through interaction with its target and its effectors, was able to disrupt downstream signaling pathways involved in cancer cell proliferation, like the MAPK/ERK pathway. These pathways are often involved in promoting cell growth, survival, and proliferation in cancer cells [237]. K-RAS activated through the

stimulation of RAF kinases (such as BRAF), activates MEK1/2 which in turn phosphorylates and activates ERK1/2. ERK1/2 translocate into the nucleus and activates transcription factors that promote the expression of genes involved in cell cycle progression and proliferation [238]. Our results showed a significant downregulation of Ras/MAP kinase pathway trough the modulation of pERK, p-p38 MAPK and β-Catenin expressions both *in vitro* and *in vivo* suggesting a role of BAY-293 in the inhibition of ATC cells proliferation and migration. In addition to reducing proliferation, BAY-293 was able to induce programmed cell death, in ATC tumor cells by disrupting survival signals mediated through K-RAS. The PI3K/AKT pathway, also regulated by KRAS, promotes cell survival and resistance to apoptosis [239]. Activates PI3K, lead to the production of PIP3 and activation of AKT, promoting cell survival and growth. Loss of PTEN function results in unchecked AKT activation. When KRAS is mutated and PTEN is lost or inactivated, there is a synergistic effect, leading to robust activation of the PI3K/AKT pathway [240]. Inhibition of KRAS activation by BAY-293 increased PTEN expression leading to improved apoptotic signaling in ATC cancer cells. Activation of the apoptotic process induced by BAY-293 treatment has been demonstrated both *in vitro* and *in vivo* and appears to be mediated by DNA fragmentation and Caspase 3 activation with concomitant increase in the levels of proapoptotic proteins such as BAD, BID or P53 and the downregulation of antiapoptotic proteins such as Bcl-2. These findings confirmed the action of BAY- 293 on the target and are consistent with preclinical studies that have demonstrated the effectiveness of BAY 293 in reducing KRAS signaling and tumor growth in cell lines [241-243]. The impact of BAY-293 on ATC proliferation was observed directly through the reduction of the expression of the proliferation marker Ki-67. Monitoring Ki-67 levels in response to BAY-293 treatment provides a valuable tool for evaluating the efficacy of this inhibitor. Activated KRAS signaling also contributes to the production of extracellular matrix (ECM) components such as collagen and fibronectin, leading tumor tissues to a fibrotic phenotype [244]. By inhibiting K-RAS activation, BAY-293 reduced ECM production and deposition, improving the fibrotic condition of ATC mice. Moreover,

through the inhibition of KRAS signaling, BAY-293 demonstrated the potential to disrupt aberrant cellular processes driven by oncogenic K-RAS, such as proliferation and uncontrolled migration, survival, and metastasis. Although further research are needed to define its clinical utility and potential as a safe and effective treatment option, BAY-293 has shown encouraging results for the treatment of ATC. After completing the study of BAY-293 in the context of ATC, research focused on investigating the inhibitory effect of SOS-1/KRAS mediated by BAY-293 in OSCC. OSCC is a subset of head and neck squamous cell carcinoma, and it is one of the most common human malignancies worldwide, ranking sixth among all human cancer. In the case of OSCC, KRAS activation facilitates several signaling pathways, including RAL, which in turn activates the NF-κB pathway highly implicated in OSCC progression [245]. KRAS has been shown to interact with the NF-κB transcription factors, RelA and RelB, to activate pro-inflammatory genes, suggesting that the NF-κB target gene signature is positively regulated by KRAS [246]. In agreement, we found an increase in NF-kB expression and a decrease in IkB-α expression in CAL-27 OSCC cells. However, treatment with the selective inhibitor of SOS-1/KRAS interaction BAY-293 was able to significantly decrease NF-kB levels and simultaneously increase IkB-α levels. In OSCC, activation of the NF-kB pathway induces the release of chemokines and cytokines, such as IL-6 and TNF- α that contribute to tumor growth by stimulating the infiltration of inflammatory cells into the tumor microenvironment. Following this, we found that the levels of TNF-α, IL-6 and COX-2, well-known biomarkers for oral cancer, were significantly augmented in CAL-27 cells, while BAY-293 treatment modulated these inflammatory players' release in a concentration-dependent manner, counteracting tumor inflammation. Furthermore, the KRAS–NF-κB pathway plays a key role in the tumor microenvironment by regulating the release of inflammatory mediators like iNOS that increase the production of reactive nitrogen species (RNS) contributing to the maintenance of the malignant phenotype. NO is a simple and multifunctional radical with numerous functions such as vascular permeability, vasodilation, angiogenesis [247]. It has been shown that the level of NO

in OSCC tissues is higher than in normal healthy mucosa, thus supporting the fact that NO plays an important role in oral cancer carcinogenesis [248]. Furthermore, it has been reported that in addition to iNOS, eNOS also modulates carcinogenesis and tumor progression via NO production and induction of angiogenesis process [249]. In addition, eNOS may be phosphorylated and activated by RAS-AKT signaling and it can in turn nitrosylate and activate wild-type RAS generating a positive feedback loop that contributes to cellular transformation and tumor maintenance [250]. In our study, we identified increased levels of nitrite and nitrate in the supernatant of CAL-27 cells, and high levels of iNOS and eNOS in protein lysate. However, BAY-293 treatment significantly reduced their levels, suggesting that modulation of SOS-1/KRAS pathway may control NO release via modulation of iNOS and eNOS. In addition, BAY-293 significantly reduced the levels of TGFβ, another pro-angiogenic marker, thus suggesting the modulation of angiogenesis. OSCC is characterized by dysregulation of the apoptotic process, a known programmed cell death process required for normal tissue development [251]. In tumor cells, overexpression of KRAS confers stimulation of cell proliferation, suppressing apoptosis. In order to inhibit apoptosis, the oncogene KRAS has been reported to upregulate anti-apoptotic proteins, including Bcl-2, and downregulate apoptosis-inducing proteins such as BAX and Caspase-3 [252]. We therefore investigated the ability of BAY-293 to modulate programmed cell death, demonstrating that selective inhibition of SOS-1/KRAS interaction increased the levels of the pro-apoptotic proteins BID, BAX, and caspase-3, and decreased the levels of the anti-apoptotic protein Bcl2. Therefore, all these findings provide a new perspective on the role of KRAS in the pathogenesis of OSCC and consider BAY-293 a possible therapeutic strategy to contrast oral cancer growth through modulating the pro-inflammatory KRAS/NF-κB pathway.

## *8. CONCLUSION*

In this project, by examining the efficacy of BAY-293 interaction in ATC and OSCC tumors, we demonstrated that blocking SOS-1/KRAS specific signaling pathway could represent a potent antitumor target. The results revealed that in ATC, the direct inhibition of SOS-1/KRAS by BAY-293 reduced tumor proliferation and growth by modulating the MAPK/ERK pathway. Additionally, in both ATC and OSCC, BAY-293 induced cellular apoptosis, thereby limiting uncontrolled proliferation.

In OSCC, BAY-293 significantly reduced pro-inflammatory markers like iNOS, COX-2, IL-6, TNFa, NFkB; however, future studies will investigate the effects of BAY-293 in an orthotopic mouse model of OSCC, in order to better understand mechanisms of action in a more complex biological context and allow for the evaluation of its effects on the tumor microenvironment. Moreover, future studies using *in vitro* gene silencing models and *in vivo* knockout models will be able to better highlights the role of KRAS-SOS1 and the selective activity of BAY-293 in the context of ATC and OSCC. On the other hand, although this SOS-1/KRAS inhibitor has shown potential antitumor effects, its long-term impact, systemic toxicity, and pharmacological response still need to be clarified due to the current lack of *in vivo* studies.Therefore, further investigation of the safety and efficacy of BAY-293 are needed.

## *REFERENCES*


1. Chow, L.Q.M. Head and Neck Cancer. *N Engl J Med* **2020**, *382*, 60-72, doi:10.1056/NEJMra1715715.
2. Deeken-Draisey, A.; Yang, G.Y.; Gao, J.; Alexiev, B.A. Anaplastic thyroid carcinoma: an epidemiologic, histologic, immunohistochemical, and molecular single-institution study. *Hum Pathol* **2018**, *82*, 140-148, doi:10.1016/j.humpath.2018.07.027.
3. Rossi, E.D.; Adeniran, A.J.; Faquin, W.C. Pitfalls in Thyroid Cytopathology. *Surg Pathol Clin* **2019**, *12*, 865-881, doi:10.1016/j.path.2019.08.001.
4. Aslan, Z.A.; Granados-Garcia, M.; Luna-Ortiz, K.; Guerrero-Huerta, F.J.; Gomez-Pedraza, A.; Namendys-Silva, S.A.; Meneses-Garcia, A.; Ordonez-Mosquera, J.M. Anaplastic thyroid cancer: multimodal treatment results. *Ecancermedicalscience* **2014**, *8*, 449, doi:10.3332/ecancer.2014.449.
5. Baloch, Z.W.; Asa, S.L.; Barletta, J.A.; Ghossein, R.A.; Juhlin, C.C.; Jung, C.K.; LiVolsi, V.A.; Papotti, M.G.; Sobrinho-Simoes, M.; Tallini, G.; et al. Overview of the 2022 WHO Classification of Thyroid Neoplasms. *Endocr Pathol* **2022**, *33*, 27-63, doi:10.1007/s12022-022-09707-3.
6. Amaral, M.; Afonso, R.A.; Gaspar, M.M.; Reis, C.P. Anaplastic thyroid cancer: How far can we go? *EXCLI J* **2020**, *19*, 800-812, doi:10.17179/excli2020-1302.
7. Bible, K.C.; Kebebew, E.; Brierley, J.; Brito, J.P.; Cabanillas, M.E.; Clark Jr, T.J.; Di Cristofano, A.; Foote, R.; Giordano, T.; Kasperbauer, J. 2021 American thyroid association guidelines for management of patients with anaplastic thyroid cancer: American thyroid association anaplastic thyroid cancer guidelines task force. *Thyroid* **2021**, *31*, 337-386.
8. Haddad, R.I.; Bischoff, L.; Ball, D.; Bernet, V.; Blomain, E.; Busaidy, N.L.; Campbell, M.; Dickson, P.; Duh, Q.Y.; Ehya, H.; et al. Thyroid Carcinoma, Version 2.2022, NCCN Clinical Practice Guidelines in Oncology. *J Natl Compr Canc Netw* **2022**, *20*, 925-951, doi:10.6004/jnccn.2022.0040.
9. Zhu, Z.; Gandhi, M.; Nikiforova, M.N.; Fischer, A.H.; Nikiforov, Y.E. Molecular profile and clinical-pathologic features of the follicular variant of papillary thyroid carcinoma: an unusually high prevalence of ras mutations. *American journal of clinical pathology* **2003**, *120*, 71-77.
10. Nikiforov, Y.E. Genetic alterations involved in the transition from well-differentiated to poorly differentiated and anaplastic thyroid carcinomas. *Endocrine pathology* **2004**, *15*, 319-327.
11. Yarbrough, W.G.; Shores, C.; Witsell, D.L.; Weissler, M.C.; Fidler, M.E.; Gilmer, T.M. ras mutations and expression in head and neck squamous cell carcinomas. *Laryngoscope* **1994**, *104*, 1337-1347, doi:10.1288/00005537-199411000-00005.
12. Volpe, J.P.; Conti, C.J.; Slaga, T.J. Characterization of mutant HA-ras gene expression in transformed murine keratinocyte lines grown under in vitro and in vivo conditions. *Mol Carcinog* **1996**, *17*, 202-206, doi:10.1002/(SICI)1098-2744(199612)17:4<202::AID-MC3>3.0.CO;2-F.
13. Prete, A.; Borges de Souza, P.; Censi, S.; Muzza, M.; Nucci, N.; Sponziello, M. Update on Fundamental Mechanisms of Thyroid Cancer. *Front Endocrinol (Lausanne)* **2020**, *11*, 102, doi:10.3389/fendo.2020.00102.

14. Jeng, H.-H. Characterization of the physiological roles of Sos-WT Ras signaling cascade in oncogenic Ras-driven tumorigenesis. New York University, 2011.
15. Menyhárd, D.K.; Pálfy, G.; Orgován, Z.; Vida, I.; Keserű, G.M.; Perczel, A. Structural impact of GTP binding on downstream KRAS signaling. *Chemical science* **2020**, *11*, 9272-9289.
16. Jančík, S.; Drábek, J.; Radzioch, D.; Hajdúch, M. Clinical relevance of KRAS in human cancers. *BioMed Research International* **2010**, *2010*.
17. Huang, L.; Guo, Z.; Wang, F.; Fu, L. KRAS mutation: from undruggable to druggable in cancer. *Signal Transduct Target Ther* **2021**, *6*, 386, doi:10.1038/s41392-021-00780-4.
18. Moore, A.R.; Rosenberg, S.C.; McCormick, F.; Malek, S. RAS-targeted therapies: is the undruggable drugged? *Nat Rev Drug Discov* **2020**, *19*, 533-552, doi:10.1038/s41573-020-0068-6.
19. Kessler, D.; Gerlach, D.; Kraut, N.; McConnell, D.B. Targeting son of sevenless 1: the pacemaker of KRAS. *Current Opinion in Chemical Biology* **2021**, *62*, 109-118.
20. Fedele, C.; Li, S.; Teng, K.W.; Foster, C.J.R.; Peng, D.; Ran, H.; Mita, P.; Geer, M.J.; Hattori, T.; Koide, A.; et al. SHP2 inhibition diminishes KRASG12C cycling and promotes tumor microenvironment remodeling. *J Exp Med* **2021**, *218*, doi:10.1084/jem.20201414.
21. Jiang, H.; Fan, Y.; Wang, X.; Wang, J.; Yang, H.; Fan, W.; Tang, C. Design, synthesis and biological evaluation of quinazoline SOS1 inhibitors. *Bioorganic & Medicinal Chemistry Letters* **2023**, *88*, 129265.
22. Plangger, A.; Rath, B.; Stickler, S.; Hochmair, M.; Lang, C.; Weigl, L.; Funovics, M.; Hamilton, G. Cytotoxicity of combinations of the pan-KRAS SOS1 inhibitor BAY-293 against pancreatic cancer cell lines. *Discov Oncol* **2022**, *13*, 84, doi:10.1007/s12672-022-00550-w.
23. Plangger, A.; Rath, B.; Hochmair, M.; Funovics, M.; Hamilton, G. Cytotoxicity of combinations of the pan-KRAS inhibitor BAY-293 against primary non-small lung cancer cells. *Transl Oncol* **2021**, *14*, 101230, doi:10.1016/j.tranon.2021.101230.
24. Wang, C.X.; Wang, T.T.; Zhang, K.D.; Li, M.Y.; Shen, Q.C.; Lu, S.Y.; Zhang, J. Pan-KRAS inhibitors suppress proliferation through feedback regulation in pancreatic ductal adenocarcinoma. *Acta Pharmacol Sin* **2022**, *43*, 2696-2708, doi:10.1038/s41401-022-00897-4.
25. Pai, S.I.; Westra, W.H. Molecular pathology of head and neck cancer: implications for diagnosis, prognosis, and treatment. *Annu Rev Pathol* **2009**, *4*, 49-70, doi:10.1146/annurev.pathol.4.110807.092158.
26. Yang, T.H.; Xirasagar, S.; Cheng, Y.F.; Chen, C.S.; Chang, W.P.; Lin, H.C. Trends in the incidence of head and neck cancer: A nationwide population-based study. *Oral Oncol* **2023**, *140*, 106391, doi:10.1016/j.oraloncology.2023.106391.
27. Gormley, M.; Creaney, G.; Schache, A.; Ingarfield, K.; Conway, D.I. Reviewing the epidemiology of head and neck cancer: definitions, trends and risk factors. *Br Dent J* **2022**, *233*, 780-786, doi:10.1038/s41415-022-5166-x.
28. Hu, J.; Yuan, I.J.; Mirshahidi, S.; Simental, A.; Lee, S.C.; Yuan, X. Thyroid Carcinoma: Phenotypic Features, Underlying Biology and Potential Relevance for Targeting Therapy. *Int J Mol Sci* **2021**, *22*, doi:10.3390/ijms22041950.
29. Benvenga, S.; Tuccari, G.; Ieni, A.; Vita, R. Thyroid gland: anatomy and physiology. *Encyclopedia of Endocrine Diseases* **2018**, *4*, 382-390.
30. Chigot, J.P.; Menegaux, F. [Review of the anatomy and physiology of the thyroid gland]. *Soins Chir* **1989**, 3-4.
31. Ashok, L.; Sivanandam, S. Diagnosis of thyroid disorder using infrared thermography. In Proceedings of the 2017 International conference of Electronics, Communication and Aerospace Technology (ICECA), 2017; pp. 37-41.

32. Cruz, J.C.; Fabrezi, M. Histology and microscopic anatomy of the thyroid gland during the larval development of Pseudis platensis (Anura, Hylidae). *J Morphol* **2020**, *281*, 122-134, doi:10.1002/jmor.21085.
33. Mullur, R.; Liu, Y.-Y.; Brent, G.A. Thyroid hormone regulation of metabolism. *Physiological reviews* **2014**.
34. Lee, J.; Yi, S.; Kang, Y.E.; Kim, H.-W.; Joung, K.H.; Sul, H.J.; Kim, K.S.; Shong, M. Morphological and functional changes in the thyroid follicles of the aged murine and humans. *Journal of pathology and translational medicine* **2016**, *50*, 426-435.
35. Rousset, B.; Dupuy, C.; Miot, F.; Dumont, J. Chapter 2 Thyroid Hormone Synthesis And Secretion. In *Endotext*, Feingold, K.R., Anawalt, B., Blackman, M.R., Boyce, A., Chrousos, G., Corpas, E., de Herder, W.W., Dhatariya, K., Dungan, K., Hofland, J., et al., Eds.; South Dartmouth (MA), 2000.
36. Giammanco, M.; Di Liegro, C.M.; Schiera, G.; Di Liegro, I. Genomic and non-genomic mechanisms of action of thyroid hormones and their catabolite 3, 5-diiodo-l-thyronine in mammals. *International Journal of Molecular Sciences* **2020**, *21*, 4140.
37. Cicatiello, A.G.; Di Girolamo, D.; Dentice, M. Metabolic effects of the intracellular regulation of thyroid hormone: old players, new concepts. *Frontiers in endocrinology* **2018**, *9*, 474.
38. Hu, J.; Yuan, I.J.; Mirshahidi, S.; Simental, A.; Lee, S.C.; Yuan, X. Thyroid carcinoma: phenotypic features, underlying biology and potential relevance for targeting therapy. *International journal of molecular sciences* **2021**, *22*, 1950.
39. Shank, J.B.; Are, C.; Wenos, C.D. Thyroid Cancer: Global Burden and Trends. *Indian J Surg Oncol* **2022**, *13*, 40-45, doi:10.1007/s13193-021-01429-y.
40. Deng, Y.; Li, H.; Wang, M.; Li, N.; Tian, T.; Wu, Y.; Xu, P.; Yang, S.; Zhai, Z.; Zhou, L.; et al. Global Burden of Thyroid Cancer From 1990 to 2017. *JAMA Netw Open* **2020**, *3*, e208759, doi:10.1001/jamanetworkopen.2020.8759.
41. Bray, F.; Ferlay, J.; Soerjomataram, I.; Siegel, R.L.; Torre, L.A.; Jemal, A. Global cancer statistics 2018: GLOBOCAN estimates of incidence and mortality worldwide for 36 cancers in 185 countries. *CA Cancer J Clin* **2018**, *68*, 394-424, doi:10.3322/caac.21492.
42. Ferlay, J.; Colombet, M.; Soerjomataram, I.; Mathers, C.; Parkin, D.M.; Pineros, M.; Znaor, A.; Bray, F. Estimating the global cancer incidence and mortality in 2018: GLOBOCAN sources and methods. *Int J Cancer* **2019**, *144*, 1941-1953, doi:10.1002/ijc.31937.
43. Berinde, G.M.; Socaciu, A.I.; Socaciu, M.A.; Cozma, A.; Rajnoveanu, A.G.; Petre, G.E.; Piciu, D. Thyroid Cancer Diagnostics Related to Occupational and Environmental Risk Factors: An Integrated Risk Assessment Approach. *Diagnostics (Basel)* **2022**, *12*, doi:10.3390/diagnostics12020318.
44. Knobel, M.; Medeiros-Neto, G. Relevance of iodine intake as a reputed predisposing factor for thyroid cancer. *Arq Bras Endocrinol Metabol* **2007**, *51*, 701-712, doi:10.1590/s0004-27302007000500007.
45. Winder, M.; Kosztyla, Z.; Boral, A.; Kocelak, P.; Chudek, J. The Impact of Iodine Concentration Disorders on Health and Cancer. *Nutrients* **2022**, *14*, doi:10.3390/nu14112209.
46. Knobel, M.; Medeiros-Neto, G. Relevance of iodine intake as a reputed predisposing factor for thyroid cancer. *Arquivos Brasileiros de Endocrinologia & Metabologia* **2007**, *51*, 701-712.
47. Betito, H.R.; Chaushu, H.; Lahav, Y.; Pinhas, S.; Warman, M.; Zornitzki, T.; Malka, L.; Cohen, J.; Lahav, G.; Cohen, O. The impact of iodine deficiency exposure on thyroid nodule cytology and pathology - A single institute, case-control study. *Am J Otolaryngol* **2024**, *45*, 104022, doi:10.1016/j.amjoto.2023.104022.
48. Horn-Ross, P.L.; Morris, J.S.; Lee, M.; West, D.W.; Whittemore, A.S.; McDougall, I.R.; Nowels, K.; Stewart, S.L.; Spate, V.L.; Shiau, A.C. Iodine and thyroid cancer risk among

women in a multiethnic population: the Bay Area Thyroid Cancer Study. *Cancer epidemiology biomarkers & prevention* **2001**, *10*, 979-985.
49. Belfiore, A.; La Rosa, G.L.; La Porta, G.A.; Giuffrida, D.; Milazzo, G.; Lupo, L.; Regalbuto, C.; Vigneri, R. Cancer risk in patients with cold thyroid nodules: relevance of iodine intake, sex, age, and multinodularity. *Am J Med* **1992**, *93*, 363-369, doi:10.1016/0002-9343(92)90164-7.
50. Chen, G.G.; Vlantis, A.C.; Zeng, Q.; van Hasselt, C.A. Regulation of cell growth by estrogen signaling and potential targets in thyroid cancer. *Curr Cancer Drug Targets* **2008**, *8*, 367-377, doi:10.2174/156800908785133150.
51. O'Grady, T.J.; Rinaldi, S.; Michels, K.A.; Adami, H.O.; Buring, J.E.; Chen, Y.; Clendenen, T.V.; D'Aloisio, A.; DeHart, J.C.; Franceschi, S.; et al. Association of hormonal and reproductive factors with differentiated thyroid cancer risk in women: a pooled prospective cohort analysis. *Int J Epidemiol* **2024**, *53*, doi:10.1093/ije/dyad172.
52. Denaro, N.; Romano, R.; Alfieri, S.; Dolci, A.; Licitra, L.; Nuzzolese, I.; Ghidini, M.; Bareggi, C.; Bertaglia, V.; Solinas, C.; et al. The Tumor Microenvironment and the Estrogen Loop in Thyroid Cancer. *Cancers (Basel)* **2023**, *15*, doi:10.3390/cancers15092458.
53. Rivas, M.; Santisteban, P. TSH-activated signaling pathways in thyroid tumorigenesis. *Mol Cell Endocrinol* **2003**, *213*, 31-45, doi:10.1016/j.mce.2003.10.029.
54. Kwong, N.; Medici, M.; Angell, T.E.; Liu, X.; Marqusee, E.; Cibas, E.S.; Krane, J.F.; Barletta, J.A.; Kim, M.I.; Larsen, P.R.; et al. The Influence of Patient Age on Thyroid Nodule Formation, Multinodularity, and Thyroid Cancer Risk. *J Clin Endocrinol Metab* **2015**, *100*, 4434-4440, doi:10.1210/jc.2015-3100.
55. Darbre, P.D. Overview of air pollution and endocrine disorders. *Int J Gen Med* **2018**, *11*, 191-207, doi:10.2147/IJGM.S102230.
56. Kruger, E.; Toraih, E.A.; Hussein, M.H.; Shehata, S.A.; Waheed, A.; Fawzy, M.S.; Kandil, E. Thyroid Carcinoma: A Review for 25 Years of Environmental Risk Factors Studies. *Cancers (Basel)* **2022**, *14*, doi:10.3390/cancers14246172.
57. Lee, M.; Morris, L.G. Genetic alterations in thyroid cancer mediating both resistance to BRAF inhibition and anaplastic transformation. *Oncotarget* **2024**, *15*, 36-48, doi:10.18632/oncotarget.28544.
58. Bahar, M.E.; Kim, H.J.; Kim, D.R. Targeting the RAS/RAF/MAPK pathway for cancer therapy: from mechanism to clinical studies. *Signal Transduct Target Ther* **2023**, *8*, 455, doi:10.1038/s41392-023-01705-z.
59. Li, X.; Jian, J.; Zhang, A.; Xiang, J.M.; Huang, J.; Chen, Y. The role of immune cells and immune related genes in the tumor microenvironment of papillary thyroid cancer and their significance for immunotherapy. *Sci Rep* **2024**, *14*, 18125, doi:10.1038/s41598-024-69187-9.
60. Buczynska, A.; Kosciuszko, M.; Kretowski, A.J.; Poplawska-Kita, A. Exploring the clinical utility of angioinvasion markers in papillary thyroid cancer: a literature review. *Front Endocrinol (Lausanne)* **2023**, *14*, 1261860, doi:10.3389/fendo.2023.1261860.
61. Christofer Juhlin, C.; Mete, O.; Baloch, Z.W. The 2022 WHO classification of thyroid tumors: novel concepts in nomenclature and grading. *Endocr Relat Cancer* **2023**, *30*, doi:10.1530/ERC-22-0293.
62. Jung, C.K.; Bychkov, A.; Kakudo, K. Update from the 2022 World Health Organization Classification of Thyroid Tumors: A Standardized Diagnostic Approach. *Endocrinol Metab (Seoul)* **2022**, *37*, 703-718, doi:10.3803/EnM.2022.1553.
63. Baloch, Z.W.; Asa, S.L.; Barletta, J.A.; Ghossein, R.A.; Juhlin, C.C.; Jung, C.K.; LiVolsi, V.A.; Papotti, M.G.; Sobrinho-Simões, M.; Tallini, G. Overview of the 2022 WHO classification of thyroid neoplasms. *Endocrine pathology* **2022**, *33*, 27-63.
64. Mete, O.; Asa, S.L. Pitfalls in the diagnosis of follicular epithelial proliferations of the thyroid. *Adv Anat Pathol* **2012**, *19*, 363-373, doi:10.1097/PAP.0b013e318271a5ac.

65. Yu, Y.; Manders, F.; Grinwis, G.C.M.; Groenen, M.A.M.; Crooijmans, R. A recurrent somatic missense mutation in GNAS gene identified in familial thyroid follicular cell carcinomas in German longhaired pointer dogs. *BMC Genomics* **2022**, *23*, 669, doi:10.1186/s12864-022-08885-y.
66. Jung, C.K.; Kim, Y.; Jeon, S.; Jo, K.; Lee, S.; Bae, J.S. Clinical utility of EZH1 mutations in the diagnosis of follicular-patterned thyroid tumors. *Hum Pathol* **2018**, *81*, 9-17, doi:10.1016/j.humpath.2018.04.018.
67. Nose, V.; Gill, A.; Teijeiro, J.M.C.; Perren, A.; Erickson, L. Overview of the 2022 WHO Classification of Familial Endocrine Tumor Syndromes. *Endocr Pathol* **2022**, *33*, 197-227, doi:10.1007/s12022-022-09705-5.
68. Wasserman, J.D.; Sabbaghian, N.; Fahiminiya, S.; Chami, R.; Mete, O.; Acker, M.; Wu, M.K.; Shlien, A.; de Kock, L.; Foulkes, W.D. DICER1 mutations are frequent in adolescent-onset papillary thyroid carcinoma. *The Journal of Clinical Endocrinology & Metabolism* **2018**, *103*, 2009-2015.
69. Juhlin, C.C.; Stenman, A.; Zedenius, J. Macrofollicular variant follicular thyroid tumors are DICER1 mutated and exhibit distinct histological features. *Histopathology* **2021**, *79*, 661-666.
70. Cameselle-Teijeiro, J.M.; Mete, O.; Asa, S.L.; LiVolsi, V. Inherited Follicular Epithelial-Derived Thyroid Carcinomas: From Molecular Biology to Histological Correlates. *Endocr Pathol* **2021**, *32*, 77-101, doi:10.1007/s12022-020-09661-y.
71. Kakudo, K.; Li, Y.; Bai, Y.; Liu, Z. Low-Risk Neoplasms in the Fifth Edition of the WHO Classification of Thyroid Tumors. In *Thyroid FNA Cytology: Differential Diagnoses and Pitfalls*; Springer: 2024; pp. 91-102.
72. Na, H.Y.; Park, S.Y. Noninvasive follicular thyroid neoplasm with papillary-like nuclear features: its updated diagnostic criteria, preoperative cytologic diagnoses and impact on the risk of malignancy. *J Pathol Transl Med* **2022**, *56*, 319-325, doi:10.4132/jptm.2022.09.29.
73. Hofman, V.; Lassalle, S.; Bonnetaud, C.; Butori, C.; Loubatier, C.; Ilie, M.; Bordone, O.; Brest, P.; Guevara, N.; Santini, J.; et al. Thyroid tumours of uncertain malignant potential: frequency and diagnostic reproducibility. *Virchows Arch* **2009**, *455*, 21-33, doi:10.1007/s00428-009-0798-7.
74. Schmid, K. Why does a thyroid tumor have to be classified as a carcinoma if it does not biologically behave like cancer? Noninvasive follicular thyroid neoplasm with papillary-like nuclear features as a model. *Der Onkologe* **2019**, *25*, 580-589.
75. Nikiforova, M.N.; Nikitski, A.V.; Panebianco, F.; Kaya, C.; Yip, L.; Williams, M.; Chiosea, S.I.; Seethala, R.R.; Roy, S.; Condello, V.; et al. GLIS Rearrangement is a Genomic Hallmark of Hyalinizing Trabecular Tumor of the Thyroid Gland. *Thyroid* **2019**, *29*, 161-173, doi:10.1089/thy.2018.0791.
76. Ho, T.K.; LaBella, F.S.; Pinsky, C. Opiate properties of SKF 525A. *Can J Physiol Pharmacol* **1978**, *56*, 550-554, doi:10.1139/y78-088.
77. O'Neill, C.J.; Vaughan, L.; Learoyd, D.L.; Sidhu, S.B.; Delbridge, L.W.; Sywak, M.S. Management of follicular thyroid carcinoma should be individualised based on degree of capsular and vascular invasion. *Eur J Surg Oncol* **2011**, *37*, 181-185, doi:10.1016/j.ejso.2010.11.005.
78. Xu, B.; Wang, L.; Tuttle, R.M.; Ganly, I.; Ghossein, R. Prognostic impact of extent of vascular invasion in low-grade encapsulated follicular cell-derived thyroid carcinomas: a clinicopathologic study of 276 cases. *Hum Pathol* **2015**, *46*, 1789-1798, doi:10.1016/j.humpath.2015.08.015.
79. Liu, Z.; Hou, P.; Ji, M.; Guan, H.; Studeman, K.; Jensen, K.; Vasko, V.; El-Naggar, A.K.; Xing, M. Highly prevalent genetic alterations in receptor tyrosine kinases and phosphatidylinositol 3-kinase/akt and mitogen-activated protein kinase pathways in

anaplastic and follicular thyroid cancers. *J Clin Endocrinol Metab* **2008**, *93*, 3106-3116, doi:10.1210/jc.2008-0273.
80. Miller, K.A.; Yeager, N.; Baker, K.; Liao, X.H.; Refetoff, S.; Di Cristofano, A. Oncogenic Kras requires simultaneous PI3K signaling to induce ERK activation and transform thyroid epithelial cells in vivo. *Cancer Res* **2009**, *69*, 3689-3694, doi:10.1158/0008-5472.CAN-09-0024.
81. Wang, H.M.; Huang, Y.W.; Huang, J.S.; Wang, C.H.; Kok, V.C.; Hung, C.M.; Chen, H.M.; Tzen, C.Y. Anaplastic carcinoma of the thyroid arising more often from follicular carcinoma than papillary carcinoma. *Ann Surg Oncol* **2007**, *14*, 3011-3018, doi:10.1245/s10434-007-9503-8.
82. Vitagliano, D.; Portella, G.; Troncone, G.; Francione, A.; Rossi, C.; Bruno, A.; Giorgini, A.; Coluzzi, S.; Nappi, T.C.; Rothstein, J.L.; et al. Thyroid targeting of the N-ras(Gln61Lys) oncogene in transgenic mice results in follicular tumors that progress to poorly differentiated carcinomas. *Oncogene* **2006**, *25*, 5467-5474, doi:10.1038/sj.onc.1209527.
83. Garcia-Rostan, G.; Zhao, H.; Camp, R.L.; Pollan, M.; Herrero, A.; Pardo, J.; Wu, R.; Carcangiu, M.L.; Costa, J.; Tallini, G. ras mutations are associated with aggressive tumor phenotypes and poor prognosis in thyroid cancer. *J Clin Oncol* **2003**, *21*, 3226-3235, doi:10.1200/JCO.2003.10.130.
84. Shonka, D.C., Jr.; Ho, A.; Chintakuntlawar, A.V.; Geiger, J.L.; Park, J.C.; Seetharamu, N.; Jasim, S.; Abdelhamid Ahmed, A.H.; Bible, K.C.; Brose, M.S.; et al. American Head and Neck Society Endocrine Surgery Section and International Thyroid Oncology Group consensus statement on mutational testing in thyroid cancer: Defining advanced thyroid cancer and its targeted treatment. *Head Neck* **2022**, *44*, 1277-1300, doi:10.1002/hed.27025.
85. Abdelmoula, N.B.; Abdelmoula, B.; Masmoudi, I.; Aloulou, S. Review Histopathological-molecular classifications of papillary thyroid cancers: Challenges in genetic practice settings. *Biomedicine & Healthcare Research* **2024**, *2*, 2-11.
86. Coca-Pelaz, A.; Rodrigo, J.P.; Agaimy, A.; Williams, M.D.; Saba, N.F.; Nuyts, S.; Randolph, G.W.; Lopez, F.; Vander Poorten, V.; Kowalski, L.P.; et al. Poorly differentiated thyroid carcinomas: conceptual controversy and clinical impact. *Virchows Arch* **2024**, *484*, 733-742, doi:10.1007/s00428-024-03752-5.
87. Volante, M.; Collini, P.; Nikiforov, Y.E.; Sakamoto, A.; Kakudo, K.; Katoh, R.; Lloyd, R.V.; LiVolsi, V.A.; Papotti, M.; Sobrinho-Simoes, M.; et al. Poorly differentiated thyroid carcinoma: the Turin proposal for the use of uniform diagnostic criteria and an algorithmic diagnostic approach. *Am J Surg Pathol* **2007**, *31*, 1256-1264, doi:10.1097/PAS.0b013e3180309e6a.
88. Asa, S.L. The Current Histologic Classification of Thyroid Cancer. *Endocrinol Metab Clin North Am* **2019**, *48*, 1-22, doi:10.1016/j.ecl.2018.10.001.
89. Hiltzik, D.; Carlson, D.L.; Tuttle, R.M.; Chuai, S.; Ishill, N.; Shaha, A.; Shah, J.P.; Singh, B.; Ghossein, R.A. Poorly differentiated thyroid carcinomas defined on the basis of mitosis and necrosis: a clinicopathologic study of 58 patients. *Cancer* **2006**, *106*, 1286-1295, doi:10.1002/cncr.21739.
90. Wong, K.S.; Dong, F.; Telatar, M.; Lorch, J.H.; Alexander, E.K.; Marqusee, E.; Cho, N.L.; Nehs, M.A.; Doherty, G.M.; Afkhami, M.; et al. Papillary Thyroid Carcinoma with High-Grade Features Versus Poorly Differentiated Thyroid Carcinoma: An Analysis of Clinicopathologic and Molecular Features and Outcome. *Thyroid* **2021**, *31*, 933-940, doi:10.1089/thy.2020.0668.
91. Xu, B.; David, J.; Dogan, S.; Landa, I.; Katabi, N.; Saliba, M.; Khimraj, A.; Sherman, E.J.; Tuttle, R.M.; Tallini, G.; et al. Primary high-grade non-anaplastic thyroid carcinoma: a retrospective study of 364 cases. *Histopathology* **2022**, *80*, 322-337, doi:10.1111/his.14550.
92. Kakudo, K.; Wakasa, T.; Ohta, Y.; Yane, K.; Ito, Y.; Yamashita, H. Prognostic classification of thyroid follicular cell tumors using Ki-67 labeling index: risk stratification

of thyroid follicular cell carcinomas. *Endocr J* **2015**, *62*, 1-12, doi:10.1507/endocrj.EJ14-0293.
93. Chernock, R.D.; Rivera, B.; Borrelli, N.; Hill, D.A.; Fahiminiya, S.; Shah, T.; Chong, A.S.; Aqil, B.; Mehrad, M.; Giordano, T.J.; et al. Poorly differentiated thyroid carcinoma of childhood and adolescence: a distinct entity characterized by DICER1 mutations. *Mod Pathol* **2020**, *33*, 1264-1274, doi:10.1038/s41379-020-0458-7.
94. Huang, N.S.; Shi, X.; Lei, B.W.; Wei, W.J.; Lu, Z.W.; Yu, P.C.; Wang, Y.; Ji, Q.H.; Wang, Y.L. An Update of the Appropriate Treatment Strategies in Anaplastic Thyroid Cancer: A Population-Based Study of 735 Patients. *Int J Endocrinol* **2019**, *2019*, 8428547, doi:10.1155/2019/8428547.
95. Kakudo, K.; Bychkov, A.; Bai, Y.; Li, Y.; Liu, Z.; Jung, C.K. The new 4th edition World Health Organization classification for thyroid tumors, Asian perspectives. *Pathol Int* **2018**, *68*, 641-664, doi:10.1111/pin.12737.
96. Zhou, S.Y.; Luo, L.X. An overview of the contemporary diagnosis and management approaches for anaplastic thyroid carcinoma. *World J Clin Oncol* **2024**, *15*, 674-676, doi:10.5306/wjco.v15.i6.674.
97. Mirabile, A.; Biafora, M.; Giordano, L.; Arrigoni, G.; Cangi, M.G.; Dell'Oca, I.; Lira Luce, F.; Di Santo, D.; Galli, A.; Tulli, M.; et al. Uncommon Site of Metastasis and Prolonged Survival in Patients with Anaplastic Thyroid Carcinoma: A Systematic Review of the Literature. *Cancers (Basel)* **2020**, *12*, doi:10.3390/cancers12092585.
98. Xu, B.; Fuchs, T.; Dogan, S.; Landa, I.; Katabi, N.; Fagin, J.A.; Tuttle, R.M.; Sherman, E.; Gill, A.J.; Ghossein, R. Dissecting Anaplastic Thyroid Carcinoma: A Comprehensive Clinical, Histologic, Immunophenotypic, and Molecular Study of 360 Cases. *Thyroid* **2020**, *30*, 1505-1517, doi:10.1089/thy.2020.0086.
99. Landa, I.; Ibrahimpasic, T.; Boucai, L.; Sinha, R.; Knauf, J.A.; Shah, R.H.; Dogan, S.; Ricarte-Filho, J.C.; Krishnamoorthy, G.P.; Xu, B.; et al. Genomic and transcriptomic hallmarks of poorly differentiated and anaplastic thyroid cancers. *J Clin Invest* **2016**, *126*, 1052-1066, doi:10.1172/JCI85271.
100. Rocha, M.L.; Schmid, K.W.; Czapiewski, P. The prevalence of DNA microsatellite instability in anaplastic thyroid carcinoma - systematic review and discussion of current therapeutic options. *Contemp Oncol (Pozn)* **2021**, *25*, 213-223, doi:10.5114/wo.2021.110052.
101. Caillou, B.; Talbot, M.; Weyemi, U.; Pioche-Durieu, C.; Al Ghuzlan, A.; Bidart, J.M.; Chouaib, S.; Schlumberger, M.; Dupuy, C. Tumor-associated macrophages (TAMs) form an interconnected cellular supportive network in anaplastic thyroid carcinoma. *PLoS One* **2011**, *6*, e22567, doi:10.1371/journal.pone.0022567.
102. Ragazzi, M.; Ciarrocchi, A.; Sancisi, V.; Gandolfi, G.; Bisagni, A.; Piana, S. Update on anaplastic thyroid carcinoma: morphological, molecular, and genetic features of the most aggressive thyroid cancer. *Int J Endocrinol* **2014**, *2014*, 790834, doi:10.1155/2014/790834.
103. Alzumaili, B.; Xu, B.; Spanheimer, P.M.; Tuttle, R.M.; Sherman, E.; Katabi, N.; Dogan, S.; Ganly, I.; Untch, B.R.; Ghossein, R.A. Grading of medullary thyroid carcinoma on the basis of tumor necrosis and high mitotic rate is an independent predictor of poor outcome. *Modern Pathology* **2020**, *33*, 1690-1701.
104. Fuchs, T.L.; Nassour, A.J.; Glover, A.; Sywak, M.S.; Sidhu, S.B.; Delbridge, L.W.; Clifton-Bligh, R.J.; Gild, M.L.; Tsang, V.; Robinson, B.G. A proposed grading scheme for medullary thyroid carcinoma based on proliferative activity (Ki-67 and mitotic count) and coagulative necrosis. *The American journal of surgical pathology* **2020**, *44*, 1419-1428.
105. Xu, B.; Fuchs, T.L.; Ahmadi, S.; Alghamdi, M.; Alzumaili, B.; Bani, M.-A.; Baudin, E.; Chou, A.; De Leo, A.; Fagin, J.A. International medullary thyroid carcinoma grading system: a validated grading system for medullary thyroid carcinoma. *Journal of Clinical Oncology* **2022**, *40*, 96-104.

106. Asa, S.L.; Mete, O. Medullary thyroid carcinoma in the IARC/WHO neuroendocrine schema. *Endocrine Pathology* **2022**, *33*, 346-347.
107. HaugenBryan, R.; AlexanderErik, K.; BibleKeith, C.; DohertyGerard, M.; MandelSusan, J.; NikiforovYuri, E.; RandolphGregory, W.; SawkaAnna, M.; SchuffKathryn, G.; ShermanSteven, I. 2015 American Thyroid Association management guidelines for adult patients with thyroid nodules and differentiated thyroid cancer: the American Thyroid Association guidelines task force on thyroid nodules and differentiated thyroid cancer. *Thyroid* **2016**.
108. Sahin, M.; Oguz, A.; Tuzun, D.; Akkus, G.; Torun, G.I.; Bahar, A.Y.; Sahin, H.; Gul, K. Effectiveness of TI-RADS and ATA classifications for predicting malignancy of thyroid nodules. *Adv Clin Exp Med* **2021**, *30*, 1133-1139, doi:10.17219/acem/139591.
109. Cibas, E.S.; Ali, S.Z. The 2017 Bethesda System for Reporting Thyroid Cytopathology. *Thyroid* **2017**, *27*, 1341-1346, doi:10.1089/thy.2017.0500.
110. Maletta, F.; Massa, F.; Torregrossa, L.; Duregon, E.; Casadei, G.P.; Basolo, F.; Tallini, G.; Volante, M.; Nikiforov, Y.E.; Papotti, M. Cytological features of "noninvasive follicular thyroid neoplasm with papillary-like nuclear features" and their correlation with tumor histology. *Hum Pathol* **2016**, *54*, 134-142, doi:10.1016/j.humpath.2016.03.014.
111. Haugen, B.R.; Alexander, E.K.; Bible, K.C.; Doherty, G.M.; Mandel, S.J.; Nikiforov, Y.E.; Pacini, F.; Randolph, G.W.; Sawka, A.M.; Schlumberger, M.; et al. 2015 American Thyroid Association Management Guidelines for Adult Patients with Thyroid Nodules and Differentiated Thyroid Cancer: The American Thyroid Association Guidelines Task Force on Thyroid Nodules and Differentiated Thyroid Cancer. *Thyroid* **2016**, *26*, 1-133, doi:10.1089/thy.2015.0020.
112. Sparano, C.; Moog, S.; Hadoux, J.; Dupuy, C.; Al Ghuzlan, A.; Breuskin, I.; Guerlain, J.; Hartl, D.; Baudin, E.; Lamartina, L. Strategies for Radioiodine Treatment: What's New. *Cancers (Basel)* **2022**, *14*, doi:10.3390/cancers14153800.
113. Filetti, S.; Bidart, J.M.; Arturi, F.; Caillou, B.; Russo, D.; Schlumberger, M. Sodium/iodide symporter: a key transport system in thyroid cancer cell metabolism. *Eur J Endocrinol* **1999**, *141*, 443-457, doi:10.1530/eje.0.1410443.
114. Teng, C.-J.; Hu, Y.-W.; Chen, S.-C.; Yeh, C.-M.; Chiang, H.-L.; Chen, T.-J.; Liu, C.-J. Use of radioactive iodine for thyroid cancer and risk for second primary malignancy: a nationwide population-based study. *Journal of the National Cancer Institute* **2016**, *108*, djv314.
115. Pasqual, E.; Schonfeld, S.; Morton, L.M.; Villoing, D.; Lee, C.; Berrington de Gonzalez, A.; Kitahara, C.M. Association between radioactive iodine treatment for pediatric and young adulthood differentiated thyroid cancer and risk of second primary malignancies. *Journal of Clinical Oncology* **2022**, *40*, 1439-1449.
116. Molenaar, R.J.; Sidana, S.; Radivoyevitch, T.; Advani, A.S.; Gerds, A.T.; Carraway, H.E.; Angelini, D.; Kalaycio, M.; Nazha, A.; Adelstein, D.J. Risk of hematologic malignancies after radioiodine treatment of well-differentiated thyroid cancer. *Journal of clinical oncology* **2018**, *36*, 1831-1839.
117. Yu, C.Y.; Saeed, O.; Goldberg, A.S.; Farooq, S.; Fazelzad, R.; Goldstein, D.P.; Tsang, R.W.; Brierley, J.D.; Ezzat, S.; Thabane, L. A systematic review and meta-analysis of subsequent malignant neoplasm risk after radioactive iodine treatment of thyroid cancer. *Thyroid* **2018**, *28*, 1662-1673.
118. Tam, S.; Amit, M.; Boonsripitayanon, M.; Cabanillas, M.E.; Busaidy, N.L.; Gunn, G.B.; Lai, S.Y.; Gross, N.D.; Sturgis, E.M.; Zafereo, M.E. Adjuvant external beam radiotherapy in locally advanced differentiated thyroid cancer. *JAMA Otolaryngology–Head & Neck Surgery* **2017**, *143*, 1244-1251.

119. Valerio, L.; Pieruzzi, L.; Giani, C.; Agate, L.; Bottici, V.; Lorusso, L.; Cappagli, V.; Puleo, L.; Matrone, A.; Viola, D.; et al. Targeted Therapy in Thyroid Cancer: State of the Art. *Clin Oncol (R Coll Radiol)* **2017**, *29*, 316-324, doi:10.1016/j.clon.2017.02.009.
120. Zhang, Y.; Xing, Z.; Liu, T.; Tang, M.; Mi, L.; Zhu, J.; Wu, W.; Wei, T. Targeted therapy and drug resistance in thyroid cancer. *Eur J Med Chem* **2022**, *238*, 114500, doi:10.1016/j.ejmech.2022.114500.
121. Jin, N.; Jiang, T.; Rosen, D.M.; Nelkin, B.D.; Ball, D.W. Synergistic action of a RAF inhibitor and a dual PI3K/mTOR inhibitor in thyroid cancer. *Clinical Cancer Research* **2011**, *17*, 6482-6489.
122. Xing, M. Molecular pathogenesis and mechanisms of thyroid cancer. *Nature Reviews Cancer* **2013**, *13*, 184-199.
123. Burrows, N.; Resch, J.; Cowen, R.; Von Wasielewski, R.; Hoang-Vu, C.; West, C.; Williams, K.; Brabant, G. Expression of hypoxia-inducible factor 1α in thyroid carcinomas. *Endocrine-related cancer* **2010**, *17*, 61.
124. Zerilli, M.; Zito, G.; Martorana, A.; Pitrone, M.; Cabibi, D.; Cappello, F.; Giordano, C.; Rodolico, V. BRAFV600E mutation influences hypoxia-inducible factor-1α expression levels in papillary thyroid cancer. *Modern Pathology* **2010**, *23*, 1052-1060.
125. Sprindzuk, M.V. Angiogenesis in malignant thyroid tumors. *World Journal of Oncology* **2010**, *1*, 221.
126. Yuan, J.; Guo, Y. Targeted therapy for anaplastic thyroid carcinoma: advances and management. *Cancers* **2022**, *15*, 179.
127. Varricchi, G.; Loffredo, S.; Marone, G.; Modestino, L.; Fallahi, P.; Ferrari, S.M.; de Paulis, A.; Antonelli, A.; Galdiero, M.R. The immune landscape of thyroid cancer in the context of immune checkpoint inhibition. *International Journal of Molecular Sciences* **2019**, *20*, 3934.
128. Hatashima, A.; Archambeau, B.; Armbruster, H.; Xu, M.; Shah, M.; Konda, B.; Lott Limbach, A.; Sukrithan, V. An evaluation of clinical efficacy of immune checkpoint inhibitors for patients with anaplastic thyroid carcinoma. *Thyroid* **2022**, *32*, 926-936.
129. Chowdhury, S.; Veyhl, J.; Jessa, F.; Polyakova, O.; Alenzi, A.; MacMillan, C.; Ralhan, R.; Walfish, P.G. Programmed death-ligand 1 overexpression is a prognostic marker for aggressive papillary thyroid cancer and its variants. *Oncotarget* **2016**, *7*, 32318.
130. Zimmer, L.; Livingstone, E.; Krackhardt, A.; Schultz, E.S.; Goppner, D.; Assaf, C.; Trebing, D.; Stelter, K.; Windemuth-Kieselbach, C.; Ugurel, S.; et al. Encorafenib, binimetinib plus pembrolizumab triplet therapy in patients with advanced BRAF(V600) mutant melanoma: safety and tolerability results from the phase I IMMU-TARGET trial. *Eur J Cancer* **2021**, *158*, 72-84, doi:10.1016/j.ejca.2021.09.011.
131. Muller, S.; Tilakaratne, W.M. Update from the 5th Edition of the World Health Organization Classification of Head and Neck Tumors: Tumours of the Oral Cavity and Mobile Tongue. *Head Neck Pathol* **2022**, *16*, 54-62, doi:10.1007/s12105-021-01402-9.
132. Tan, Y.; Wang, Z.; Xu, M.; Li, B.; Huang, Z.; Qin, S.; Nice, E.C.; Tang, J.; Huang, C. Oral squamous cell carcinomas: state of the field and emerging directions. *Int J Oral Sci* **2023**, *15*, 44, doi:10.1038/s41368-023-00249-w.
133. Harada, H.; Kikuchi, M.; Asato, R.; Hamaguchi, K.; Tamaki, H.; Mizuta, M.; Hori, R.; Kojima, T.; Honda, K.; Tsujimura, T.; et al. Characteristics of oral squamous cell carcinoma focusing on cases unaffected by smoking and drinking: A multicenter retrospective study. *Head Neck* **2023**, *45*, 1812-1822, doi:10.1002/hed.27398.
134. Jerjes, W.; Upile, T.; Petrie, A.; Riskalla, A.; Hamdoon, Z.; Vourvachis, M.; Karavidas, K.; Jay, A.; Sandison, A.; Thomas, G.J.; et al. Clinicopathological parameters, recurrence, locoregional and distant metastasis in 115 T1-T2 oral squamous cell carcinoma patients. *Head Neck Oncol* **2010**, *2*, 9, doi:10.1186/1758-3284-2-9.
135. Ogden, G.R. Alcohol and oral cancer. *Alcohol* **2005**, *35*, 169-173, doi:10.1016/j.alcohol.2005.04.002.

136. Jeng, J.H.; Chang, M.C.; Hahn, L.J. Role of areca nut in betel quid-associated chemical carcinogenesis: current awareness and future perspectives. *Oral Oncol* **2001**, *37*, 477-492, doi:10.1016/s1368-8375(01)00003-3.
137. Schiffman, M.; Castle, P.E.; Jeronimo, J.; Rodriguez, A.C.; Wacholder, S. Human papillomavirus and cervical cancer. *Lancet* **2007**, *370*, 890-907, doi:10.1016/S0140-6736(07)61416-0.
138. Feldman, D.; Krishnan, A.V.; Swami, S.; Giovannucci, E.; Feldman, B.J. The role of vitamin D in reducing cancer risk and progression. *Nat Rev Cancer* **2014**, *14*, 342-357, doi:10.1038/nrc3691.
139. Stechschulte, S.A.; Kirsner, R.S.; Federman, D.G. Vitamin D: bone and beyond, rationale and recommendations for supplementation. *Am J Med* **2009**, *122*, 793-802, doi:10.1016/j.amjmed.2009.02.029.
140. Markopoulos, A.K. Current aspects on oral squamous cell carcinoma. *Open Dent J* **2012**, *6*, 126-130, doi:10.2174/1874210601206010126.
141. Usman, S.; Jamal, A.; Teh, M.T.; Waseem, A. Major Molecular Signaling Pathways in Oral Cancer Associated With Therapeutic Resistance. *Front Oral Health* **2020**, *1*, 603160, doi:10.3389/froh.2020.603160.
142. Li, Q.; Tie, Y.; Alu, A.; Ma, X.; Shi, H. Targeted therapy for head and neck cancer: signaling pathways and clinical studies. *Signal Transduct Target Ther* **2023**, *8*, 31, doi:10.1038/s41392-022-01297-0.
143. Peng, Q.; Deng, Z.; Pan, H.; Gu, L.; Liu, O.; Tang, Z. Mitogen-activated protein kinase signaling pathway in oral cancer. *Oncol Lett* **2018**, *15*, 1379-1388, doi:10.3892/ol.2017.7491.
144. Caruntu, A.; Moraru, L.; Lupu, M.; Vasilescu, F.; Dumitrescu, M.; Cioplea, M.; Popp, C.; Dragusin, A.; Caruntu, C.; Zurac, S. Prognostic Potential of Tumor-Infiltrating Immune Cells in Resectable Oral Squamous Cell Carcinoma. *Cancers (Basel)* **2021**, *13*, doi:10.3390/cancers13092268.
145. Sasahira, T.; Kirita, T. Hallmarks of Cancer-Related Newly Prognostic Factors of Oral Squamous Cell Carcinoma. *Int J Mol Sci* **2018**, *19*, doi:10.3390/ijms19082413.
146. Rivera, C.; Oliveira, A.K.; Costa, R.A.P.; De Rossi, T.; Paes Leme, A.F. Prognostic biomarkers in oral squamous cell carcinoma: A systematic review. *Oral Oncol* **2017**, *72*, 38-47, doi:10.1016/j.oraloncology.2017.07.003.
147. Xiao, W.; Li, J.; Hu, J.; Wang, L.; Huang, J.R.; Sethi, G.; Ma, Z. Circular RNAs in cell cycle regulation: Mechanisms to clinical significance. *Cell Prolif* **2021**, *54*, e13143, doi:10.1111/cpr.13143.
148. Wu, C.C.; Xiao, Y.; Li, H.; Mao, L.; Deng, W.W.; Yu, G.T.; Zhang, W.F.; Sun, Z.J. Overexpression of FAM3C is associated with poor prognosis in oral squamous cell carcinoma. *Pathol Res Pract* **2019**, *215*, 772-778, doi:10.1016/j.prp.2019.01.019.
149. Brands, M.T.; Brennan, P.A.; Verbeek, A.L.M.; Merkx, M.A.W.; Geurts, S.M.E. Follow-up after curative treatment for oral squamous cell carcinoma. A critical appraisal of the guidelines and a review of the literature. *Eur J Surg Oncol* **2018**, *44*, 559-565, doi:10.1016/j.ejso.2018.01.004.
150. Paleri, V.; Urbano, T.G.; Mehanna, H.; Repanos, C.; Lancaster, J.; Roques, T.; Patel, M.; Sen, M. Management of neck metastases in head and neck cancer: United Kingdom National Multidisciplinary Guidelines. *J Laryngol Otol* **2016**, *130*, S161-S169, doi:10.1017/S002221511600058X.
151. Brahmer, J.R.; Tykodi, S.S.; Chow, L.Q.; Hwu, W.J.; Topalian, S.L.; Hwu, P.; Drake, C.G.; Camacho, L.H.; Kauh, J.; Odunsi, K.; et al. Safety and activity of anti-PD-L1 antibody in patients with advanced cancer. *N Engl J Med* **2012**, *366*, 2455-2465, doi:10.1056/NEJMoa1200694.

152. Lee, W.S.; Ye, Z.; Cheung, A.M.S.; Goh, Y.P.S.; Oh, H.L.J.; Rajarethinam, R.; Yeo, S.P.; Soh, M.K.; Chan, E.H.L.; Tan, L.K.; et al. Effective Killing of Acute Myeloid Leukemia by TIM-3 Targeted Chimeric Antigen Receptor T Cells. *Mol Cancer Ther* **2021**, *20*, 1702-1712, doi:10.1158/1535-7163.MCT-20-0155.
153. Barbacid, M. ras genes. *Annu Rev Biochem* **1987**, *56*, 779-827, doi:10.1146/annurev.bi.56.070187.004023.
154. Hodge, R.G.; Schaefer, A.; Howard, S.V.; Der, C.J. RAS and RHO family GTPase mutations in cancer: twin sons of different mothers? *Crit Rev Biochem Mol Biol* **2020**, *55*, 386-407, doi:10.1080/10409238.2020.1810622.
155. Goitre, L.; Trapani, E.; Trabalzini, L.; Retta, S.F. The Ras superfamily of small GTPases: the unlocked secrets. *Methods Mol Biol* **2014**, *1120*, 1-18, doi:10.1007/978-1-62703-791-4_1.
156. Karnoub, A.E.; Weinberg, R.A. Ras oncogenes: split personalities. *Nat Rev Mol Cell Biol* **2008**, *9*, 517-531, doi:10.1038/nrm2438.
157. Prior, I.A.; Harding, A.; Yan, J.; Sluimer, J.; Parton, R.G.; Hancock, J.F. GTP-dependent segregation of H-ras from lipid rafts is required for biological activity. *Nat Cell Biol* **2001**, *3*, 368-375, doi:10.1038/35070050.
158. Volmar, A.Y.; Guterres, H.; Zhou, H.; Reid, D.; Pavlopoulos, S.; Makowski, L.; Mattos, C. Mechanisms of isoform-specific residue influence on GTP-bound HRas, KRas, and NRas. *Biophys J* **2022**, *121*, 3616-3629, doi:10.1016/j.bpj.2022.07.005.
159. Castellano, E.; Santos, E. Functional specificity of ras isoforms: so similar but so different. *Genes Cancer* **2011**, *2*, 216-231, doi:10.1177/1947601911408081.
160. Sung, P.J.; Tsai, F.D.; Vais, H.; Court, H.; Yang, J.; Fehrenbacher, N.; Foskett, J.K.; Philips, M.R. Phosphorylated K-Ras limits cell survival by blocking Bcl-xL sensitization of inositol trisphosphate receptors. *Proc Natl Acad Sci U S A* **2013**, *110*, 20593-20598, doi:10.1073/pnas.1306431110.
161. Simanshu, D.K.; Nissley, D.V.; McCormick, F. RAS Proteins and Their Regulators in Human Disease. *Cell* **2017**, *170*, 17-33, doi:10.1016/j.cell.2017.06.009.
162. Han, C.W.; Jeong, M.S.; Jang, S.B. Structure, signaling and the drug discovery of the Ras oncogene protein. *BMB Rep* **2017**, *50*, 355-360, doi:10.5483/bmbrep.2017.50.7.062.
163. Han, C.W.; Jeong, M.S.; Jang, S.B. Understand KRAS and the Quest for Anti-Cancer Drugs. *Cells* **2021**, *10*, doi:10.3390/cells10040842.
164. Xu, D.; Shao, Q.; Zhou, C.; Mahmood, A.; Zhang, J. In Silico Analysis of nsSNPs of Human KRAS Gene and Protein Modeling Using Bioinformatic Tools. *ACS Omega* **2023**, *8*, 13362-13370, doi:10.1021/acsomega.3c00804.
165. Han, C.W.; Jeong, M.S.; Jang, S.B. Understand KRAS and the quest for anti-cancer drugs. *Cells* **2021**, *10*, 842.
166. Prior, I.A.; Hancock, J.F. Ras trafficking, localization and compartmentalized signalling. *Semin Cell Dev Biol* **2012**, *23*, 145-153, doi:10.1016/j.semcdb.2011.09.002.
167. Ash, L.J.; Busia-Bourdain, O.; Okpattah, D.; Kamel, A.; Liberchuk, A.; Wolfe, A.L. KRAS: Biology, Inhibition, and Mechanisms of Inhibitor Resistance. *Curr Oncol* **2024**, *31*, 2024-2046, doi:10.3390/curroncol31040150.
168. Schlessinger, J. Cell signaling by receptor tyrosine kinases. *Cell* **2000**, *103*, 211-225, doi:10.1016/s0092-8674(00)00114-8.
169. Hennig, A.; Markwart, R.; Esparza-Franco, M.A.; Ladds, G.; Rubio, I. Ras activation revisited: role of GEF and GAP systems. *Biol Chem* **2015**, *396*, 831-848, doi:10.1515/hsz-2014-0257.
170. Liu, P.; Wang, Y.; Li, X. Targeting the untargetable KRAS in cancer therapy. *Acta Pharm Sin B* **2019**, *9*, 871-879, doi:10.1016/j.apsb.2019.03.002.

171. Bahar, M.E.; Kim, H.J.; Kim, D.R. Targeting the RAS/RAF/MAPK pathway for cancer therapy: from mechanism to clinical studies. *Signal transduction and targeted therapy* **2023**, *8*, 455.
172. Liceras-Boillos, P.; Jimeno, D.; Garcia-Navas, R.; Lorenzo-Martin, L.F.; Menacho-Marquez, M.; Segrelles, C.; Gomez, C.; Calzada, N.; Fuentes-Mateos, R.; Paramio, J.M.; et al. Differential Role of the RasGEFs Sos1 and Sos2 in Mouse Skin Homeostasis and Carcinogenesis. *Mol Cell Biol* **2018**, *38*, doi:10.1128/MCB.00049-18.
173. Tiacci, E.; Trifonov, V.; Schiavoni, G.; Holmes, A.; Kern, W.; Martelli, M.P.; Pucciarini, A.; Bigerna, B.; Pacini, R.; Wells, V.A.; et al. BRAF mutations in hairy-cell leukemia. *N Engl J Med* **2011**, *364*, 2305-2315, doi:10.1056/NEJMoa1014209.
174. Castellano, E.; Downward, J. RAS Interaction with PI3K: More Than Just Another Effector Pathway. *Genes Cancer* **2011**, *2*, 261-274, doi:10.1177/1947601911408079.
175. Castellano, E.; Downward, J. Role of RAS in the regulation of PI 3-kinase. *Curr Top Microbiol Immunol* **2010**, *346*, 143-169, doi:10.1007/82_2010_56.
176. Vivanco, I.; Sawyers, C.L. The phosphatidylinositol 3-Kinase AKT pathway in human cancer. *Nat Rev Cancer* **2002**, *2*, 489-501, doi:10.1038/nrc839.
177. Mantovani, A.; Balkwill, F. RalB signaling: a bridge between inflammation and cancer. *Cell* **2006**, *127*, 42-44.
178. Yan, C.; Theodorescu, D. RAL GTPases: Biology and Potential as Therapeutic Targets in Cancer. *Pharmacol Rev* **2018**, *70*, 1-11, doi:10.1124/pr.117.014415.
179. Luo, J.; Manning, B.D.; Cantley, L.C. Targeting the PI3K-Akt pathway in human cancer: rationale and promise. *Cancer cell* **2003**, *4*, 257-262.
180. Lavoie, H.; Gagnon, J.; Therrien, M. ERK signalling: a master regulator of cell behaviour, life and fate. *Nat Rev Mol Cell Biol* **2020**, *21*, 607-632, doi:10.1038/s41580-020-0255-7.
181. Valderrabano, P.; Eszlinger, M.; Stewardson, P.; Paschke, R. Clinical value of molecular markers as diagnostic and prognostic tools to guide treatment of thyroid cancer. *Clinical endocrinology* **2023**, *98*, 753-762.
182. Goldner, W.S.; Angell, T.E.; McAdoo, S.L.; Babiarz, J.; Sadow, P.M.; Nabhan, F.A.; Nasr, C.; Kloos, R.T. Molecular Variants and Their Risks for Malignancy in Cytologically Indeterminate Thyroid Nodules. *Thyroid* **2019**, *29*, 1594-1605, doi:10.1089/thy.2019.0278.
183. Gilani, S.M.; Abi-Raad, R.; Garritano, J.; Cai, G.; Prasad, M.L.; Adeniran, A.J. RAS mutation and associated risk of malignancy in the thyroid gland: An FNA study with cytology-histology correlation. *Cancer Cytopathol* **2022**, *130*, 284-293, doi:10.1002/cncy.22537.
184. Liu, F.-T.; Patterson, R.J.; Wang, J.L. Intracellular functions of galectins. *Biochimica et Biophysica Acta (BBA)-General Subjects* **2002**, *1572*, 263-273.
185. Shalom-Feuerstein, R.; Plowman, S.J.; Rotblat, B.; Ariotti, N.; Tian, T.; Hancock, J.F.; Kloog, Y. K-ras nanoclustering is subverted by overexpression of the scaffold protein galectin-3. *Cancer research* **2008**, *68*, 6608-6616.
186. Inohara, H.; Honjo, Y.; Yoshii, T.; Akahani, S.; Yoshida, J.i.; Hattori, K.; Okamoto, S.; Sawada, T.; Raz, A.; Kubo, T. Expression of galectin-3 in fine-needle aspirates as a diagnostic marker differentiating benign from malignant thyroid neoplasms. *Cancer: Interdisciplinary International Journal of the American Cancer Society* **1999**, *85*, 2475-2484.
187. Saggiorato, E.; Aversa, S.; Deandreis, D.; Arecco, F.; Mussa, A.; Puligheddu, B.; Cappia, S.; Conticello, S.; Papotti, M.; Orlandi, F. Galectin-3: presurgical marker of thyroid follicular epithelial cell-derived carcinomas. *Journal of endocrinological investigation* **2004**, *27*, 311-317.
188. Martinez-Limon, A.; Joaquin, M.; Caballero, M.; Posas, F.; de Nadal, E. The p38 Pathway: From Biology to Cancer Therapy. *Int J Mol Sci* **2020**, *21*, doi:10.3390/ijms21061913.

189. Yu, W.; Imoto, I.; Inoue, J.; Onda, M.; Emi, M.; Inazawa, J. A novel amplification target, DUSP26, promotes anaplastic thyroid cancer cell growth by inhibiting p38 MAPK activity. *Oncogene* **2007**, *26*, 1178-1187, doi:10.1038/sj.onc.1209899.
190. Nylen, C.; Mechera, R.; Marechal-Ross, I.; Tsang, V.; Chou, A.; Gill, A.J.; Clifton-Bligh, R.J.; Robinson, B.G.; Sywak, M.S.; Sidhu, S.B.; et al. Molecular Markers Guiding Thyroid Cancer Management. *Cancers (Basel)* **2020**, *12*, doi:10.3390/cancers12082164.
191. Tadokoro, K.; Ueda, M.; Ohshima, T.; Fujita, K.; Rikimaru, K.; Takahashi, N.; Enomoto, S.; Tsuchida, N. Activation of oncogenes in human oral cancer cells: a novel codon 13 mutation of c-H-ras-1 and concurrent amplifications of c-erbB-1 and c-myc. *Oncogene* **1989**, *4*, 499-505.
192. Murugan, A.K.; Munirajan, A.K.; Tsuchida, N. Ras oncogenes in oral cancer: the past 20 years. *Oral Oncol* **2012**, *48*, 383-392, doi:10.1016/j.oraloncology.2011.12.006.
193. Hoa, M.; Davis, S.L.; Ames, S.J.; Spanjaard, R.A. Amplification of wild-type K-ras promotes growth of head and neck squamous cell carcinoma. *Cancer Res* **2002**, *62*, 7154-7156.
194. Sinevici, N.; O'Sullivan, J. Oral cancer: Deregulated molecular events and their use as biomarkers. *Oral Oncol* **2016**, *61*, 12-18, doi:10.1016/j.oraloncology.2016.07.013.
195. El Hanbuli, H.M.; Abou Sarie, M.A. KRAS Protein Expression in Oral Squamous Cell Carcinoma: A Potential Marker for Progression and Prognosis. *Iran J Pathol* **2022**, *17*, 469-479, doi:10.30699/IJP.2022.550727.2856.
196. Cascetta, P.; Marinello, A.; Lazzari, C.; Gregorc, V.; Planchard, D.; Bianco, R.; Normanno, N.; Morabito, A. KRAS in NSCLC: State of the Art and Future Perspectives. *Cancers (Basel)* **2022**, *14*, doi:10.3390/cancers14215430.
197. Spencer-Smith, R.; O'Bryan, J.P. Direct inhibition of RAS: Quest for the Holy Grail? *Semin Cancer Biol* **2019**, *54*, 138-148, doi:10.1016/j.semcancer.2017.12.005.
198. Zhu, Z.; Golay, H.G.; Barbie, D.A. Targeting pathways downstream of KRAS in lung adenocarcinoma. *Pharmacogenomics* **2014**, *15*, 1507-1518, doi:10.2217/pgs.14.108.
199. Evelyn, C.R.; Duan, X.; Biesiada, J.; Seibel, W.L.; Meller, J.; Zheng, Y. Rational design of small molecule inhibitors targeting the Ras GEF, SOS1. *Chem Biol* **2014**, *21*, 1618-1628, doi:10.1016/j.chembiol.2014.09.018.
200. Jiang, H.; Fan, Y.; Wang, X.; Wang, J.; Yang, H.; Fan, W.; Tang, C. Design, synthesis and biological evaluation of quinazoline SOS1 inhibitors. *Bioorg Med Chem Lett* **2023**, *88*, 129265, doi:10.1016/j.bmcl.2023.129265.
201. Hillig, R.C.; Sautier, B.; Schroeder, J.; Moosmayer, D.; Hilpmann, A.; Stegmann, C.M.; Werbeck, N.D.; Briem, H.; Boemer, U.; Weiske, J.; et al. Discovery of potent SOS1 inhibitors that block RAS activation via disruption of the RAS-SOS1 interaction. *Proc Natl Acad Sci U S A* **2019**, *116*, 2551-2560, doi:10.1073/pnas.1812963116.
202. Harwood, S.J.; Smith, C.R.; Lawson, J.D.; Ketcham, J.M. Selected Approaches to Disrupting Protein-Protein Interactions within the MAPK/RAS Pathway. *Int J Mol Sci* **2023**, *24*, doi:10.3390/ijms24087373.
203. Cucinotta, L.; Mannino, D.; Casili, G.; Repici, A.; Crupi, L.; Paterniti, I.; Esposito, E.; Campolo, M. Prolyl oligopeptidase inhibition ameliorates experimental pulmonary fibrosis both in vivo and in vitro. *Respir Res* **2023**, *24*, 211, doi:10.1186/s12931-023-02519-x.
204. Sewell, W.; Reeb, A.; Lin, R.Y. An orthotopic mouse model of anaplastic thyroid carcinoma. *J Vis Exp* **2013**, doi:10.3791/50097.
205. Nucera, C.; Nehs, M.A.; Mekel, M.; Zhang, X.; Hodin, R.; Lawler, J.; Nose, V.; Parangi, S. A novel orthotopic mouse model of human anaplastic thyroid carcinoma. *Thyroid* **2009**, *19*, 1077-1084, doi:10.1089/thy.2009.0055.
206. Scuderi, S.A.; Casili, G.; Basilotta, R.; Lanza, M.; Filippone, A.; Raciti, G.; Puliafito, I.; Colarossi, L.; Esposito, E.; Paterniti, I. NLRP3 Inflammasome Inhibitor BAY-117082

Reduces Oral Squamous Cell Carcinoma Progression. *Int J Mol Sci* **2021**, *22*, doi:10.3390/ijms222011108.
207. Basilotta, R.; Lanza, M.; Filippone, A.; Casili, G.; Mannino, D.; De Gaetano, F.; Chisari, G.; Colarossi, L.; Motta, G.; Campolo, M.; et al. Therapeutic Potential of Dimethyl Fumarate in Counteract Oral Squamous Cell Carcinoma Progression by Modulating Apoptosis, Oxidative Stress and Epithelial-Mesenchymal Transition. *Int J Mol Sci* **2023**, *24*, doi:10.3390/ijms24032777.
208. Cheng, N.; Diao, H.; Lin, Z.; Gao, J.; Zhao, Y.; Zhang, W.; Wang, Q.; Lin, J.; Zhang, D.; Jin, Y.; et al. Benzyl Isothiocyanate Induces Apoptosis and Inhibits Tumor Growth in Canine Mammary Carcinoma via Downregulation of the Cyclin B1/Cdk1 Pathway. *Front Vet Sci* **2020**, *7*, 580530, doi:10.3389/fvets.2020.580530.
209. Ohnishi, K.; Ota, I.; Yane, K.; Takahashi, A.; Yuki, K.; Emoto, M.; Hosoi, H.; Ohnishi, T. Glycerol as a chemical chaperone enhances radiation-induced apoptosis in anaplastic thyroid carcinoma cells. *Mol Cancer* **2002**, *1*, 4, doi:10.1186/1476-4598-1-4.
210. Thackaberry, E.A.; Wang, X.; Schweiger, M.; Messick, K.; Valle, N.; Dean, B.; Sambrone, A.; Bowman, T.; Xie, M. Solvent-based formulations for intravenous mouse pharmacokinetic studies: tolerability and recommended solvent dose limits. *Xenobiotica* **2014**, *44*, 235-241, doi:10.3109/00498254.2013.845706.
211. Nucera, C.; Nehs, M.A.; Nagarkatti, S.S.; Sadow, P.M.; Mekel, M.; Fischer, A.H.; Lin, P.S.; Bollag, G.E.; Lawler, J.; Hodin, R.A.; et al. Targeting BRAFV600E with PLX4720 displays potent antimigratory and anti-invasive activity in preclinical models of human thyroid cancer. *Oncologist* **2011**, *16*, 296-309, doi:10.1634/theoncologist.2010-0317.
212. Fanfone, D.; Stanicki, D.; Nonclercq, D.; Port, M.; Vander Elst, L.; Laurent, S.; Muller, R.N.; Saussez, S.; Burtea, C. Molecular Imaging of Galectin-1 Expression as a Biomarker of Papillary Thyroid Cancer by Using Peptide-Functionalized Imaging Probes. *Biology (Basel)* **2020**, *9*, doi:10.3390/biology9030053.
213. Scuderi, S.A.; Casili, G.; Ardizzone, A.; Forte, S.; Colarossi, L.; Sava, S.; Paterniti, I.; Esposito, E.; Cuzzocrea, S.; Campolo, M. KYP-2047, an inhibitor of prolyl-oligopeptidase, reduces glioblastoma proliferation through angiogenesis and apoptosis modulation. *Cancers* **2021**, *13*, 3444.
214. Plangger, A.; Rath, B.; Hochmair, M.; Funovics, M.; Hamilton, G. Cytotoxicity of combinations of the pan-KRAS inhibitor BAY-293 against primary non-small lung cancer cells. *Translational Oncology* **2021**, *14*, 101230.
215. Kim, H.J.; Lee, H.N.; Jeong, M.S.; Jang, S.B. Oncogenic KRAS: signaling and drug resistance. *Cancers* **2021**, *13*, 5599.
216. Schubert, L.; Mariko, M.L.; Clerc, J.; Huillard, O.; Groussin, L. MAPK Pathway Inhibitors in Thyroid Cancer: Preclinical and Clinical Data. *Cancers (Basel)* **2023**, *15*, doi:10.3390/cancers15030710.
217. Jeong, W.J.; Ro, E.J.; Choi, K.Y. Interaction between Wnt/beta-catenin and RAS-ERK pathways and an anti-cancer strategy via degradations of beta-catenin and RAS by targeting the Wnt/beta-catenin pathway. *NPJ Precis Oncol* **2018**, *2*, 5, doi:10.1038/s41698-018-0049-y.
218. Zhu, W.; Xie, B. PLK4 inhibitor exhibits antitumor effect and synergizes sorafenib via arresting cell cycle and inactivating Wnt/β-catenin pathway in anaplastic thyroid cancer. *Cancer Biology & Therapy* **2023**, *24*, 2223383.
219. Carnero, A.; Paramio, J.M. The PTEN/PI3K/AKT Pathway in vivo, Cancer Mouse Models. *Front Oncol* **2014**, *4*, 252, doi:10.3389/fonc.2014.00252.
220. Xu, L.L.; Li, C.C.; An, L.Y.; Dai, Z.; Chen, X.Y.; You, Q.D.; Hu, C.; Di, B. Selective apoptosis-inducing activity of synthetic hydrocarbon-stapled SOS1 helix with d-amino acids in H358 cancer cells expressing KRAS(G12C). *Eur J Med Chem* **2020**, *185*, 111844, doi:10.1016/j.ejmech.2019.111844.

221. Piersma, B.; Hayward, M.-K.; Weaver, V.M. Fibrosis and cancer: A strained relationship. *Biochimica et Biophysica Acta (BBA)-Reviews on Cancer* **2020**, *1873*, 188356.
222. Silver Karcioglu, A.; Iwata, A.J.; Pusztaszeri, M.; Abdelhamid Ahmed, A.H.; Randolph, G.W. The American Thyroid Association (ATA) integrates molecular testing into its framework for managing patients with anaplastic thyroid carcinoma (ATC): Update on the 2021 ATA ATC guidelines. *Cancer Cytopathol* **2022**, *130*, 174-180, doi:10.1002/cncy.22519.
223. Tallini, G.; Garcia-Rostan, G.; Herrero, A.; Zelterman, D.; Viale, G.; Bosari, S.; Carcangiu, M.L. Downregulation of p27KIP1 and Ki67/Mib1 labeling index support the classification of thyroid carcinoma into prognostically relevant categories. *Am J Surg Pathol* **1999**, *23*, 678-685, doi:10.1097/00000478-199906000-00007.
224. Zhao, M.; Sano, D.; Pickering, C.R.; Jasser, S.A.; Henderson, Y.C.; Clayman, G.L.; Sturgis, E.M.; Ow, T.J.; Lotan, R.; Carey, T.E.; et al. Assembly and initial characterization of a panel of 85 genomically validated cell lines from diverse head and neck tumor sites. *Clin Cancer Res* **2011**, *17*, 7248-7264, doi:10.1158/1078-0432.CCR-11-0690.
225. Chen, S.; Hu, H.; Miao, S.; Zheng, J.; Xie, Z.; Zhao, H. Anti-tumor effect of cisplatin in human oral squamous cell carcinoma was enhanced by andrographolide via upregulation of phospho-p53 in vitro and in vivo. *Tumour Biol* **2017**, *39*, 1010428317705330, doi:10.1177/1010428317705330.
226. Jiang, L.; Ji, N.; Zhou, Y.; Li, J.; Liu, X.; Wang, Z.; Chen, Q.; Zeng, X. CAL 27 is an oral adenosquamous carcinoma cell line. *Oral Oncol* **2009**, *45*, e204-207, doi:10.1016/j.oraloncology.2009.06.001.
227. Pereira, F.; Ferreira, A.; Reis, C.A.; Sousa, M.J.; Oliveira, M.J.; Preto, A. KRAS as a Modulator of the Inflammatory Tumor Microenvironment: Therapeutic Implications. *Cells* **2022**, *11*, doi:10.3390/cells11030398.
228. Hirst, D.G.; Robson, T. Nitrosative stress in cancer therapy. *Front Biosci* **2007**, *12*, 3406-3418, doi:10.2741/2322.
229. Sheffels, E.; Kortum, R.L. The Role of Wild-Type RAS in Oncogenic RAS Transformation. *Genes (Basel)* **2021**, *12*, doi:10.3390/genes12050662.
230. Vivekanandhan, S.; Mukhopadhyay, D. Genetic status of KRAS influences Transforming Growth Factor-beta (TGF-beta) signaling: An insight into Neuropilin-1 (NRP1) mediated tumorigenesis. *Semin Cancer Biol* **2019**, *54*, 72-79, doi:10.1016/j.semcancer.2018.01.014.
231. Jagadeeshan, S.; Novoplansky, O.Z.; Cohen, O.; Kurth, I.; Hess, J.; Rosenberg, A.J.; Grandis, J.R.; Elkabets, M. New insights into RAS in head and neck cancer. *Biochim Biophys Acta Rev Cancer* **2023**, *1878*, 188963, doi:10.1016/j.bbcan.2023.188963.
232. Novoplansky, O.; Jagadeeshan, S.; Regev, O.; Menashe, I.; Elkabets, M. Worldwide Prevalence and Clinical Characteristics of RAS Mutations in Head and Neck Cancer: A Systematic Review and Meta-Analysis. *Front Oncol* **2022**, *12*, 838911, doi:10.3389/fonc.2022.838911.
233. Are, C.; Shaha, A.R. Anaplastic thyroid carcinoma: biology, pathogenesis, prognostic factors, and treatment approaches. *Annals of surgical oncology* **2006**, *13*, 453-464.
234. Ito, K.i.; Hanamura, T.; Murayama, K.; Okada, T.; Watanabe, T.; Harada, M.; Ito, T.; Koyama, H.; Kanai, T.; Maeno, K. Multimodality therapeutic outcomes in anaplastic thyroid carcinoma: improved survival in subgroups of patients with localized primary tumors. *Head & neck* **2012**, *34*, 230-237.
235. Xu, B.; Ghossein, R. Genomic landscape of poorly differentiated and anaplastic thyroid carcinoma. *Endocrine pathology* **2016**, *27*, 205-212.
236. Stringer, B.M.; Rowson, J.M.; Parkar, M.H.; Seid, J.M.; Hearn, P.R.; Wynford-Thomas, D.; Ingemansson, S.; Woodhouse, N.; Goyns, M.H. Detection of the H-RAS oncogene in human thyroid anaplastic carcinomas. *Experientia* **1989**, *45*, 372-376, doi:10.1007/BF01957483.

237. Guo, Y.J.; Pan, W.W.; Liu, S.B.; Shen, Z.F.; Xu, Y.; Hu, L.L. ERK/MAPK signalling pathway and tumorigenesis. *Experimental and therapeutic medicine* **2020**, *19*, 1997-2007.
238. Ullah, R.; Yin, Q.; Snell, A.H.; Wan, L. RAF-MEK-ERK pathway in cancer evolution and treatment. In Proceedings of the Seminars in cancer biology, 2022; pp. 123-154.
239. De Luca, A.; Maiello, M.R.; D'Alessio, A.; Pergameno, M.; Normanno, N. The RAS/RAF/MEK/ERK and the PI3K/AKT signalling pathways: role in cancer pathogenesis and implications for therapeutic approaches. *Expert opinion on therapeutic targets* **2012**, *16*, S17-S27.
240. Davies, E.J.; Marsh Durban, V.; Meniel, V.; Williams, G.T.; Clarke, A.R. PTEN loss and KRAS activation leads to the formation of serrated adenomas and metastatic carcinoma in the mouse intestine. *The Journal of pathology* **2014**, *233*, 27-38.
241. Wilhelm, S.M.; Carter, C.; Tang, L.; Wilkie, D.; McNabola, A.; Rong, H.; Chen, C.; Zhang, X.; Vincent, P.; McHugh, M. BAY 43-9006 exhibits broad spectrum oral antitumor activity and targets the RAF/MEK/ERK pathway and receptor tyrosine kinases involved in tumor progression and angiogenesis. *Cancer research* **2004**, *64*, 7099-7109.
242. Ju, C.; Zhou, M.; Du, D.; Wang, C.; Yao, J.; Li, H.; Luo, Y.; He, F.; He, J. EIF4A3-mediated circ_0042881 activates the RAS pathway via miR-217/SOS1 axis to facilitate breast cancer progression. *Cell Death & Disease* **2023**, *14*, 559.
243. Chen, T.; Tang, X.; Wang, Z.; Feng, F.; Xu, C.; Zhao, Q.; Wu, Y.; Sun, H.; Chen, Y. Inhibition of Son of Sevenless Homologue 1 (SOS1): Promising therapeutic treatment for KRAS-mutant cancers. *European Journal of Medicinal Chemistry* **2023**, 115828.
244. Dias Carvalho, P.; Mendonça, S.; Martins, F.; Oliveira, M.J.; Velho, S. Modulation of Fibroblast Phenotype by Colorectal Cancer Cell-Secreted Factors Is Mostly Independent of Oncogenic KRAS. *Cells* **2022**, *11*, 2490.
245. Dey, S.; Singh, A.K.; Singh, A.K.; Rawat, K.; Banerjee, J.; Agnihotri, V.; Upadhaya, D. Critical pathways of oral squamous cell carcinoma: molecular biomarker and therapeutic intervention. *Med Oncol* **2022**, *39*, 30, doi:10.1007/s12032-021-01633-4.
246. Guo, Q.; Jin, Y.; Chen, X.; Ye, X.; Shen, X.; Lin, M.; Zeng, C.; Zhou, T.; Zhang, J. NF-kappaB in biology and targeted therapy: new insights and translational implications. *Signal Transduct Target Ther* **2024**, *9*, 53, doi:10.1038/s41392-024-01757-9.
247. Reddy, T.P.; Glynn, S.A.; Billiar, T.R.; Wink, D.A.; Chang, J.C. Targeting Nitric Oxide: Say NO to Metastasis. *Clin Cancer Res* **2023**, *29*, 1855-1868, doi:10.1158/1078-0432.CCR-22-2791.
248. Sangle, V.A.; Chaware, S.J.; Kulkarni, M.A.; Ingle, Y.C.; Singh, P.; Pooja, V.K. Elevated tissue nitric oxide in oral squamous cell carcinoma. *J Oral Maxillofac Pathol* **2018**, *22*, 35-39, doi:10.4103/jomfp.JOMFP_27_16.
249. Su, C.W.; Chien, M.H.; Lin, C.W.; Chen, M.K.; Chow, J.M.; Chuang, C.Y.; Chou, C.H.; Liu, Y.C.; Yang, S.F. Associations of genetic variations of the endothelial nitric oxide synthase gene and environmental carcinogens with oral cancer susceptibility and development. *Nitric Oxide* **2018**, *79*, 1-7, doi:10.1016/j.niox.2018.06.005.
250. Lim, K.H.; Ancrile, B.B.; Kashatus, D.F.; Counter, C.M. Tumour maintenance is mediated by eNOS. *Nature* **2008**, *452*, 646-649, doi:10.1038/nature06778.
251. He, S.; Chakraborty, R.; Ranganathan, S. Proliferation and Apoptosis Pathways and Factors in Oral Squamous Cell Carcinoma. *Int J Mol Sci* **2022**, *23*, doi:10.3390/ijms23031562.
252. Ferreira, A.; Pereira, F.; Reis, C.; Oliveira, M.J.; Sousa, M.J.; Preto, A. Crucial Role of Oncogenic KRAS Mutations in Apoptosis and Autophagy Regulation: Therapeutic Implications. *Cells* **2022**, *11*, doi:10.3390/cells11142183.